1-1-1986

Linear viscoelasticity of crosslinking polymers at the gel point/

Francois H. Chambon
University of Massachusetts Amherst

LINEAR VISCOELASTICITY OF CROSSLINKING POLYMERS AT THE GEL POINT

A Dissertation Presented

By

FRANCOIS CHAMBON

Submitted to the Graduate School of the
University of Massachusetts in partial fulfillment
of the requirements for the degree of

DOCTOR OF PHILOSOPHY

September 1986

Polymer Science and Engineering

LINEAR VISCOELASTICITY OF CROSSLINKING

POLYMERS AT THE GEL POINT

A Dissertation Presented

By

FRANCOIS CHAMBON

Approved as to style and content by:

Professor H. Henning Winter
Chairperson of Committee

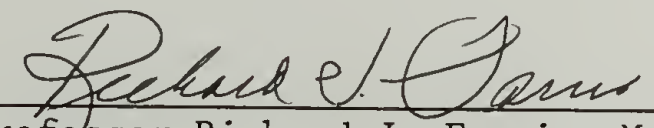

Professor Richard J. Farris, Member

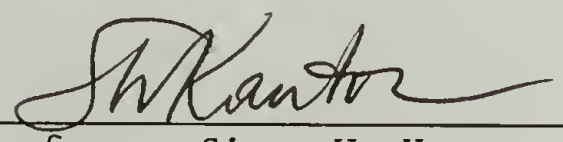

Professor Simon W. Kantor, Member

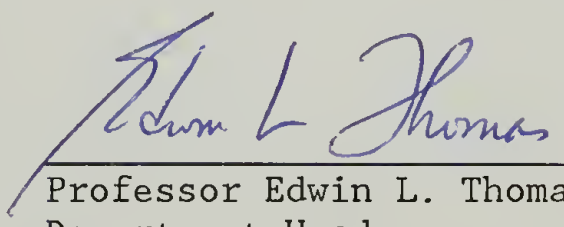

Professor Edwin L. Thomas
Department Head
Polymer Science and Engineering

ACKNOWLEDGMENTS

It is a real pleasure and honor to acknowledge here my great indebtedness to Professor H. Henning Winter under whose general direction this dissertation has been written. His enthusiastic guidance and scholarly assistance are in great measure responsible for whatever merits this study may have.

My sincere thanks also go to Professors Richard J. Farris and Simon W. Kantor for stimulating discussion, help and encouragement during the course of this research.

I am also obliged to Professor J. D. Ferry for a variety of helpful comments and criticisms as well.

Several people made this study easier. These are: Professor T. McCarthy and his students, Dr. S. Curran from Monsanto Chemical Co., Dr. Z. Petrovic, Dr. P. Morganelli, Mr. L. Coyne and Mr. E. Holly. I am greatly indebted to them for their help.

A word of gratitude is finally due to the many friends and colleagues whom I have met in Amherst. I am particularly grateful to Chris, Faith, and Tom, for invaluable assistance and supportive friendship.

Acknowledgment is herewith made to the Center for the University of Massachusetts and Industry Research in Polymers (CUMIRP) for continuous financial support of this work.

ABSTRACT

LINEAR VISCOELASTICITY OF CROSS-LINKING POLYMERS AT THE GEL POINT

September 1986

Francois Chambon

Ingenieur, INSA Lyon

Ph.D., University of Massachusetts

Directed by: Professor H. Henning Winter

Cross-linking polymers undergo a phase transition from liquid to solid at a critical extent of reaction. This phenomenon is called gelation. In this study, the evolution of the linear viscoelastic properties of two end-linking polymers were studied through the gelation transition. The polymers selected were a model polydimethylsiloxane (PDMS), and a model polyurethane (PU) of cross-link functionality four and three respectively.

Analysis of the rheological experiments led to the discovery that, at the gel point, the linear relaxation modulus obeys a power law, St^{-n}. An exponent value of $n=1/2$ was found for gels with balanced stoichiometry and for gels with excess of cross-linker while exponents values of $1/2<n<1$ were found for cross-linker deficient gels. The gel 'strength', S, was found to be strongly dependent on molecular parameters, but in a way not yet understood. The observed rheological behavior is consistent

with the results of recently developed fractals theories. A fractal dimension of 2 is predicted for gels with balanced stoichiometry; this value increases for non stoichiometric gels.

The Gel Equation, a constitutive equation based on the power law relaxation behavior, was formulated. It describes the observed rheological behavior at the gel point and predicts the classical attributes of a gel, namely infinite steady shear viscosity and zero equilibrium modulus. The simplicity and clarity of the Gel Equation suggests its universal validity for cross-linking polymers at the gel point.

TABLE OF CONTENTS

LIST OF TABLES

LIST OF FIGURES

CHAPTER I

INTRODUCTION

The introduction of chemical cross-links into an uncross-linked polymer converts it from a viscoelastic liquid to a viscoelastic solid, creating a three dimensional network. At some critical extent of the cross-linking reaction the material undergoes a phase transition from liquid to solid, a phenomenon which is called gelation. Because of the increasing use of thermosetting systems in polymer applications, there is considerable interest in elucidating the relationship between network formation and rheological properties. While the rheological behavior of the starting polymeric liquid and of the final tridimensional network are rather well understood, very little is known about linear viscoelastic properties at intermediate stages of the growing network structure. Further development and novel applications of reactive polymer processing largely depend on a thorough understanding of these properties and our the ability to model them.

The objective of this research is to understand the evolution of the linear viscoelastic properties of cross-linking polymers during the gelation transition and to formulate a constitutive equation which describes the rheological behavior <u>at</u> the gel point. Several processes may contribute to this transition besides the connection of molecular strands by chemical cross-linking: physical entanglements among the macromolecular strands, vitrification as the glass transition tempera-

ture rises with increasing extent of reaction, phase separation of the reaction components or products, and crystallization. This study is not concerned with gelation in its most general sense but specifically with the phase transition due to chemical cross-linking.

A polymer is said to be at the gel point (GP) if its steady shear viscosity is infinite and its equilibrium modulus is zero (Flory, 1953). The transition is understood to occur when at least one of the molecules of the cross-linking polymer has grown very large and has reached the dimensions of the macroscopic sample (Stauffer et al., 1982). At this stage (i.e. critical extent of reaction), an irreversible gel has been formed.

Branching theories based on combinatorial methods have been proposed to describe the phenomenon of gelation (Flory, 1941, 1953; Stockmayer, 1943, 1944; Gordon, 1962; Miller and Macosko, 1976, 1979). Newer models based on percolation theory have also been formulated (Stauffer, 1981; Stauffer et al., 1982). While the former approach does not take into account the effects of intramolecular reactions, the latter tends to overestimate them. Recently, a different model which considers gelation as a completely random process has been developed (Leung and Eichinger, 1984), and the effect of intramolecular reactions has been more realistically quantified (Shy and Eichinger, 1985; Shy et al., 1985). In the case of end-linking polymers, theoretical predictions agree reasonably well with classical determinations (e.g. spectroscopy, titration) of the critical extent of reaction, even though the universal character of the transition is still debated (Stauffer, 1981). Verification of these predictions with rheological measurements may not settle

the question of universality (Adam et al., 1981, 1985), but such experiments remain of the greatest interest in understanding the different stages of network formation (Bibbo and Valles, 1984).

There are presently two accepted methods for the rheological study of cross-linking polymers. In the first method (Lipshitz and Macosko, 1976; Castro, Macosko and Perry, 1984; Apicella, Masi and Nicolais, 1984), the polymer is subjected to shear flow while in its liquid state. The measured viscosity increases with increasing extent of reaction until the stress reaches the limit of the instrument or until the material breaks. For characterization beyond the gel point, the material is subjected to strain (or stress) and the steady state modulus (or compliance) is measured during its growth with increasing extent of reaction (Farris and Lee, 1983; Choy and Plazeck, to be published). Measurements in either the liquid state or the solid state give reliable data around GP. However the transition itself is defined by a singular behavior which is not accessible to these experiments except by extrapolation, as shown in Figure 1.1.

In the second method (Macosko and Mussatti, 1972; Tung and Dynes, 1982; Marin and Monge, 1984), the reacting mixture is subjected to small amplitude oscillatory shear deformations and the loss and storage moduli are recorded as a function of the extent of reaction. This method has the advantage of a continuous measurement of the viscoelastic properties as the polymer goes through the transition. However the data give no direct indication of the specific instant at which gelation occurs.

Neither of the two previous methods is able to give sufficient information concerning the rheological behavior at intermediate stages

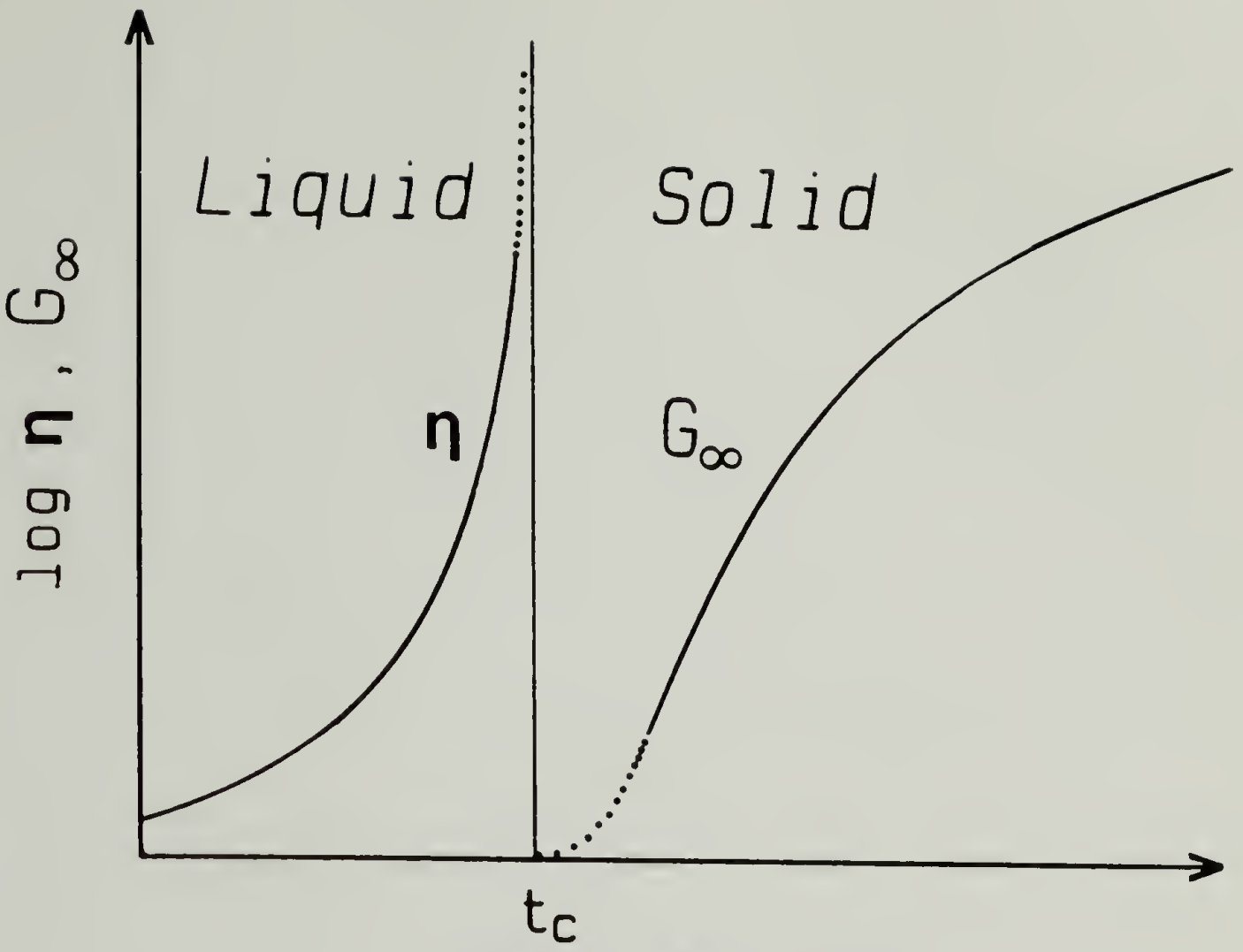

Figure 1.1. Schematic of steady shear viscosity and equilibrium modulus of a cross-linking polymer. No such experiments are possible in the close vicinity of the transition from liquid to solid.

of the cross-linking process. Only a few studies have been reported where such investigations were carried out (Valentine et al., 1968; Vinogradov, Gartsman and Garelik, 1974). These authors measured respectively the retardation spectrum and the loss and storage moduli of polybutadiene samples with various cross-link densities. But as Ferry (1980) pointed out, these results are subject to some reservations because of the discontinuous nature of the cross-linking process utilized. Even in these studies, data very close to and at the transition itself are missing.

Previously described rheological experiments give an indication of the increasing cross-link density without giving sufficient information to formulate constitutive equations. Problems arise from the fact that the stress in a cross-linking polymer is time dependent due to two different phenomena: the viscoelastic behavior in transient deformations, and the changing chemical composition as the network is forming with time. In this research, these two time dependencies have been separated and rheological data through the gelation process have been obtained.

For this purpose, two suitable cross-linking polymers, a polydimethylsiloxane and a polyurethane, have been selected. For these systems, gelation can be observed without the interference of any other phenomenon such as vitrification, phase separation or crystallization. Characterization of the components and material preparation are the topic of chapter two. The linear viscoelastic properties of the cross-linking polymers are measured at different stages of network formation. Two different techniques are used to successfully perform these measurements.

With the first cross-linking system, polydimethysiloxane, the curing reaction is stopped at chosen extents of reaction close to GP. The linear viscoelastic properties of the stable samples obtained are then recorded. Results of the measurements performed with balanced stoichiometry are presented in chapter three. Their analysis leads to the formulation of the Gel Equation, a constitutive equation for polymers at GP. In chapter four, this equation is generalized to describe the rheological behavior of gels formed with imbalanced stoichiometry.

With the second cross-linking system, polyurethane, the curing reaction is not stopped. Instead, the curing kinetics are kept very slow and the material can be regarded as stable during the time necessary for rheological characterization. Analysis of the results, given in chapter five, suggests universal validity of the gel equation.

In chapter six, rheological measurements are complemented by Fourier transform infrared (FTIR) and nuclear magnetic resonance (NMR) spectroscopy experiments which give respectively a measure of the extent of reaction and of the changes of chain mobility during network formation. The results are compared with the predictions of gelation theories.

Finally, concluding remarks and suggestions for future research in the field of cross-linking polymers at GP are presented in chapter seven.

CHAPTER II

MODEL POLYMERS

Two cross-linking polymers were chosen for this study, a cross-linking polydimethylsiloxane (PDMS) and a cross-linking polyurethane (PU). Both systems are known to produce elastomeric networks with very well defined structural characteristics (i.e. model networks) which are formed by end-linking primary chains in very specific chemical reactions (Mark and Sullivan, 1977; Valles and Macosko, 1981; Mark, 1982; Meyers, Bye and Merill, 1980; Sung and Mark, 1981; Mark, 1982; Feger et al., 1984). The two systems, however, involve different cross-linking processes and have different functionalities. The characteristics of the systems, the purification of their components, and the materials' preparation are given in this chapter.

2.1 Cross-linking PDMS

PDMS networks were prepared by the hydrosilation reaction of tetrakis(dimethylsiloxy)silane and α,ω-divinyl terminated linear PDMS prepolymer in the presence of cis-dichlorobis(diethylsulfide)platinum (II) catalyst. The structural formulas of these compounds are shown in Figure 2.1. This system was suggested by the previous work of Valles and Macosko (1979). It was chosen for its well defined chemical nature, the need of catalysis, the availability of prepolymers with different

a)

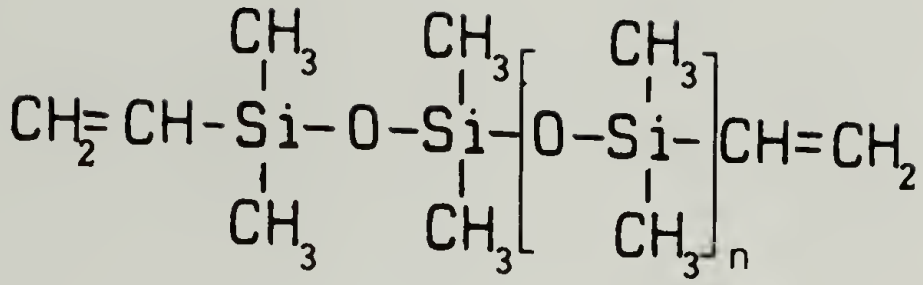

b)

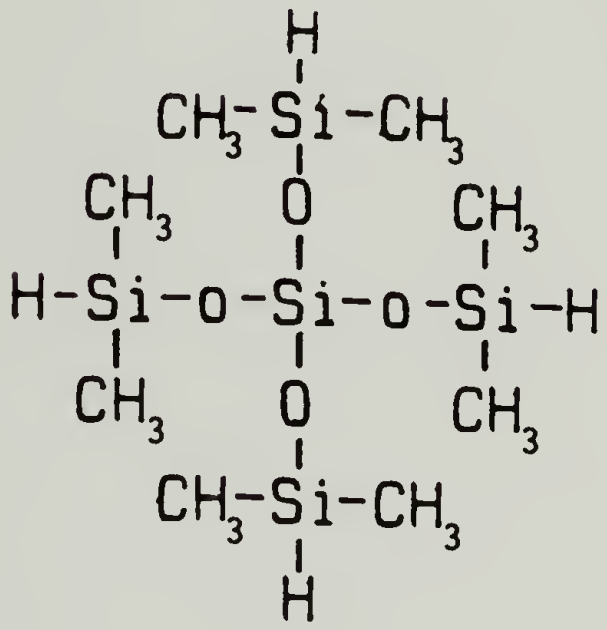

c)

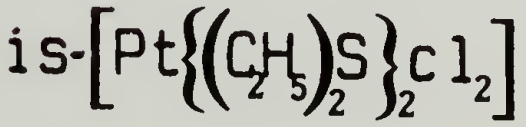

Figure 2.1. PDMS system: a) α,ω-divinyl terminated linear PDMS;b) tetrakis-(dimethylsiloxy)silane; c)cis-dichlorobis(diethylsulfide)platinum(II);

molecular weights, and the elastomeric nature of the samples after cross-linking.

2.1.1 Prepolymer

The prepolymer was purchased from Petrarch System Inc. A molecular weight below the entanglement limit for PDMS was chosen. Prior to use the prepolymer was filtered and held for 12 hours at 140°C under high vacuum. About 1.1 wt% low molecular weight volatiles were removed in this process. This amount corresponded to the expected 1 to 2 wt% low molecular weight cyclics, primarily siloxane octamer (D_8), claimed by Petrarch to be present.

The number average molecular weight, $\bar{M}_n$, and the molecular weight distribution, $\bar{M}_w/\bar{M}_n$, were measured by vapor pressure osmometry (VPO) and gel permeation chromatography (GPC). The results of these measurements are summarized in Table 2.1. Their accuracy is expected to be ±20%.

End group analysis was performed at Monsanto Chemical Co.in collaboration with Dr. S. Curran. The vinyl concentration was determined by HNMR using deuterated chloroform as solvent and toluene as an internal standard at a concentration of 1.32×10^{-4} mole toluene/g PDMS. Double precision data acquisition mode was employed for improved accuracy. The vinyl concentration was determined by direct proportionality to the ratio of the peak areas corresponding to the vinyl and the methyl groups respectively, as shown in Figure 2.2. The vinyl concentration was found to be 1.58×10^{-4} mole vinyl/g PDMS with a precision of ±3%. The presence of silanol end groups (instead of vinyl) was

Table 2.1. Molecular weight of α,ω-divinyl terminated PDMS prepolymer

Technique	$\bar{M}_n$	$\bar{M}_w$	$\bar{M}_w/\bar{M}_n$
VPO	10300		
GPC in chloroform Polystyrene standards	12060	23312	1.93
GPC in toluene Universal calibration	14860	33566	2.26

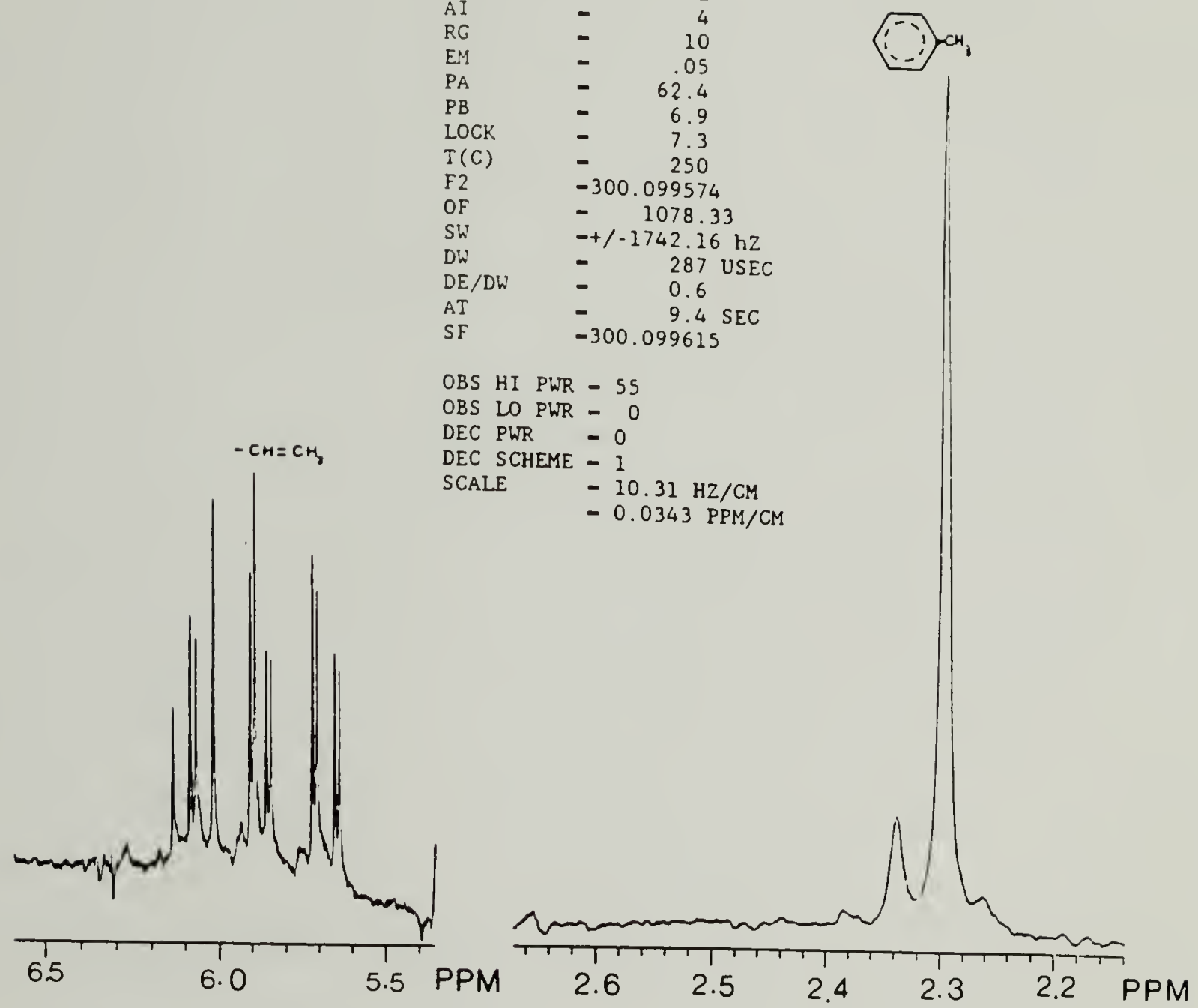

Figure 2.2. End group analysis of PDMS prepolymer by HNMR.

checked by Si_{29}NMR on a mixture of PDMS prepolymer and deuterated chloroform. Such end groups were not detected, but it should be mentioned that the technique employed is not sensitive at very low concentrations (i.e. below 5%). As a result, if a vinyl functionality of 2 is assumed, the NMR measurement indicates $\tilde{M}_n$=12658 which is in relatively good agreement with the GPC measurements.

2.1.2 Cross-linker

The cross-linker was purchased from Petrarch System Inc. It was distilled prior to use with a Perkin Elmer spinning band column. The pressure in the column was set at 7mm of Hg. The temperatures of the pot and of the head were 80°C and 68°C respectively. The distillation process was monitored by parallel determination of the purity of each cut. Gas-liquid chromatograpy (GC) was used for these latter measurements using a 10% OV101 column and an oven temperature of 150°C. After distillation, the cross-linker was obtained with a purity higher than 99.99% as determined by GC. The chromatograms before and after distillation are shown in Figure 2.3. After purification, the cross-linker was stored in a Schlank type storage flask under nitrogen.

The functionality of the distilled cross-linker was measured by Si_{29}NMR on a neat sample. A peak due to the glass tube should appear at the same shift as the peak of the tetrahedral silicone structure at -105ppm. This peak was suppressed by the Hahn spin echo effect as shown in Figure 2.4. The number of silane groups was directly determined by the ratio of the peak areas at -5ppm and -105ppm respectively. A func-

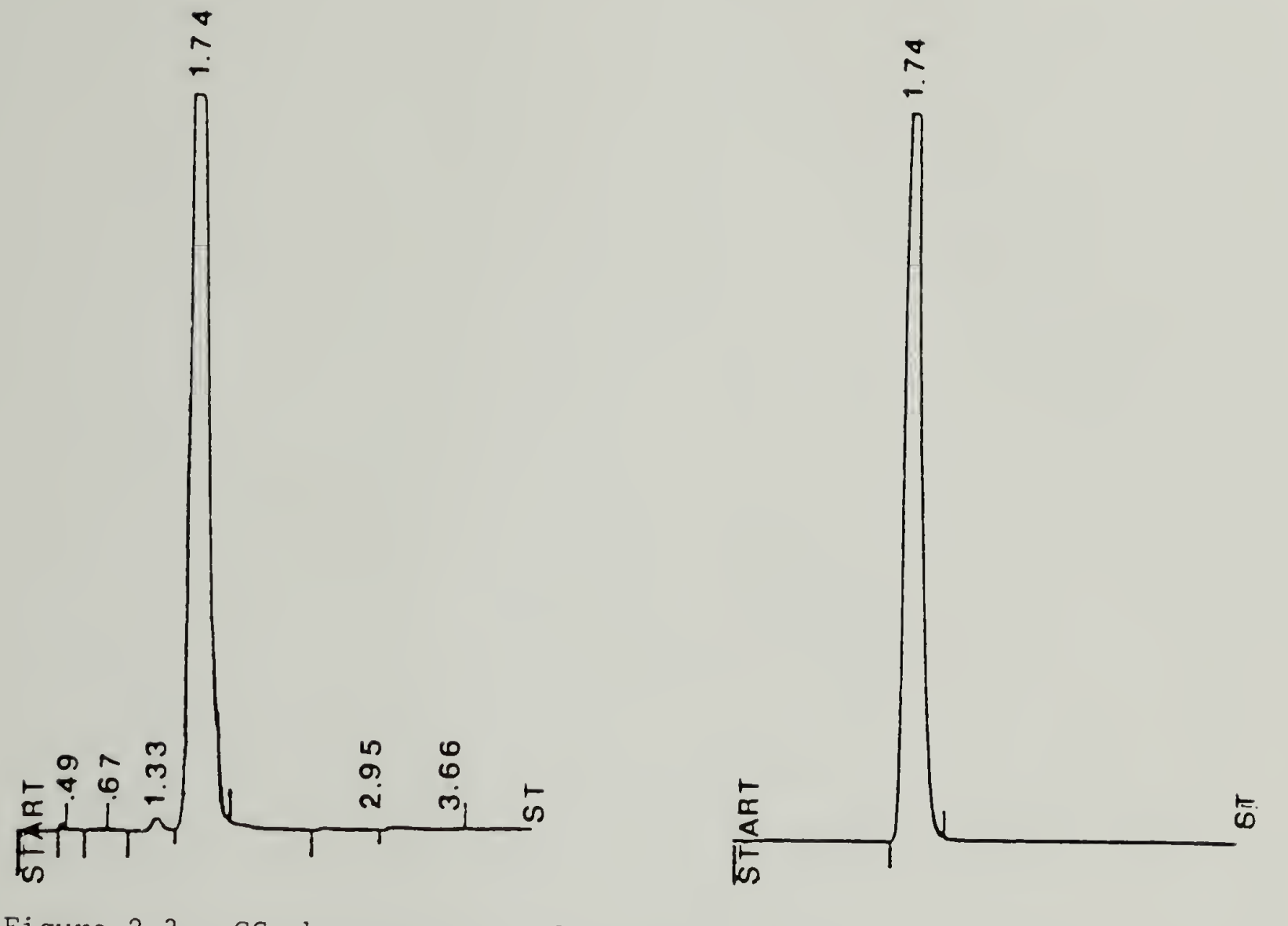

Figure 2.3. GC chromatograms of the cross-linker: a) before distillation; b) after distillation.

CROSSLINKER/GLASS SUPRESSED BY
HAHN ECHO

GARED DECOUPLER/HAHN SPIN ECHO

P2	=	46.25 USEC
P4	=	92.50 USEC
D5	=	200.00 SEC
L1	=	63
NA	=	290
SIZE	=	16384
ADC	=	12
AI	=	9
RG	=	10
SW	=	+/-7142.84 HZ
DW	=	70 USEC
DE/DW	=	60
AT	=	573.44 MSEC
F2	=	-300.099906
OF	=	-2700.16
SF	=	59.618446
EM	=	2.00
PA	=	326.5
PB	=	180.3
LOCK	=	7.3

OBS HI PWR = 60
OBS LO PWR = 100
DEC PWR = 63
DEC SCHEME = 1
SCALE = 420.16 HZ/CM
= 7.0476 PPM/CM

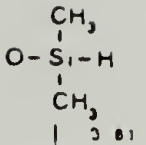

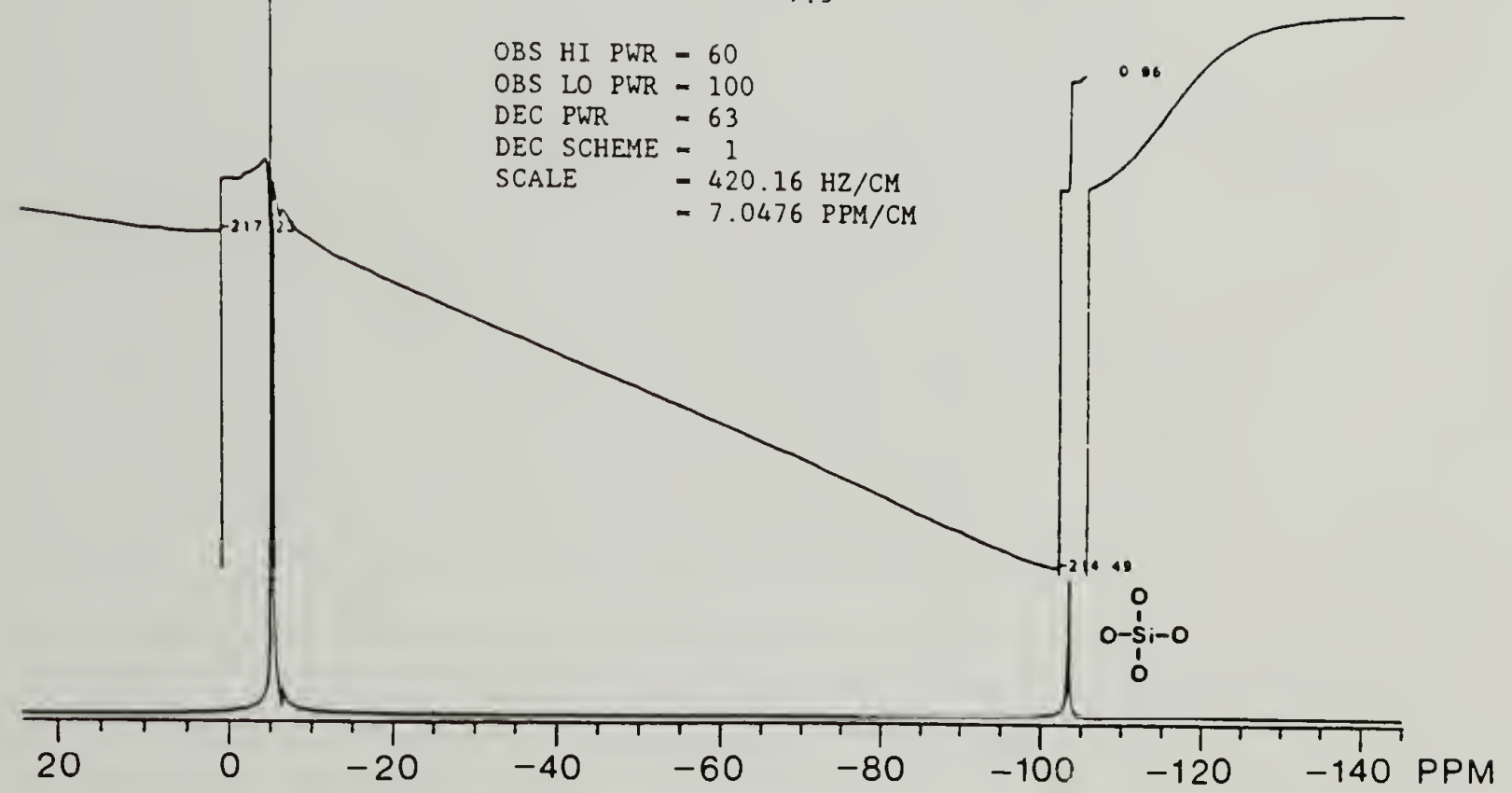

Figure 2.4. End group analysis of tetrakis(dimethylsiloxy)silane cross-linker by Si_{29} NMR.

tionality of 3.97 was found which is very close to the ideal value of 4.

2.1.3 Catalyst

The cis-dichlorobis(diethylsulfide)platinum(II) catalyst was synthesized by closely following the procedure of Kauffman and Cowan (1960) but with one third of the amount of starting material they use (i.e. 1.38g of potassium tetrachloride and 1.20g of distilled diethyl sulfide). The cis isomer was obtained in high purity after four successive recrystallizations. Its measured melting point after air-drying overnight was found to be 104°C instead of 107°C as reported by Kauffman and Cowan.

Following synthesis, the yellowish crystals of the platinum compound were dissolved in distilled, dry toluene. The catalyst was prepared in the form of a 1.8×10^{-3} molar solution of platinum in toluene and stored under nitrogen.

2.1.4 Material Preparation

Small size batches, typically 15g of PDMS, were mixed at room temperature in a nitrogen atmosphere to prevent moisture absorption (Macosko and Benjamin, 1981; Fisher and Gottlieb, 1986). The PDMS prepolymer was first mixed with the catalyst for one hour and degassed for ten minutes. The cross-linker was then added in controlled amounts, and the mixture was stirred for ten to fifteen additional minutes and again degassed for two minutes. The volumes of catalyst and cross-

linker were added using a 1ml gas tight Hamilton syringe. The stoichiometric ratio of the reactants, r= [silane]/[vinyl], was adjusted using the results of the NMR end group analysis. The platinum concentration, 5.32×10^{-5} and 7.6×10^{-5} mole Pt/mole vinyl for the samples with balanced and imbalanced stoichiometries respectively, was chosen to be the minimum level needed to reach the highest final modulus with the slowest possible kinetics. The amount of toluene (from the catalyst) incorporated into the reactants was less than 0.7 wt%, most of which is expected to leave during the first degassing operation.

After mixing the reactants, the preparation was placed into several small containers which were stored in liquid nitrogen. A glove bag with a nitrogen atmosphere was used for the transfer operation. By using this procedure, samples from the same batch and therefore with the same composition could be kept for several days and used for different experiments.

2.1.5 Catalyst Poisoning

Valles and Macosko (1979) reported that traces of elemental sulfur poison the catalyst almost instantaneously. This effect can be used to stop the hydrosilation reaction at chosen stages of the cross-linking process. Other compounds are also known to annihilate the platinum catalyst very efficiently, among them dimethylformamide (DMF) and tetramethylethylenediamine (TMEDA). Both sulfur and TMEDA were used in this study.

Elemental sulfur was used for the experiments at balanced stoichiometry. In these experiments the hydrosylation reaction was stopped before and after the gel point by using a sulfur solution in toluene. Toluene, a good solvent for PDMS, enabled the diffusion of sulfur molecules throughout the polymeric material. In order to minimize the amount of toluene introduced into the samples a concentrated sulfur solution, 0.33 molar, was prepared. Samples 25mm in diameter and about 0.6mm thickness were used. The sample thickness was optimized to obtain the most efficient poisoning conditions along with accurate rheological measurements. The hydrosilation reaction was stopped at chosen extent of the cross-linking reaction by spraying the poisonning solution on the surface of the samples. The molar ratio of sulfur to platinum utilized was less than 1000 and the amount of toluene introduced into the samples was less than 2 wt%. Details of the poisoning procedure as well as measurements demonstrating the efficiency of the process and the properties of the samples after poisoning are presented in chapter three, sections 3.3.1 and 3.3.2.

In the experiments at imbalanced stoichiometry, TMEDA was used instead of sulfur. There were several reasons for changing the poison compound and for chosing TMEDA. First, TMEDA has two electron donor sites (i.e. bidentate ligand) instead of one for sulfur (i.e. monodentate ligand) and will therefore deactivate the platinum catalyst more efficiently (Cotton and Wilkinson, 1972). Secondly, TMEDA is a liquid at room temperature and will diffuse more easily than sulfur through the polymeric material. Finally, the presence of small sulfur aggregates in

the samples after poisoning was incompatible with light scattering experiments which will be done in a future study.

TMEDA (Aldrich Chemical Co.) was prepared in the form of a 0.6 molar solution in toluene. The samples used were of the same shape as those previously described, and the molar ratio of TMEDA to platinum employed was also about 1000. Measurements presented in sections 3.3.1 and 4.1 indicate that the cross-linking reaction stops immediately after poisoning. The type of measurements performed, however, did not clearly demonstrate whether TMEDA is a more effective poison than sulfur.

Several other methods for stopping the cross-linking reaction were considered: thermal quenching of the system while cross-linking, changing the stoichiometric ratio of the reactants, and end-capping all the functional groups.

For the first method the cross-linking process is 'frozen' at different stages of the developing network by a drastic reduction of molecular mobility. For this technique to be successful, temperatures close to the glass transition of the already formed network structure must be used. Under these conditions, measurements presented in chapter five of this research indicate that vitrification will interfere with gelation which is inadequate for the study of gelation as an independent phenomenon. In addition, thermal quenching of the reactants would not allow the use of time-temperature superposition (Ferry, 1980) which would make the determination of rheological functions over wide ranges of time or frequency impossible. Finally, in the particular case of the PDMS system, crystallization will occur, independently of the cross-link

density, well before vitrification. As a result, at the low temperatures required for sufficiently decreasing the reaction rate, unacceptable interference from crystallization is to be expected.

The second method (i.e. changing the stoichiometric ratio of the reactants) is not suitable either. The intermediate stages (i.e. gel state, Adam et al., 1985) of the developing network at balanced stoichiometry cannot even be approximated by a simple change of the stoichiometric ratio. This is clearly shown by the measurements presented in chapters four and five of this study. Finally, with the third method (i.e. end-capping all the functional groups), strong disturbances of the already formed network structure have to be expected.

Poisoning the catalyst only required the introduction of a small number of foreign molecules into the samples, which can be done rapidly and without altering the network structure. By contrast, end-capping all the functional groups with a liquid compound would require longer diffusion times and would result in inhomogeneous samples. An alternative would be to use a pressurized gas. Sulfide gas (i.e. hydrogen sulfide) would probably be suitable to stop the hydrosilation reaction. Its use, however, would require cumbersome safety precautions and this possibility was not given further consideration.

2.2 Cross-linking PU

The constituents of the system are α,ω-dihydroxypoly(propylene oxide) (PPO) of nominal molecular weights 425, 1000, 2000 and tris(4-isocyanatophenyl)thiophosphate (DRF) for which structural formulas are

a)

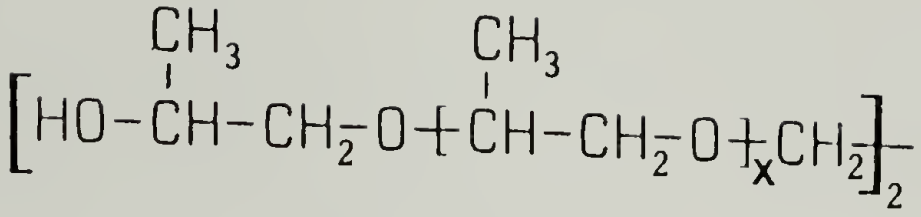

b)

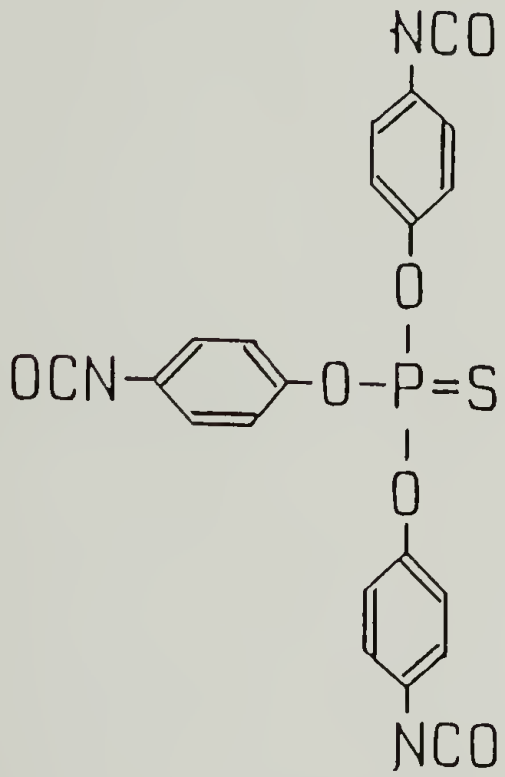

Figure 2.5. PU system: a) α,ω-dihydroxypoly(propylene oxide) (PPO); b) tris(4-isocyanatophenyl)thiophosphate (DRF).

shown in Figure 2.5. Advantages of this system are that: 1) the initial compounds are well characterized and can be readily obtained with a high degree of purity; 2) the linear PPO component is available at different molecular weights with narrow polydispersity; 2) the well defined chemistry of the cross-linking process (Feger et al., 1984; Feger and MacKnight, 1985) makes it possible to form nearly perfect networks and; 3) the reaction kinetics at room temperature are slow.

This system was suggested by the previous work of Feger and MacKnight (1984, 1985). In this research the purification of the compounds and the materials' preparation were carried out by Pr. Z.S. Petrovic and Dr. P. Morganelli for the networks at balanced stoichiometry and imbalanced stoichiometry respectively. Details of the procedure employed for these syntheses are given in the following two sections.

2.2.1 Components Characterization

The PPO prepolymers (Aldrich Chemical Co.) were dried prior to use by preparing a 50% (v/v) solution in benzene and distilling the benzene-water azeotrope. Residual benzene was removed under vacuum with mild heating (temperatures less than 90°C to avoid PPO oxidation). The water content, measured by Karl Fisher titration, was found to be 0.024$\pm$.002%.

The number average molecular weights and the molecular weight distributions were measured (Petrovic and MacKnight, personal communication) by VPO and GPC. The hydroxyl content was determined by an acetyl chloride titration method. In all three systems, the PPO prepolymers

were found to be quasi-monodisperse ($\bar{M}_w/\bar{M}_n<1.02$) and their functionality was very close to 2 as shown in Table 2.2.

The triisocyanate crosslinker was obtained as a 20% solution in methylene chloride (Mobay Chemical Co., Desmodur DRF). Approximately 100ml of the yellow solution was concentrated in a flask, under reduced pressure, to one-half to one-third of the original volume. The flask was stored for one to two days at 4°C, in a dessicator, to begin crystallization. The flask was then placed at -18°C for three additional days to allow further crystallization. The yellow solution was decanted and the triisocyanate was then recrystallized by dissolving in a minimum amount of dry benzene and allowing the solution to stand at 4°C for two to three days. Finally, the crystals were isolated by decanting, dissolved in dry benzene, and freeze dried. The isocyanate purity was 97-98% as determined by titration (ASTM D 1638-74).

2.2.2 Material Preparation

The reaction mixtures were prepared under nitrogen in a glove box. The diol and the triisocyanate were weighed into a reaction vessel to achieve the desired stoichiometry. The vessel was then sealed and degassed on a vacuum line. The reactants were mixed at 90°C with magnetic stirring until a clear colorless solution was obtained. Higher temperatures are unsuitable due to the risk of allophanate formation and carbodiimide formation (Odian, 1981). The mixture was vented with nitrogen after five to fifteen minutes and a sample was quickly trans-

Table 2.2. α,ω-Dihydroxypoly (propylene oxides) (PPO) characterization

Polymer	$\bar{M}_n$ (GPC)	$\bar{M}_w/\bar{M}_n$ (GPC)	Functionality (Titration)
PPO425	454	1.013	1.93
PPO1000	965	1.007	1.88
PPO2000	2018	1.006	1.94

ferred to the rheometer where curing was allowed at 30°C under a nitrogen atmosphere. The remaining mixture was transferred to dry vials and stored in liquid nitrogen.

CHAPTER III

LINEAR VISCOELASTIC PROPERTIES OF CROSS-LINKING PDMS DURING NETWORK FORMATION - BALANCED STOICHIOMETRY

A method is presented to stop the cross-linking reaction of PDMS networks at intermediate stages of the curing process. The developing network is represented by a discrete set of samples with increasing extent of reaction and the linear viscoelastic properties of these samples are measured. Experiments performed through the gel transition clearly indicate how GP is approached and passed during the nework formation. Rheological data very near GP are analyzed. Results of this analysis lead to the formulation of a constitutive equation for cross-linking polymers, with balanced stoichiometry, at GP.

3.1 Rheological Test of the Stoichiometry

The stoichiometric ratio, r, of the PDMS system is defined here as the ratio of silane to vinyl groups. For non-stoichiometric systems, most of the structural irregularities obtained at complete conversion of the least abundant functional groups are, in addition of the inner loops, dangling ends. Networks with such imperfections have a lower number of elastically active macromolecular strands and therefore exhibit a lower elasticity (Treolar, 1975).

Computer simulations of end-linked elastomers in bulk (Leung and

Eichinger, 1984) show that even when loop formation is accounted for, the most perfect networks are always obtained at balanced stoichiometry. However, it has often been observed that the maximum elasticity of the final network does not occur at balanced stoichiometry, but instead at stoichiometric ratios slightly higher than unity (Macosko and Benjamin, 1981; Macosko and Saam, 1985). Several explanations can account for this discrepancy. Among the most credible is the fact that computer simulations fail to take into account both side reactions leading to an increased number of dangling ends, and reactants with imperfect functionality (i.e. PDMS chains with only one vinyl group).

The stoichiometric ratio corresponding to the maximum elasticity, but not to chemical stoichiometry, has been called effective stoichiometry, r_e, (Macosko and Saam, 1985). This definition of stoichiometry is adopted in the present study. In the following, balanced stoichiometry will always stand for the composition which leads to the final network with the highest elasticity.

In order to determine the composition corresponding to the balanced stoichiometry for the PDMS system, a set of networks with increasing silane concentration was synthesized by following the procedure described in section 2.1.4. After mixing, the liquid samples were transferred to the rheometer, a Rheometrics Dynamic Mechanical Spectrometer. Reaction between the 25mm diameter parallel disks was allowed to take place overnight at 34°C followed by two additional hours at 130°C. A nitrogen atmosphere was used for the first stage of the curing process. The dynamic storage modulus, G′, of the fully cured samples was

measured at low frequency, ω_0=0.5 rad/s, and small shear strain amplitude, γ=0.01. The frequency was chosen to be sufficiently low to fall well within the terminal plateau region of the cross-linked elastomers. As a result the value of the modulus measured is close to the equilibrium modulus of the network and is directly representative of its elasticity. Results of these measurements are shown in Figure 3.1.

A maximum of the storage modulus is observed at r close to 1.3 instead of the ideal value of 1. Similar observations with the hydrosilation reaction have recently been reported, however with a different prepolymer (Macosko and Saam, 1985). Possible causes for such a deviation have been mentioned earlier and will be discussed in more detail in chapter six. For the moment we limit ourselves to remark that even though the PDMS system is well purified and well characterized it is not ideal, and that the balanced stoichiometry of this system occurs at $r_e \simeq 1.3$.

It is unfortunate, however, that the tangent of the phase angle, tanδ, could not be measured with sufficient accuracy on the fully cured networks (e.g. tn$\delta < 10^{-2}$ outside the limit of resolution of the rheometer). Since tanδ is a direct measure of the dampening in the material it should exhibit a minimum for the most perfect network. It would have been informative to see whether the network with the highest elasticity, $r=r_e$, is also the most perfect one.

It is equally interesting to note the asymetric shape of the curve of the storage modulus shown in Figure 3.1. Networks with $r \simeq 1.2$ and $r \simeq 1.6$ exhibit approximately the same elasticity. This observation is in complete agreement with the results of the computer simulations made by

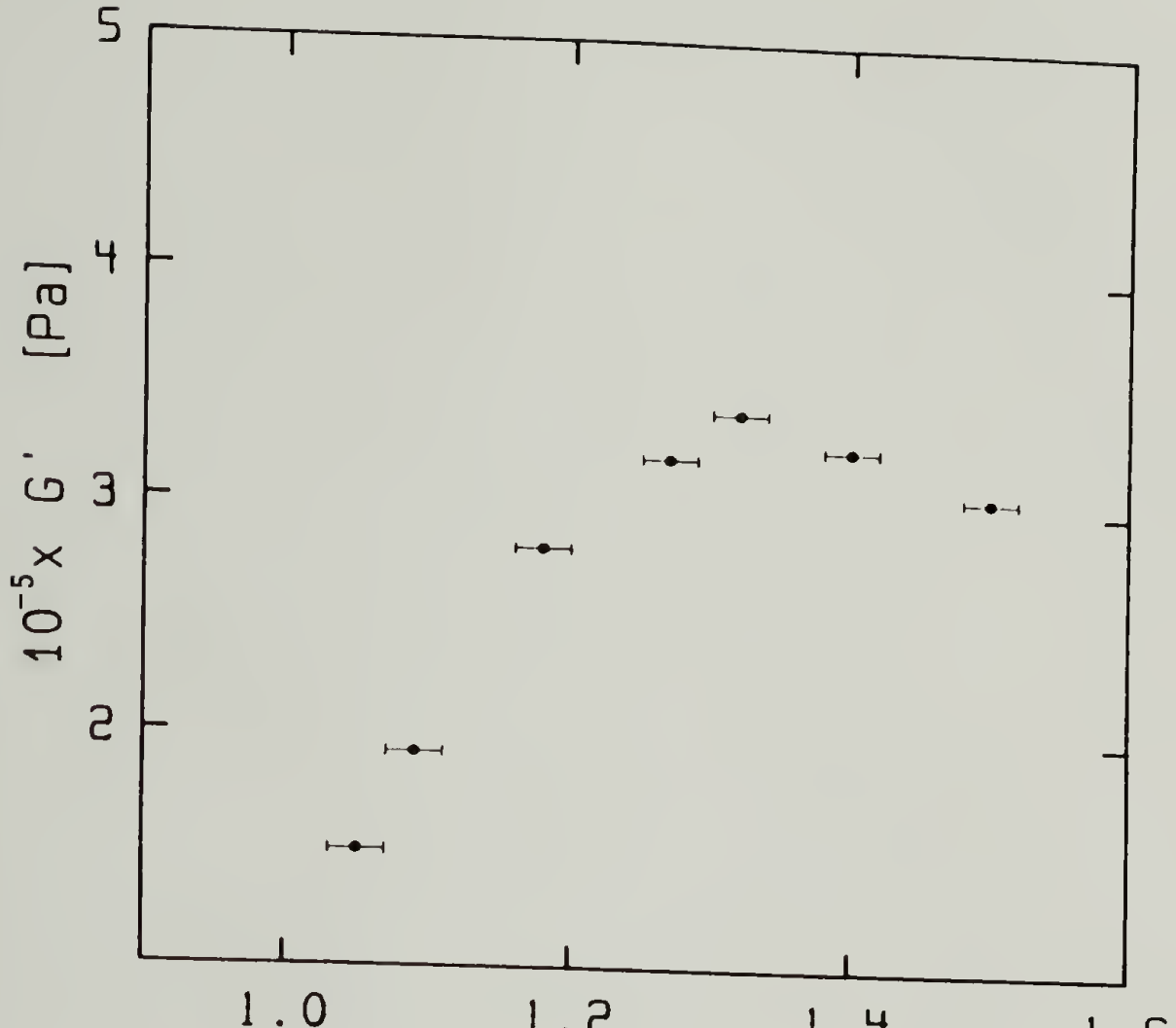

Figure 3.1. Storage modulus, G', of fully cured PDMS samples as a function of the stoichiometric ratio, r, at T=34°C and ω_0=0.5rad/s.

Leung and Eichinger (1984) on a similar system. These authors mentioned that cross-link deficient mixtures would produce less effective elastic networks than those using excess cross-linker. In addition, they calculated that networks 10% deficient in silane groups exhibit the same degree of perfection than those with 30% excess silane groups with respect to stoichiometry. This prediction is quantatively verified here if it is assumed that structural perfection and network elasticity are equivalent quantities.

3.2 Rheology of the Curing Material

PDMS samples with balanced stoichiometry, r=1.32±0.05, were prepared by following the procedure described in section 2.1.4. All the samples were removed from liquid nitrogen prior to use, and reacted isothermally at 34°C. The time elapsed between thawing and starting the isothermal reaction was kept constant in all cases. A nitrogen atmosphere was used to prevent moisture absorption. In this section the samples were used to record the evolution of the dynamic storage, $G'(\omega_0,t)$, and loss, $G''(\omega_0,t)$, shear moduli during the cross-linking reaction. All the mechanical measurements were performed with a Rheometrics Dynamic Mechanical Spectrometer using 25mm parallel disk geometry and a medium range transducer with a maximum torque of 2000 grams force cm. The cone and plate geometry could not be used because of the slight volume change occuring during the reaction. This shrinkage gives rise to an extra normal force which was corrected by readjusting the gap

when needed. All the measurements were carried out within the range of linear viscoelasticity.

The change in dynamic storage and loss moduli during isothermal cure is shown in Figure 3.2. In a typical curing curve, the viscous behavior of the oligomeric starting material dominates the initial part of the experiment. The loss modulus is large while the storage modulus is still negligible. With increasing molecular weight, the storage modulus rises sharply until it intersects and then exceeds the loss modulus. The storage modulus keeps increasing with increasing cross-link density while the loss modulus goes through a slight maximum. Both moduli level off as the reaction comes to completion.

The frequency of oscillation, ω_0, was chosen as low as possible to minimize the disturbances imposed on the developing network. By continuously decreasing the shear strain amplitude from 2.0 to 0.0005 the increase of the linear viscoelastic material properties was accurately followed over six decades in modulus. Continuous readjustment of the strain level was needed so that the deformation remained within the range of linear viscoelasticity at each step of the developing network and that the torque level stayed sufficiently high to be accurately measured (i.e. above 2 grams force cm).

Samples from the same batch have the same history. As a result,the curing curves obtained were extremely reproducible. Shifts of less than $\pm$1 minute were observed from one sample to another as long as the flow histories imposed during the cross-linking reaction were sufficiently similar. Because of the well defined procedure employed during the sample preparation and because of the high purity of the reactants,

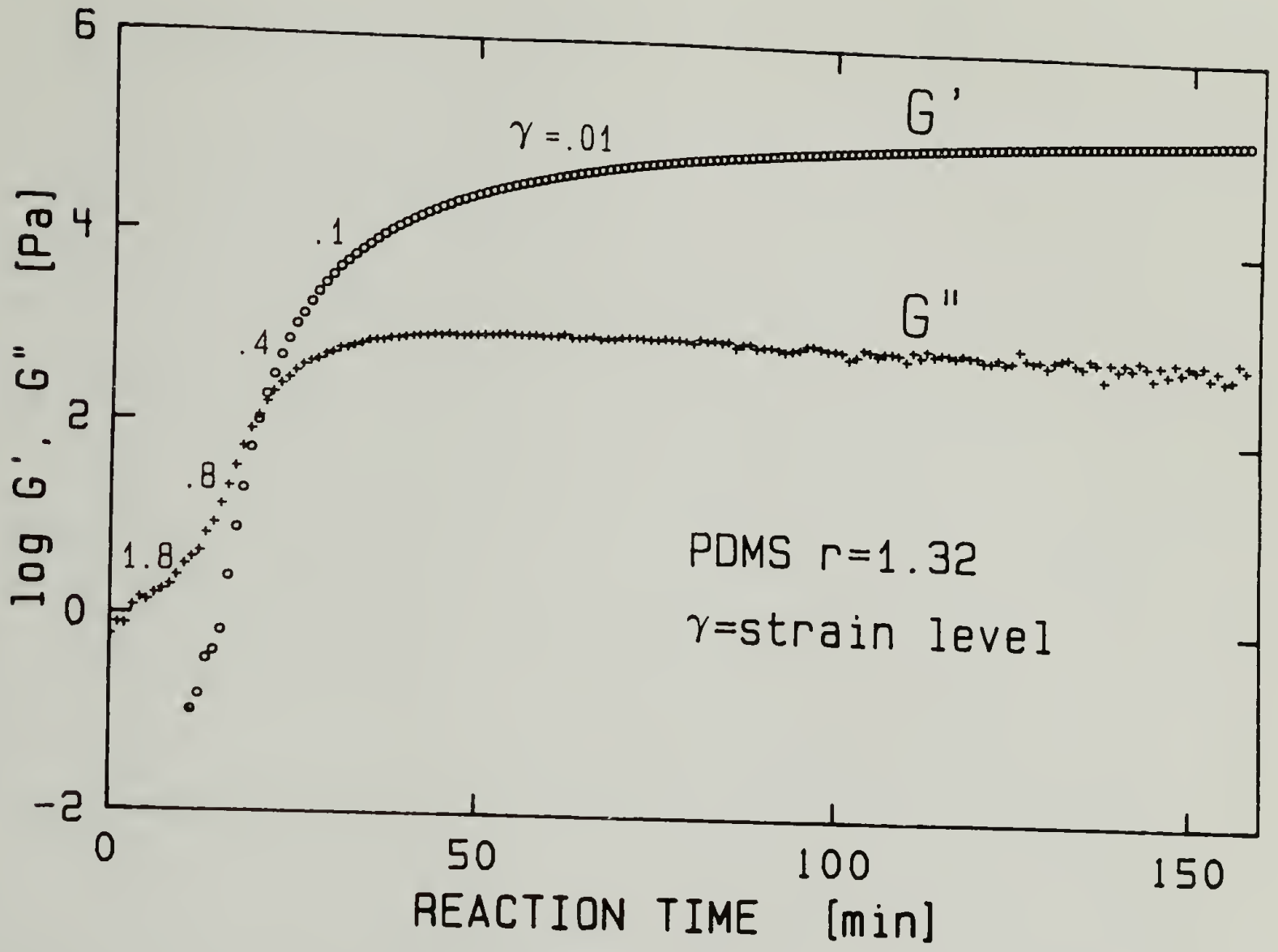

Figure 3.2. Curing curve of PDMS with balanced stoichiometry, in an oscillatory shear experiment at constant temperature, T=34°C, and constant frequency, ω_0=0.5rad/s. t=0 marks the beginning of the rheological measurement but not the beginning of the crosslinking process. The strain level, γ, is continuously decreased as the material solidifies.

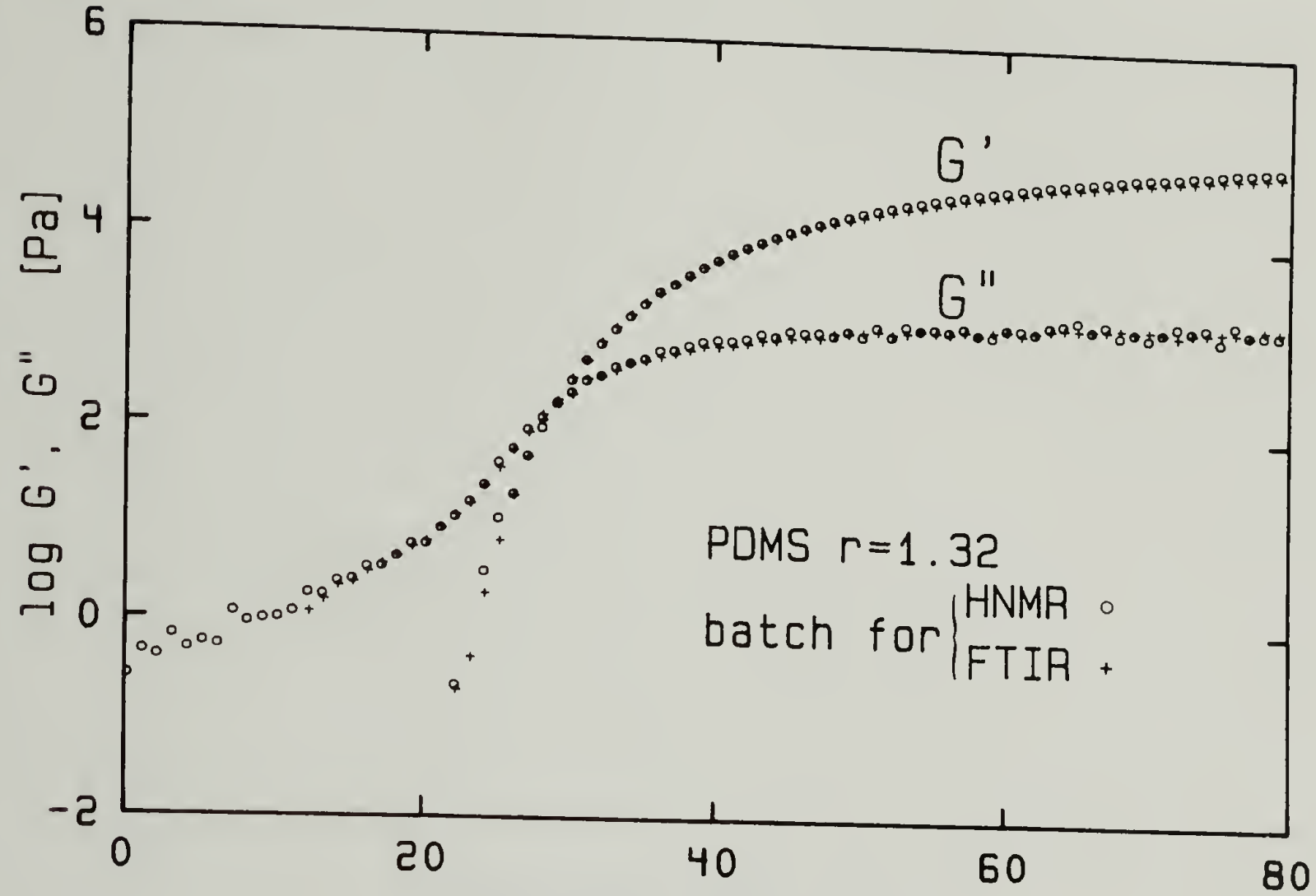

Figure 3.3. Curing curve of PDMS with balanced stoichiometry, at T=34°C and ω_0=0.5rad/s. Reproducibility of the curing kinetics with two samples from a different batch

a very high reproducibility from batch to batch was also obtained as shown in Figure 3.3. Such reproducible reaction kinetics will be of prime interest for future experiments.

3.3 Rheology at Different Stages of Network Formation

The curing curves previously presented give an indication of the increasing cross-link density and allow for a continuous measurement of the viscoelastic properties as the polymer goes through GP. The data, however, give no indication of the rheological behavior of the transient states of the developing network nor of the specific instant at which the transition occurs. In order to obtain more detailed information, the cross-linking reaction must be stopped. This procedure is now presented.

3.3.1 Stopping the Cross-linking Reaction in the Rheometer

Samples which are stable, homogeneous and representative of the intermediate stages of the developing network need to be obtained. A very effective way to achieve this goal was discussed in section 2.1.5, namely the poisoning of the catalyst with a solution of elemental sulfur in toluene. An easy way to stop the cross-linking reaction would be to immerse the cross-linking samples in the poisoning solution when an intermediate state needs to be conserved. However, even close to GP,such a procedure would lead to partial loss of the sol fraction in the incompletely cured material and also to samples of inadequate shape

for accurate rheological measurements. It was found that samples close to the gel point were extremely sticky and could hardly be manipulated without being overstretched. As a result, a method had to be used where the samples could be prepared with the exact disk-like shape needed to fit in the rheomoter. Ideally the samples had to be prepared in the rheometer itself.

The simple procedure shown in Figure 3.4 was developed for this purpose. A removable cup was mounted around the bottom plate of the rheometer. The height of the edge above the plate's surface could be adjusted to the exact value required for the sample thickness (typically 0.7mm) by simply sliding the cup along the plate. The liquid sample was then poured into the gap formed by the surface of the plate and the edge of the cup and was allowed to react in a nitrogen atmosphere. At this stage, the top plate of the rheometer was left well above the free surface of the sample. The cup was required to obtain a sample with a flat free surface. Without the cup a meniscus would form which would be undesirable for rheological experiments. It is important to note that the samples were reacted in a quiescent state. At chosen times on the curing curve, Figure 3.3, the reaction was stopped by spraying about $3x10^{-2}$ cc of the 0.33 molar sulfur solution in toluene (i.e. one or two sprays with a small atomizer). Details of the chemical composition of the samples and of the poisoning solution employed are reported in chapter 2. With this procedure, a good distribution of the sulfur solution on the sample surface was obtained and a minimum amount of solvent was needed. Immediately after spraying the sulfur solution, the cup was slided down along the bottom plate of the rheometer and the

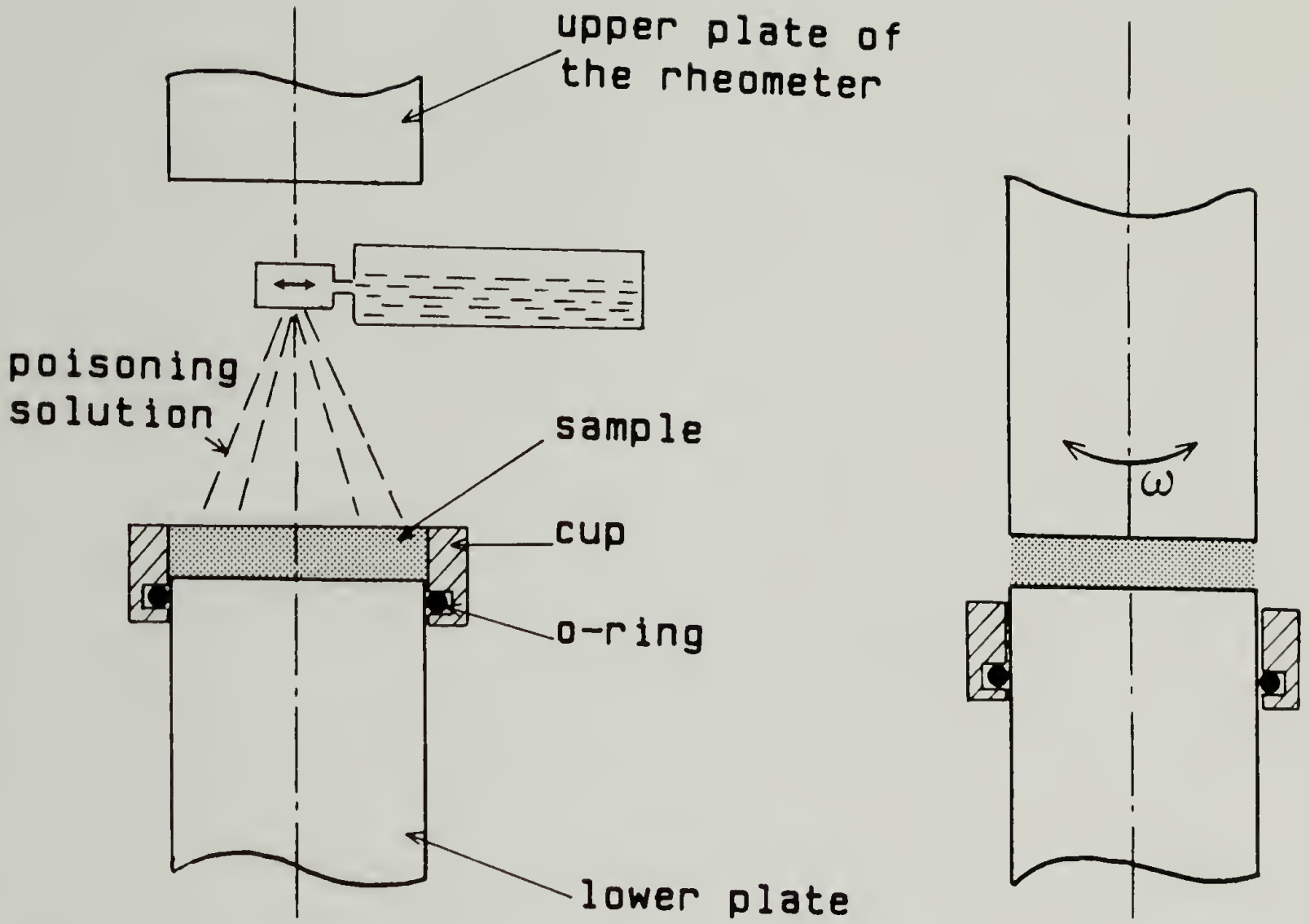

Figure 3.4. Schematic of the poisoning procedure: a) before poisoning, the sample is allowed to cure at rest without touching the upper plate; b) after poisoning, the cup is lowered and the upper plate is positioned.

upper plate was positioned as shown in Figure 3.4. At this point, rheological measurements could be started.

About two to three minutes were necessary between the poisoning time and the first measurement. However in all the cases studied, this elapsed time was sufficient to obtain completely stopped reactions with stabilized values of the loss and storage moduli as shown in Figure 3.5. Prior to further rheological characterization, the poisoned samples were heated for two hours at 120°C in order to attempt to boil the slight amount of toluene introduced during the poisoning process. After cooling down to 34°C slight decreases of G" were often observed while G' did not change noticeably. It was difficult to determine with certainty whether these slight variations of G" were caused by a loss of toluene even though this appears to be the most consistent explanation. At all stages of the cross-linking process, the samples obtained after poisoning were stable, homogeneous, and representative of the actual network structure as will be shown in the next section.

3.3.2 Rheology of the Stopped Samples

From earlier experiments, Tung and Dynes (1982) suggested that the time of intersection of $G'(\omega_0,t)$ and $G''(\omega_0,t)$ on the curing curve, (see Figure 3.3), marks the time of gelation. However, they report that the time of intersection was found to be a function of the frequency of the oscillatory shear experiment. This could indicate that the time of intersection might be close to but not identical with the transition time. The instant of the transition must be strictly material dependent

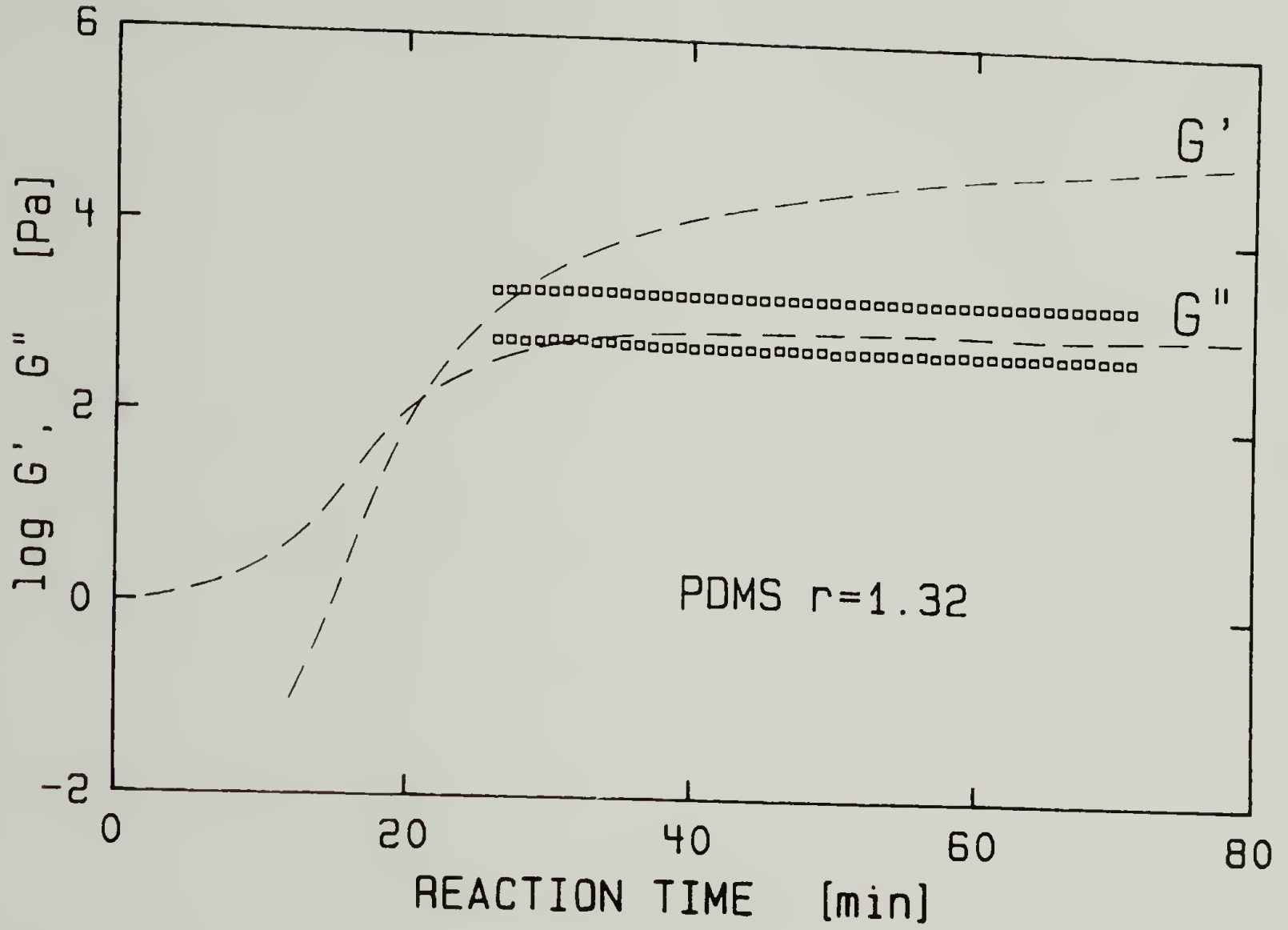

Figure 3.5. Stability of the storage modulus,G', and the loss modulus, G", after poisoning of the catalyst with sulfur. The dashed lines represent the regular curing curve.

and cannot depend on the frequency of the rheological test unless there are other masking effects such as influence of flow on the chemical reaction or interference of a second phenomenon such as vitrification.

In order to obtain complementary information, the cross-linking reaction of the PDMS was stopped according to the previously described procedure at different times, t_i, on the curing curve close to the intersection of $G'(\omega_0,t)$ and $G''(\omega_0,t)$. As represented by the dark squares in Figure 3.6, the dynamic loss and stotage moduli of the partially reacted samples superimposed very well upon the data measured on the continuously curing samples. The instant of poisoning and the instant of superimposition on the curing curve were always the same within two to three minutes which is about the limit of the reproducibility between two samples of the same batch. It was therefore concluded that the partially cured samples were homogeneous and representative of the intermediate stages of the curing process. Since the partially reacted samples were cured in a quiescent state, section 3.3.1, their good superposition on the curing curve suggests that the flow imposed to the samples during the cross-linking did not disturb nor modify this process.

The partially cured samples were stable beyond 180°C but an increase of both moduli attributed to oxidation was observed above 200°C. This temperature stability allowed the use of time-temperature equivalence (Ferry, 1980) in order to obtain master curves of the reduced storage, $G'(a_T\omega,t_i)$, and loss, $G''(a_T\omega,t_i)$, moduli versus frequency at different stages of the cross-linking process. This study required the use of parallel disk geometry since gap corrections must be made to

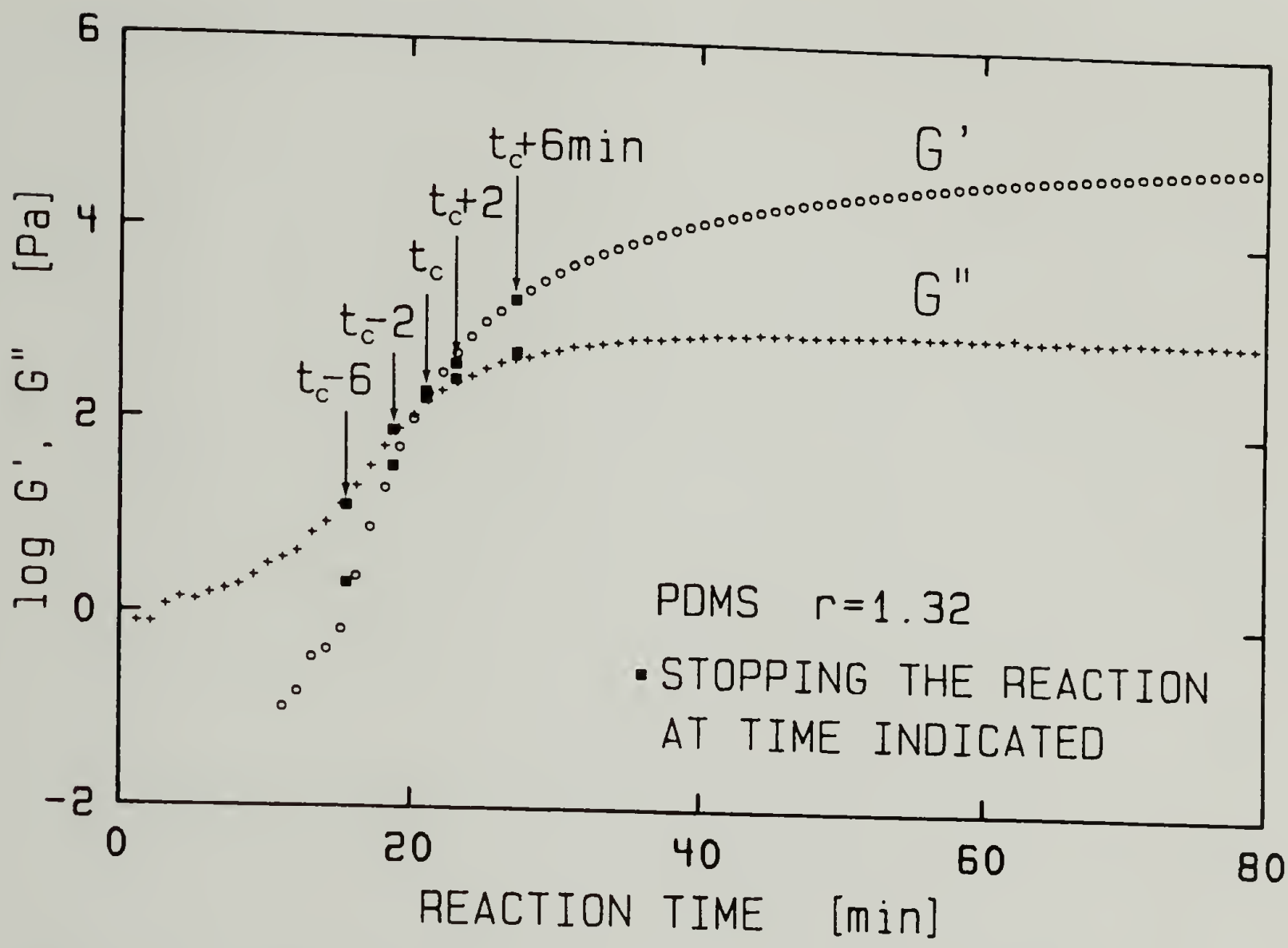

Figure 3.6. Curing curve of PDMS with balanced stoichiometry, at T=34°C and ω_0=0.5rad/s. The loss and storage moduli of the poisoned samples are represented by the dark squares.

compensate for variations in sample volume during the temperature changes.

The frequency dependence of the reduced storage and loss moduli and of the reduced complex viscosity $\eta^*(a_T\omega, t_i)$ at different stages of the cross-linking process are presented in Figures 3.7 and 3.8. In these figures t_c stands for critical time as will be sown in the next section.Viscoelastic data at temperatures between -50°C (below which the PDMS samples crystallize) and +180°C could be shifted to form single curves. The temperature shift factors (Ferry, 1980) are

$$a_T(T,T_0) = \exp[\frac{E}{R}(\frac{1}{T} - \frac{1}{T_0})]; \; b_T = \frac{\rho(T_0)T_0}{\rho(T)T} \qquad (3.1).$$

The shift factor a_T followed an Arrhenius relation as shown in Figure 3.9. Arrhenius behavior is expected since the experiments were performed much above the glass transition temperature. The vertical shift factor was estimated from the changes in sample thickness with temperature.

At the times t_c-6min and t_c-2min shown in Figure 3.7, both G′ and G" decrease to zero at low frequency and approach the limiting behavior $G' \sim \omega^2$ and $G'' \sim \omega$ characteristic of polymeric liquids (Ferry, 1980). On the other hand, at t_c+2min and t_c+6min a plateau value of G′ is clearly observed at low frequency which indicates that the material possesses a permanent elasticity. This plateau region which appears only in G′, has to be distinguished from characteristic plateau regions in both G′ and G" for entangled polymers. The same observations can be made with the

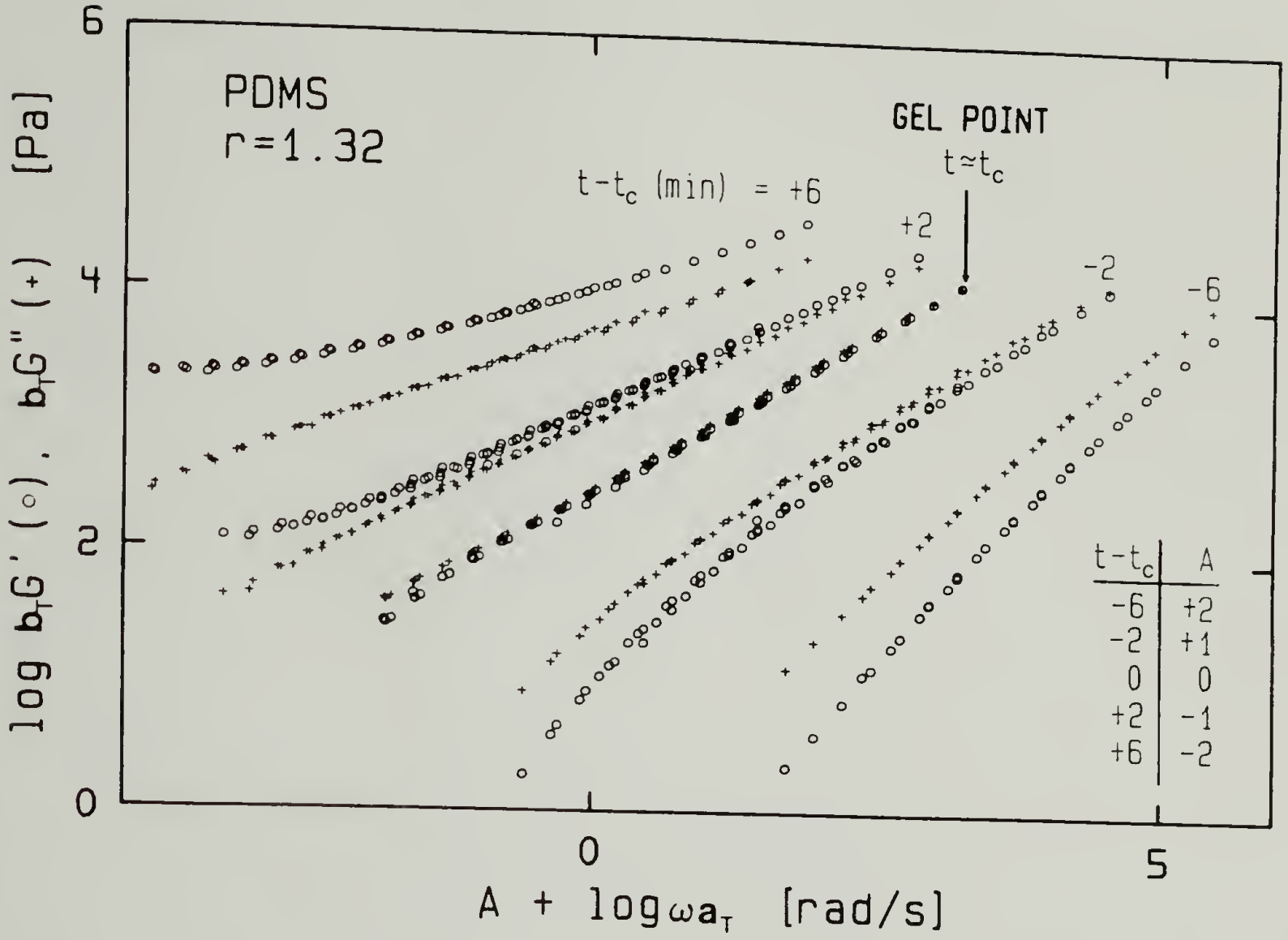

Figure 3.7. Reduced storage and loss moduli at intermediate states of conversion for PDMS with balanced stoichiometry. t_c is the instant of intersection (see Figure 3.6) of G′ and G". The curves were shifted side-ways (factor A) to avoid overlap.

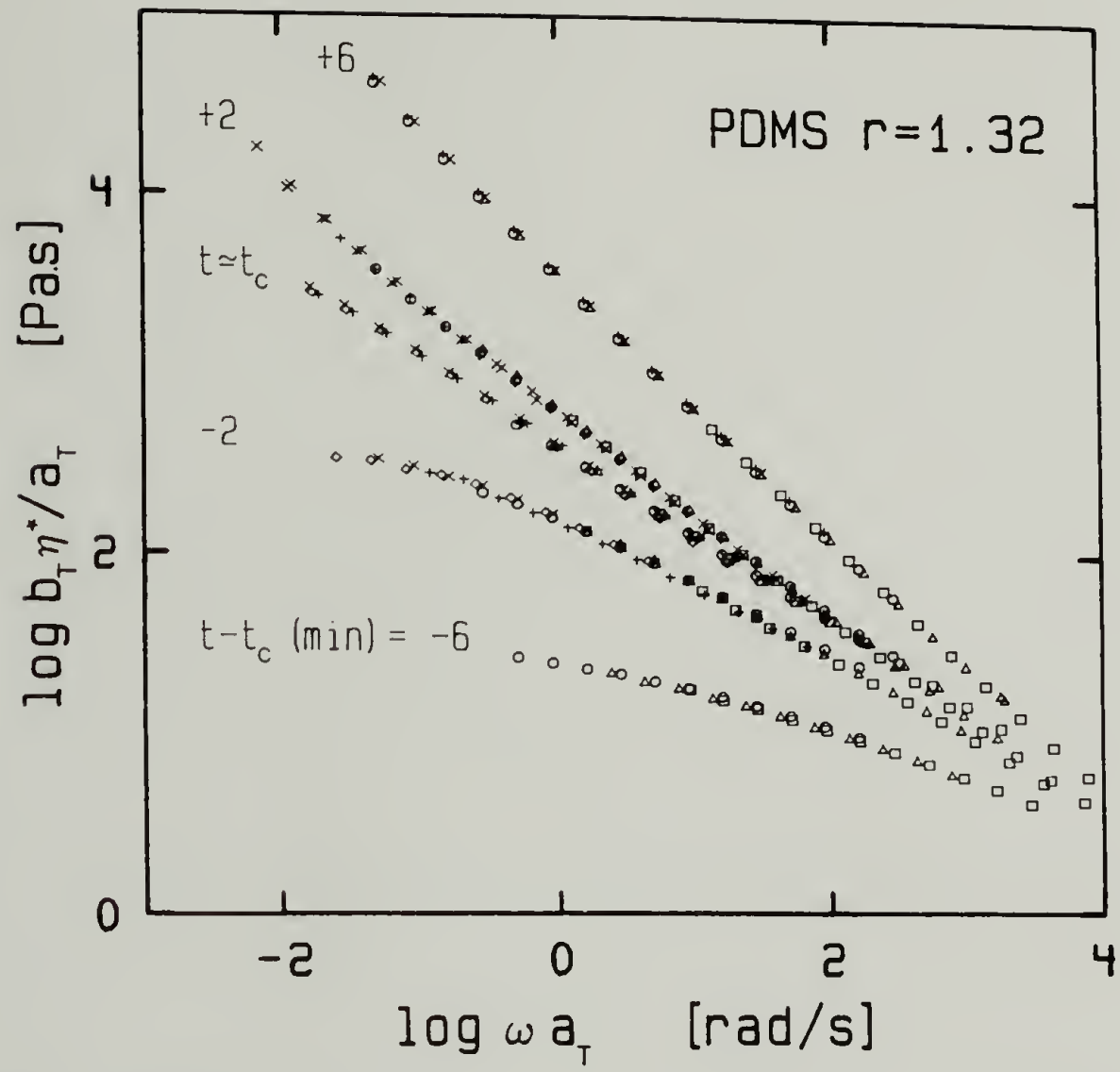

Figure 3.8. Reduced complex viscosity at intermediate states of conversion for PDMS with balanced stoichiometry.

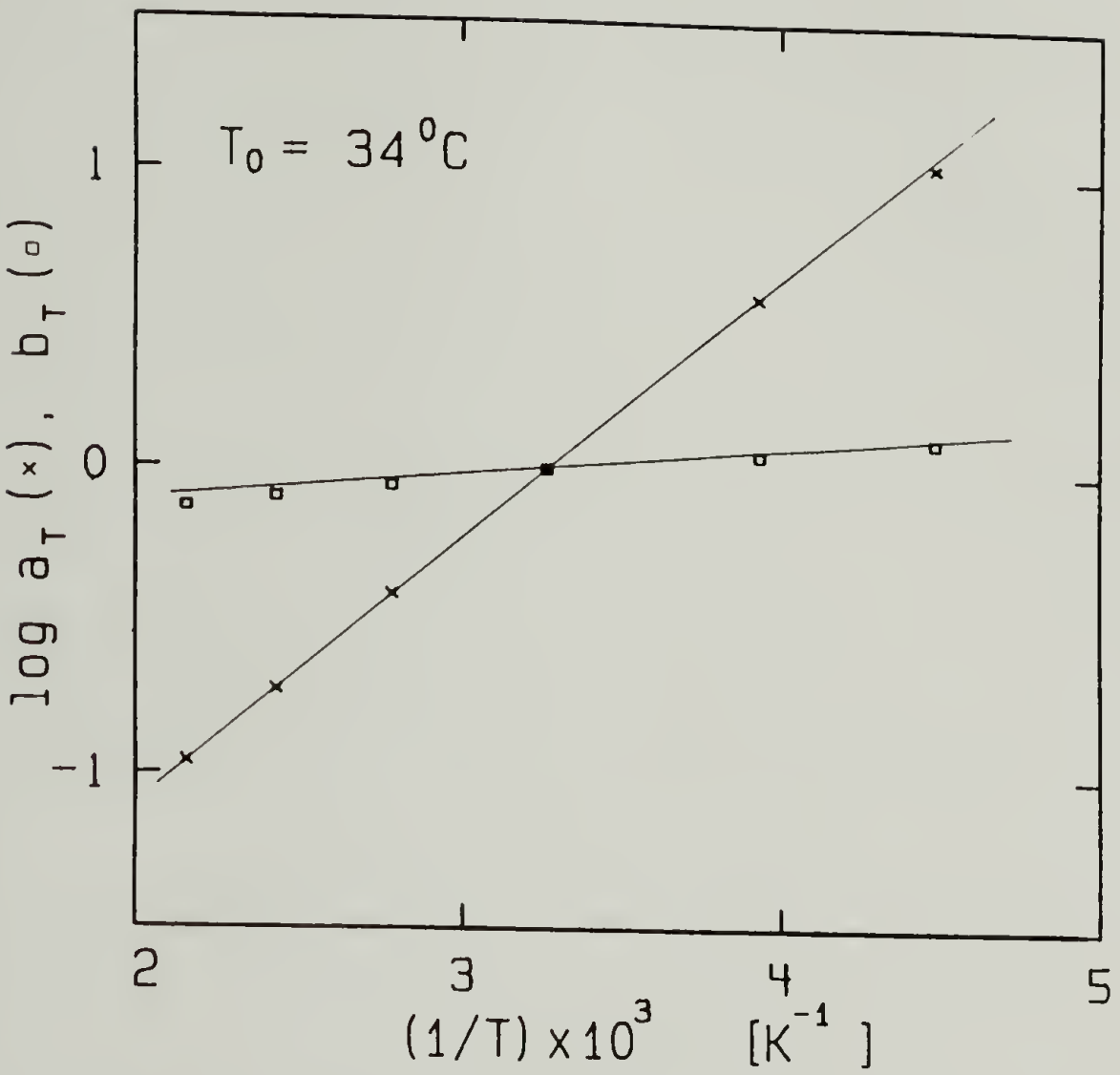

Figure 3.9. Measured temperature shift factors of PDMS with balanced stoichiometry at $t \simeq t_c$.

curves of η^* shown in Figure 3.8. At t_c-2min, a typical curve for polymeric liquids is observed where the viscosity reaches a finite plateau value, the zero steady shear viscosity, at low frequency. At t_c+2min, the low frequency end of the viscosity curve diverges towards infinity as expected for a solid material. These observations clearly indicate that the transition from liquid to solid has occured between the instants t_c-2min and t_c+2min. This implies that an infinitely large macromolecule which can sustain a stress for an infinitely long period of time has formed throughout the cross-linking sample; that is to say that the material gelled between these two instants. Analysis of the experimental data for the material at $t \simeq t_c$, is presented in the following section. Results of this analysis demonstrate that the material is very close to a critical state.

3.4 Analysis of Linear Viscoelasticity at GP

3.4.1 Experimental Observations

As seen in Figure 3.10 the partially cured sample at $t \simeq t_c$ exhibited congruency of the reduced moduli

$$b_T G'_c = b_T G''_c = C(a_T \omega)^{1/2} \qquad (3.2).$$

The subscript c indicates that the material with congruent moduli is at a critical state. The material constant C is independent of temperature.

For clarification, this condition of G'=G" over a wide temperature

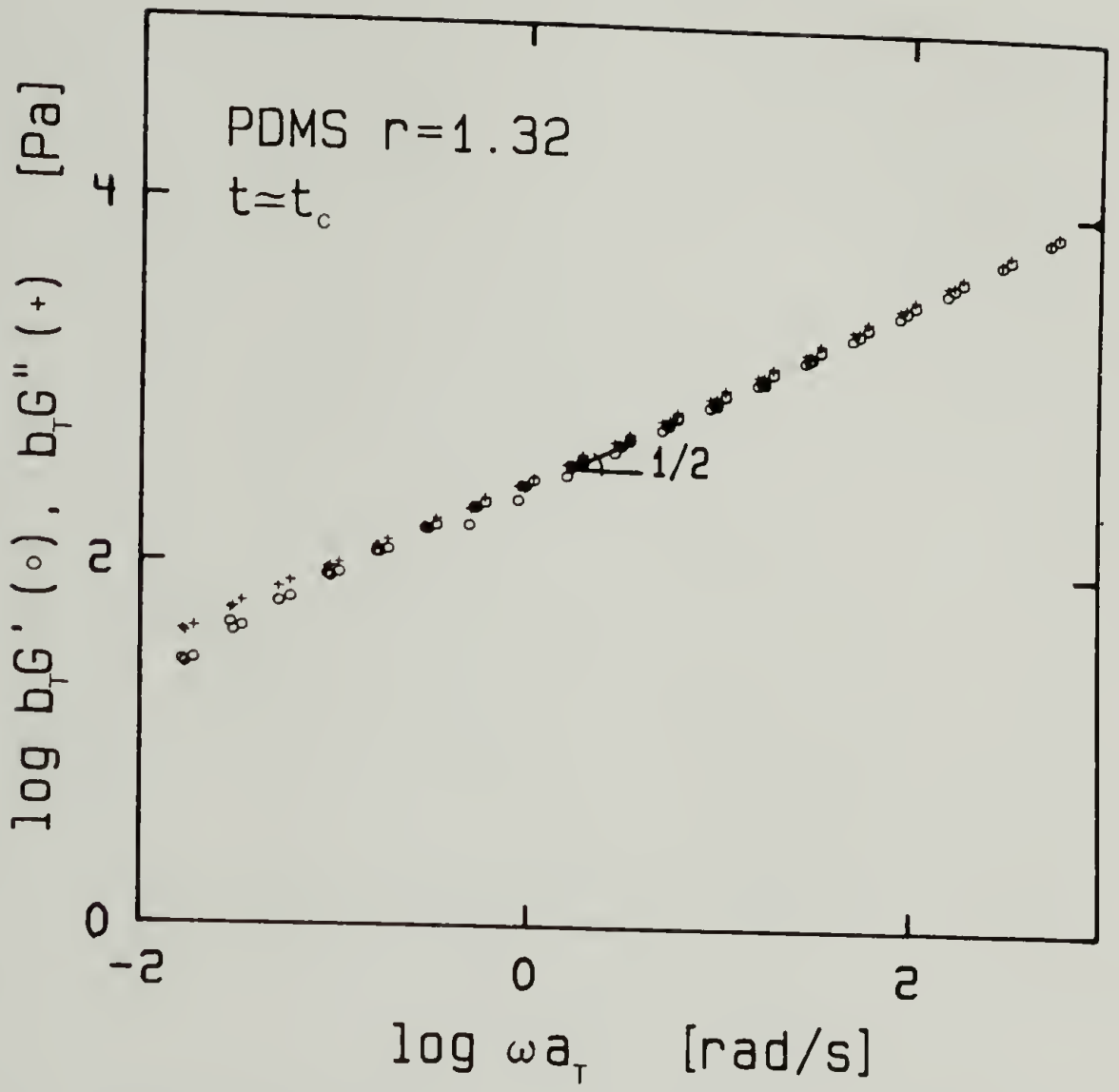

Figure 3.10. Reduced storage and loss moduli at $t \simeq t_c$ for PDMS with balanced stoichiometry.

and frequency range has to be distinguished from frequency-dependent crossover points which have been observed with most polymeric liquids (Ferry, 1980). This study is solely concerned with materials which exhibit congruence, G'=G", over a wide frequency range and not just an intersection at a specific frequency value. The crossover phenomenon will not be discussed further.

Linear viscoelastic theory, as applied to Eq. (3.2), predicts a steady shear viscosity

$$\eta_0 = \lim_{\omega \to 0} (G''_c/\omega) = C \lim_{\omega \to 0} (\omega^{-1/2}) \to \infty \qquad (3.3)$$

and an equilibrium modulus

$$G_\infty = \lim_{\omega \to 0} (G'_c) = C \lim_{\omega \to 0} (\omega^{1/2}) = 0 \qquad (3.4).$$

Infinite viscosity and zero equilibrium modulus are properties of a material at the liquid/solid transition (Flory, 1953). However, Eqs. (3.3) and (3.4) involve the zero frequency limit which is outside the experimental range.

It would be interesting to know the range of validity of the power law behavior which was observed over more than 5 decades in frequency and which is expected to continue over an even wider range. Of special interest is the region of low frequency which, as shown above, is responsible for the observation of the critical behavior. It is clear, however, that further measurements would not be able to solve this uncertainty. At very low frequency, the sample would exhibit either liquid behavior ($G' \sim \omega^2$; $G'' \sim \omega$) or solid behavior (G'=const.; $G'' \sim \omega$) since it is not possible to stop the reaction precisely at GP. This precise

point is, by definition, a purely theoretical limit which is not accessible to actual experiments.

By contrast, the high frequency region is of lesser interest. At very high frequency, the power law behavior will be masked by the onset of vitrification as an other transition phenomenon. In this study the material properties are investigated very far from the glass transition so that only the rubbery behavior at the gel point is analyzed. We therefore hypothesize that the power law behavior is not restricted in frequency range,

$$G'(T,\omega) = G''(T,\omega) = \sqrt{\pi/2}\ S(T)\omega^n, \qquad 0< \omega <\infty,$$

$$\text{with } S(T) = \sqrt{2/\pi}\ Ca_T^{1/2}/b_T \tag{3.5}$$

and test whether this hypothesis violates the relation of Kramers (1927) and Kronig (1926),

$$\frac{G'(\omega)}{\omega^2} = \frac{2}{\pi}\int_0^\infty \frac{G''(x)/x}{\omega^2 - x^2}\ dx \tag{3.6}$$

which involves an integral of the loss and storage moduli over the entire frequency range. The factor $\sqrt{\pi/2}$ is introduced for future convenience. Equation (3.5) is introduced twice into the Kramers-Kronig relation, Eq. (3.6), without specifying the value of n (which is expected to be about 1/2 from experiment). The values of the material constant C and of the temperature shift factors have no influence. The resulting equation, after arrangement,

$$1 = \frac{2}{\pi}\int_0^\infty y^{n-1}(1 - y^2)^{-1}\ dy, \tag{3.7}$$

has solutions

$$n = 1/2,\ -3/2,\ -7/2,\ -11/2... \tag{3.8}$$

The only valid solution, however, is $n=1/2$ since $n<1/2$ would predict a relaxation modulus which increases with time and therefore would violate thermodynamics principles. It is important to note that this proof is restricted to a power-law as defined in Eq. (3.5). It does not exclude the possible existence of another type of function which satisfies the congruency $G'=G"$.

The verification of Kramers-Kronig relation indicates that 1) the hypothesis of a power law over the entire frequency range does not violate the principles of the theory of linear viscoelasticity 2) the experimentally found value of the exponent $n=1/2$ is the only possible value which will give rise to congruent moduli over the entire frequency range.

These results are rather surpising. However it still has to be shown that congruent $G'=G"$ provides a well defined method for detecting GP of cross-linking polymers with balanced stoichiometry. This can be done through the use of a constitutive equation which will be developed in the following sections.

3.4.2 Relaxation Modulus

The extra stress in any viscoelastic liquid or solid at constant density can be described by a general constitutive equation (Bird, Armstrong and Hassager, 1977)

$$\underline{\tau}(t) = \int_{-\infty}^{t} G(t-t') \, \underline{\dot{\gamma}}(t') \, dt' \tag{3.9}$$

in which the relaxation modulus G(t-t') contains the material properties. Kinematics determines the rate of deformation tensor

$$\underline{\dot{\gamma}}(t') = \nabla v(x,t') + (\nabla v(x,t'))^{T} \tag{3.10}.$$

where v is the velocity. Equation (3.9) is valid as long as the memorized strain is kept within the linear region of the material. The extent of the linear region is difficult to define since a nonlinear constitutive equation is required. However, the lack of definition is no real problem since linear behavior can always be confirmed experimentally by repeated tests at increasing strain magnitude.

Equation (3.9) is suitable for describing the stress in the cross-linking material at its transition from liquid to solid since it is applicable to the liquid state as well as to the solid state and since the relaxation changes smoothly during the transition (as will be shown). As a result, the oscillatory shear data shown in Figure 3.10 can be analyzed through this constitutive equation. The kinematics of oscillatory shear is introduced into Eq. (3.9) to define the storage and loss moduli,

$$G'(\omega) = \omega \int_{0}^{\infty} G(t)\sin(\omega t)dt \tag{3.11}$$

$$G''(\omega) = \omega \int_{0}^{\infty} G(t)\cos(\omega t)dt \tag{3.12}.$$

As shown earlier, congruency of $G'(\omega)$ and $G''(\omega)$ over the entire frequency range requires that Eq. (3.11) and (3.12) are equal and proportional to $\omega^{1/2}$. Fourier transform tables list a unique solution for the relaxation modulus which satisfies all these conditions

$$G(t) = St^{-1/2} \qquad 0< t < \infty \qquad (3.13)$$

where the only material parameter, S [Pa $s^{1/2}$], is called the 'strength' of the network at GP.

This is a result which contradicts several observations which seemed to be generally valid for viscoelastic materials. First, a single material constant is the only adjustable parameter here, while viscoelastic liquids or solids require a relaxation time spectrum. Secondly, the modulus is infinite at the limit of zero time but the limiting modulus of viscoelastic liquids or solids is finite. This latter deviation is a consequence of the fact that vitrification was ignored in the starting hypothesis, Eq. (3.5). Finally, the relaxation time does not occur exponentially in time. Further experiments are however required to establish confidence in such unusual behavior.

Equation (3.13) which is valid over the entire time range represents a continuous relaxation spectrum. Such a spectrum, $H(\lambda)$, is conventionally defined as (Bird, Armstrong and Hassager, 1977)

$$G(t) = \int_0^\infty \frac{H(\lambda)}{\lambda} \exp(-t/\lambda)d\lambda \qquad (3.14).$$

By equating Eqs. (3.13) and (3.14) the continuous relaxation spectrum can be calculated

$$H(\lambda) = S(\pi\lambda)^{-1/2} \qquad (3.15).$$

It is interesting to note that, at GP, the material behaves like the polymer component of the Rouse model (1953) for dilute polymer solutions at the limit of high frequency,

$$1 \ll \lambda_{max}\omega \qquad (3.16).$$

For polymer solutions, the Rouse limit is reached by applying high frequencies (Ferry, 1980). However, this limit can also be reached by generating a material of extremely long relaxation time. Such Rouse-like behavior has been predicted for undiluted polymers below the entanglement level (Bueche, 1952; Ferry, 1980). At the gel point, the relaxation time is infinitely long and the power law behavior with a slope of 1/2 can be expected even at the limit of $\omega \to 0$. This coincidence with the Rouse behavior suggests the possibility of expressing the relaxation modulus as a sum of exponential as is often done for viscoelastic liquids. The discrete spectrum at GP can be written as

$$G(t) = St^{-1/2} = \lim_{\lambda_{max}\to\infty} \frac{2S}{\sqrt{\pi\lambda_{max}}} \sum_{i=1}^{\infty} \exp(-ti^2/\lambda_{max}) \qquad (3.17)$$

The spacing of the relaxation times is the same as in a Rouse spectrum. The spectrum is normalized to obtain the value of S at t=1s. No additional material parameter needs to be introduced when defining the discrete spectrum.

3.4.3 The Gel Equation

The constitutive equation for extra stress at GP is formulated by introducing the relaxation modulus at the transition, Eq. (3.13), into the general equation for viscoelastic materials previously defined, Eq. (3.9). In the limit of small strains and small strain rates it takes the simple form

$$\underline{\underline{\tau}}(t) = S \int_{-\infty}^{t} (t-t')^{-1/2} \, \underline{\underline{\dot{\gamma}}}(t') \, dt' \qquad (3.18).$$

the density is assumed to be constant. The only material parameter in the gel equation is the strength S. It can be measured in an oscillatory shear experiment without stopping the cross-linking reaction. The value of S is determined by G' at the time of its intersection with G", as shown in Figure 3.6. This parameter is defined as

$$S = G'_c [\pi\omega_0/2]^{-1/2}, \qquad (3.19)$$

where ω_0 is the frequency of the experiment. The PDMS used in these experiments has a strength of 226 Pa $s^{1/2}$ at T=34°C. The temperature dependence is found to be

$$S(T) = S(T_0) a_T^{1/2} / b_T \qquad (3.20)$$

hence S decreases with temperature.

3.4.4 Predictions of Gel Equation

Equation (3.18) obviously predicts congruent $G'(\omega)$ and $G''(\omega)$ since its derivation is based on the same condition. It now remains to be shown that it also predicts the behavior at GP, namely infinite steady shear viscosity and zero equilibrium modulus (Flory, 1953). Many experiments can be conceived for defining the viscoelastic phase transition. The predictions of Eq. (3.18) for transient shear viscosity and transient shear modulus are tested here since these quantities can actually be measured in a shear rheometer.

The first experiment gives the transient shear viscosity during start-up of shear flow at constant rate; the material is defined to be at GP if the time dependent viscosity grows to infinity without reaching the steady state. This is a more precise definition than 'infinite' steady shear viscosity which obviously cannot be verified in an experiment.

The stress is modeled by defining the time dependent shear rate and by introducing it into Eq. (3.18). The sample is kept at rest during times $t<0$; at time $t=0$ and thereafter, the sample is sheared at constant rate $\dot{\gamma}_{12}$. The resulting shear viscosity is calculated as

$$\eta(t) = \frac{\tau_{12}(t)}{\dot{\gamma}_{12}} = S \int_0^t (t-t')^{1/2}\, dt' = 2St^{1/2} \quad \text{for } 0< t \qquad (3.21).$$

The shear viscosity grows with time without ever reaching steady state. This satisfies the first condition of GP.

The second experiment measures the transient modulus during shear stress relaxation at rest after a rapid strain; the material is defined

to be at GP if the stress relaxes to zero and hence the equilibrium modulus is zero.

The stress is again modeled by defining the time-dependent shear rate and by introducing it into Eq. (3.18). The sample is subjected to a rapid shear with a shear rate,

$$\dot{\gamma}_{12}(t) = \begin{cases} 0 & \text{for } t < 0 \\ \dot{\gamma}_0 & \text{for } 0 < t < t_0 \\ 0 & \text{for } t_0 < t \end{cases} \qquad (3.22).$$

The total shear strain of this experiment amounts to $\dot{\gamma}_0 t_0$. With this strain history, the transient modulus is calculated as

$$g(t) = \frac{\tau_{12}(t)}{\dot{\gamma}_0 t_0} = \frac{S}{t_0} \int_0^t (t-t')^{-1/2} \, dt' ; \; t_0 < t$$

$$= St^{-1/2} 2/[1 + (1-t_0/t)^{1/2}] \qquad (3.23).$$

The duration, t_0, of the shearing motion in a rapid strain experiment is very short compared to that of the relaxation experiment. The equation for the transient shear modulus simplifies to

$$g(t) = St^{-1/2}, \qquad (3.24)$$

as expected from the equation for the relaxation modulus. The transient shear modulus approaches zero at long times. Therefore, the equilibrium modulus is equal to zero. This satisfies the second criterion of GP.

It is important to note that the short time contribution to the above predicted behaviors would be very small. This supports the starting hypothesis, Eq. (3.5), where the actual polymeric behavior at short

times has been ignored.

In summary, the gel equation, Eq. (3.18), is able to describe the known rheological phenomena at GP. Analysis of the experiments confirms that congruency of G′ and G" is a property of the PDMS polymer with balanced stoichiometry at the critical state.

3.4.5 Finite Strain Measure

An infinitesimal strain measure was selected when formulating the constitutive equation. This is permissible for studying material behavior in the limit of very small strain. However, continuum mechanics principles (objectivity) are violated by such an equation when applied to finite strains. The infinitesimal strain measure has to be replaced by a finite measure. Possible formulations for the stress are

$$\underline{\underline{\tau}}(t) = -S \int_{-\infty}^{t} (t-t')^{-1/2} \frac{\partial}{\partial t'} \left(\underline{\underline{C}}_t^{-1}(t')\right) dt' \qquad (3.25)$$

or

$$\underline{\underline{\tau}}(t) = -\frac{S}{2} \int_{-\infty}^{t} (t-t')^{-3/2} \left[\underline{\underline{C}}_t^{-1}(t') - \underline{\underline{1}}\right] dt' \qquad (3.26)$$

with a Finger strain tensor $\underline{\underline{C}}_t^{-1}(t')$ and a unit tensor $\underline{\underline{1}}$, definitions of which are given in standard continuum mechanics texts (Malvern,1969). Volume changes are assumed to be negligibly small (ρ=const.). The two equations are identical and transformation from one to another is possible by partial integration. The available data were taken at small strain and therefore do not give any indication of a suitable choice of finite strain measure. However the behavior at finite strain is outside

the scope of this research and shall have to be investigated in a future study.

3.5 Discussion

An extremely simple relation between stress and strain, the Gel Equation (3.18) or (3.25), describes the known rheological phenomena of a polydimethylsiloxane network at its gel point (GP). The constitutive equation is based on the congruence hypothesis Eq. (5), which says that there exists an intermediate state of the material at which $G'(\omega)$ and $G''(\omega)$ are congruent functions over the entire range $0< \omega< \infty$.

A new material property has been defined, the strength of the gel, S, with a dimension of Pa $s^{1/2}$. It is easily measured in a single oscillatory shear experiment during the cross-linking reaction. S depends, in some general way which is not yet known, on molecular structure. For engineering applications, one would like to know how S depends on reaction conditions and whether there exists a relation between S and the final network properties after complete conversion.

For the PDMS polymer with balanced stoichiometry, GP is given by the intersection of the loss and storage moduli on the curing curve seen in Figure 3.6. In this particular case, this makes it possible to measure the exact instant of gelation without having to stop the cross-linking reaction.

The relaxation modulus at GP was shown to exhibit a power law behavior with a Rouse-like character, section 3.4.2. The short power law region often observed with polymeric materials at intermediate

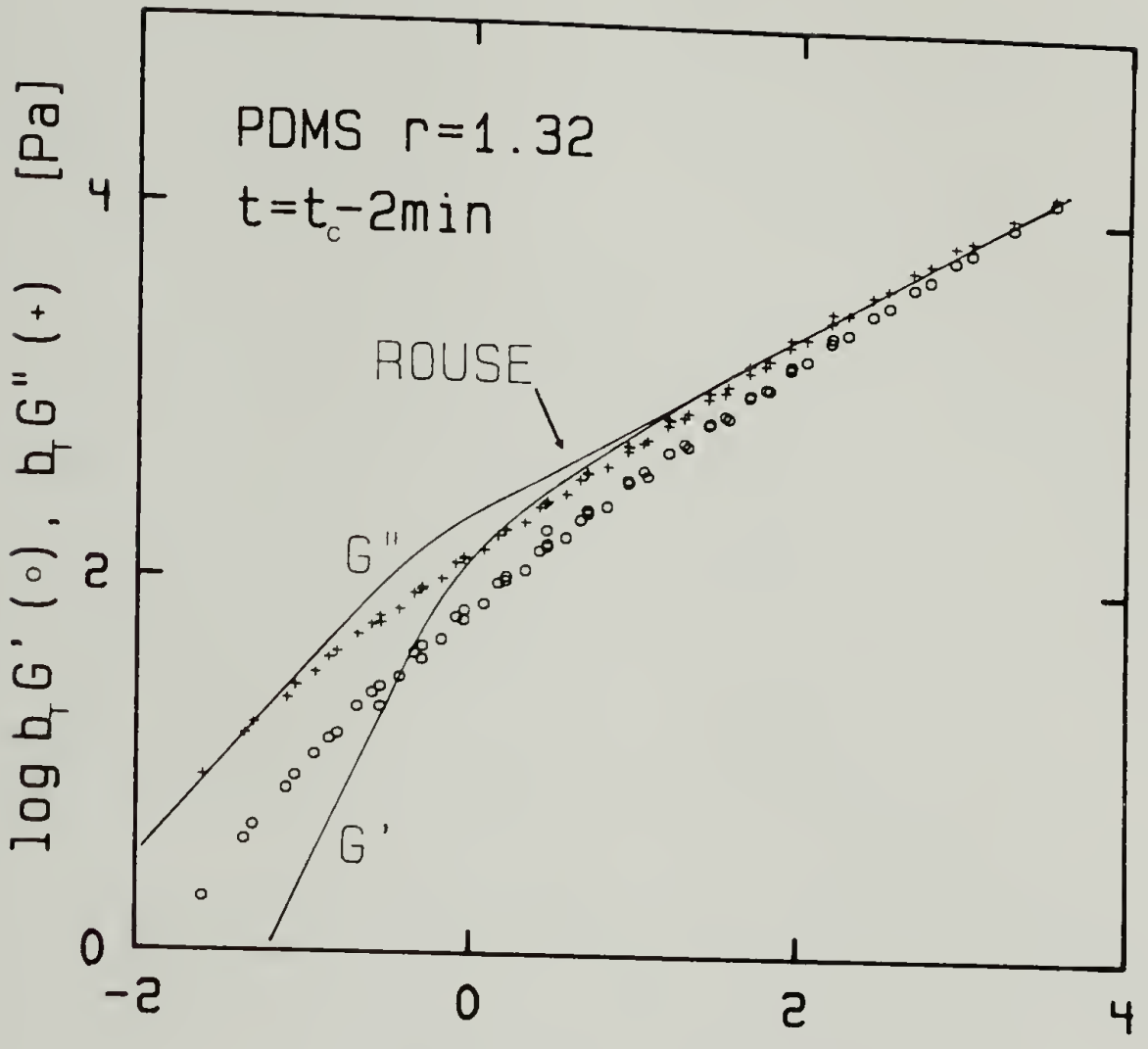

Figure 3.11. Comparison of Rouse spectrum with the behavior of PDMS at t_c-2min (see Figure 3.6).

frequencies (Roovers and Graessley, 1981; Larson, 1985) is overstretched for the polymer at GP. This results in a shift of the terminal zone towards lower and lower frequencies as GP is approached. It is important to note, however, that the behavior in the vicinity of GP cannot be described with a Rouse model. For instance, the rheological behavior at t_c-2min does not correspond to a Rouse spectrum with finite longest relaxation time, as shown in Figure 3.11. The same conclusion applies just after GP where the rheological behavior at t_c+2min cannot be satisfactorily predicted from the Mooney (1959) modification of the Rouse model for cross-linked polymers. This suggests that the extraordinarily broad power law region observed on the material at GP may not only be caused by a large increase of the relaxation times but also by the development of a particular polymeric structure with unusual rheological behavior.

It is important to mention that previous studies with cross-linking polymers (Lipshitz and Macosko, 1976; Castro and Macosko, 1984) often neglected the occurence of shear thinning effects in the pre-gel region. This study suggests a different behavior. If the Cox and Merz (1958) rule is assumed to be valid for branched polymers, which is likely, the complex viscosity curves shown in Figure 3.8 strongly support the existence of an important shear thinning effect before GP.

In conclusion, the simplicity and clarity of the Gel Equation implies that it may be universally valid for end-linking polymers with balanced stoichiometry. Experiments on other polymer systems are needed to support such a far reaching conclusion.

C H A P T E R I V

EFFECT OF STOICHIOMETRY ON LINEAR VISCOELASTIC PROPERTIES AT GEL POINT

The validity of the Gel Equation must be tested with different materials at GP. As discussed in section 3.1, a simple way to produce a new material with a cross-linking polymer is to change the stoichiometric ratio of the reactants. For this purpose, the cross-linking reaction of PDMS networks with imbalanced stoichiometry is stopped at different stages of the developing network. The linear viscoelastic properties at GP are measured and compared to those obtained for balanced stoichiometry (chapter three). The previously developed Gel Equation is generalized to take into account the effect of the stoichiometric ratio. The power law relaxation behavior at GP is confirmed. Gels formed with different stoichiometric ratios can now be distinguished by their rheological behavior. The results are consistent with recently developed fractal theories.

4.1 Rheology of Curing Material and of 'Stopped' Samples

PDMS samples with imbalanced stoichiometry, $r=0.91\pm0.05$, were prepared by following the procedure described in section 2.1.4. A stoichiometric ratio well below the balanced stoichiometry ($r_e \simeq 1.3$) was chosen since, as discussed in section 3.1, cross-linker deficiencies are

more effective than cross-linker excesses in creating network imperfections. When compared with networks of balanced stoichiometry, systems with $r<1.3$ are expected to exhibit more drastic changes in their rheological properties than systems with $r>1.3$ at intermediate states of network developmemt.

The experimental conditions used to measure the changes in dynamic storage and loss moduli during isothermal cure were similar to those described in section 3.1. The reproducibility of the reaction kinetics from one sample to another was again ± 1 minute. The curing curve measured at 34°C is shown in Figure 4.1. A typical evolution, similar to that of the curing network with balanced stoichiometry shown in Figure 3.6, is observed. Viscous behavior dominates the initial part of the experiment, $G" >> G'$, and elastic behavior dominates the final stages of the reaction, $G' >> G"$. Direct comparison of the rates of reaction between the two curing curves cannot be done since, as mentioned in section 2.1.4, the amount of catalyst employed in the two experiments was slightly different. However, from the previous study the instant of gelation is expected to occur at the crossover point of the loss and storage moduli on the curing curve. In order to verify whether this criterion is still valid for networks with imbalanced stoichiometry, the cross-linking reaction was stopped at different stages in the vicinity of this point.

Partially cured samples were obtained by following the procedure presented in section 3.1. A solution of TMEDA in toluene was used for poisoning the cross-linker instead of the elemental sulfur used in the earlier experiments. Details of the chemical composition of the samples

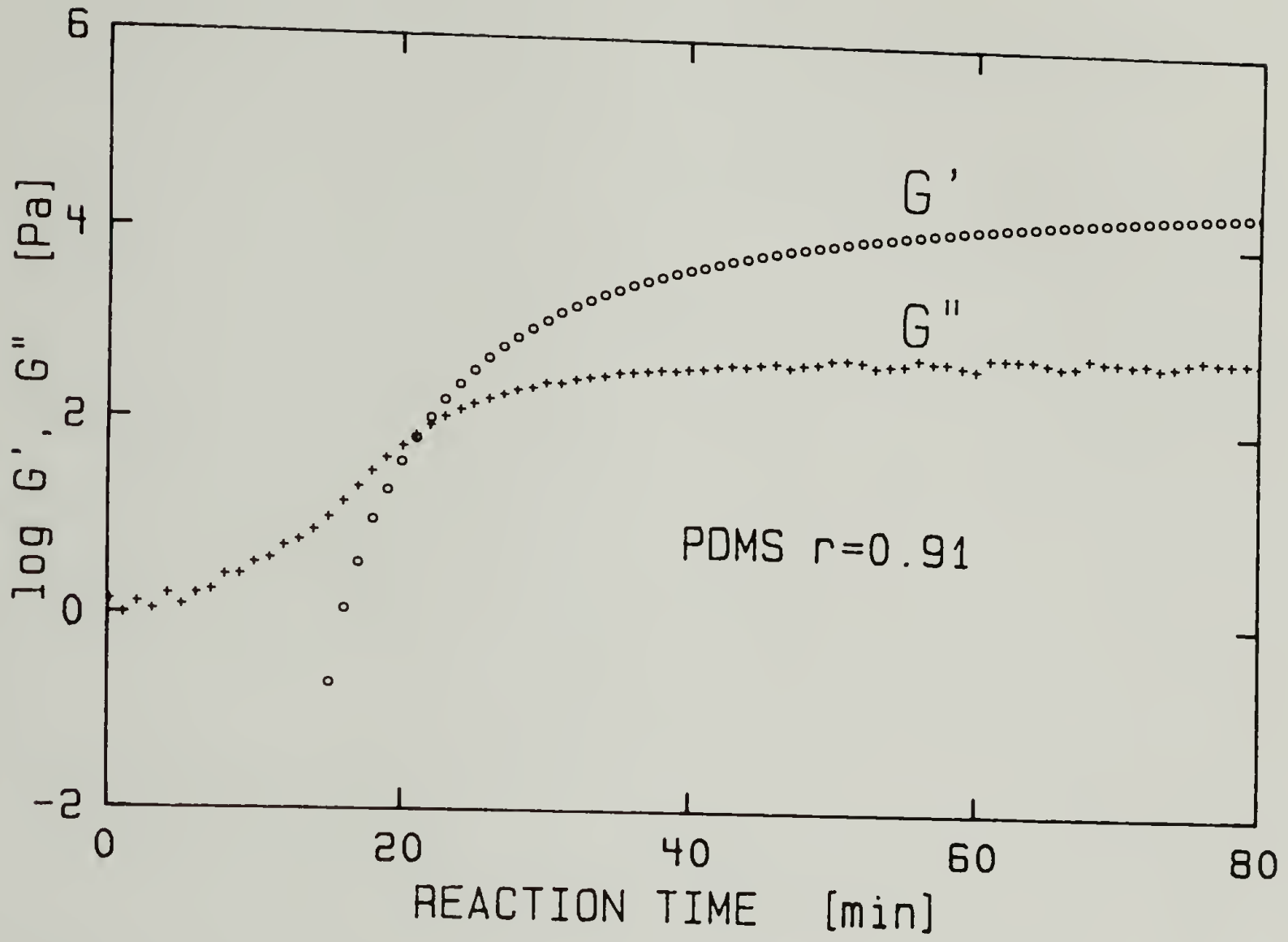

Figure 4.1. Curing curve of PDMS with imbalanced stoichiometry, at T=34°C and ω_0=0.5rad/s.

and of the poisoning solution are reported in chapter two. Rheological measurements showing the effectiveness of TMEDA are shown in Figure 4.2. These measurements were started about three minutes after spraying the poisoning solution on the surface of the samples. As indicated in Figure 4.2, the instant of poisoning and the instant of superposition on the curing curve are in very good agreement. Prior to further rheological experiments, the partially cured samples were heated for two hours at 140°C. Very slight changes of the storage and loss moduli were noticed after cooling down to 34°C as shown in Figure 4.2 and as previously discussed in section 3.3.1. These rheological measurements cannot distinguish between the efficiencies of TMEDA and elemental sulfur as poisoning compound for stopping the cross-linking reaction. TMEDA was however preferred for the reasons discussed in section 2.1.5.

As shown by the dark squares in Figure 4.3, the developing network was represented by a discrete set of stable samples with increasing extents of reaction. The good superposition observed indicates that partially cured samples were homogeneous and representative of the intermediate stages of the cross-linking process. In addition, the temperature stability of the poisoned samples allowed the application of time-temperature superposition (Ferry, 1980) from -50°C to +140°C. The PDMS samples crystallize below -50°C and the dynamic moduli of these samples were too low to enable accurate measurements above +140°C. Master curves of the reduced storage, $G'(\omega_0,t_i)$, and loss, $G''(\omega_0,t_i)$, moduli versus frequency at different times, t_i,on the curing curve are presented in Figure 4.4. An evolution of the rheological properties comparable to that of PDMS networks with balanced stoichiometry (see

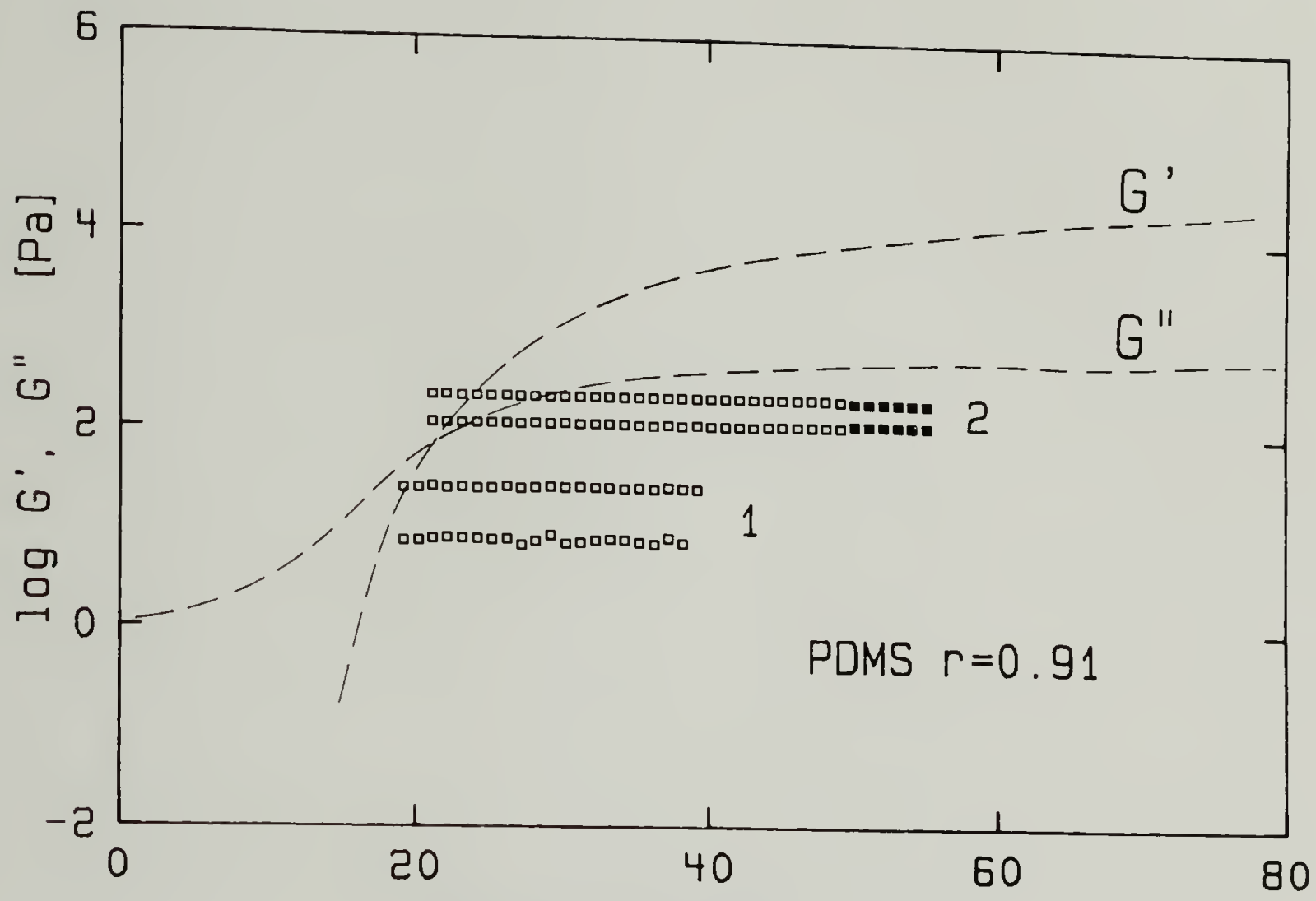

Figure 4.2. Stability of the storage modulus,G', and the loss modulus, G", after poisoning of the catalyst with TMEDA, (□) before heating to 140°C, (■) after 2 hours at 140°C. The dashed lines represent the regular curing curve. 1) poisoned at t=19min and superimposes with t=18min; 2) poisoned at t=21min and superimposes with t=23min.

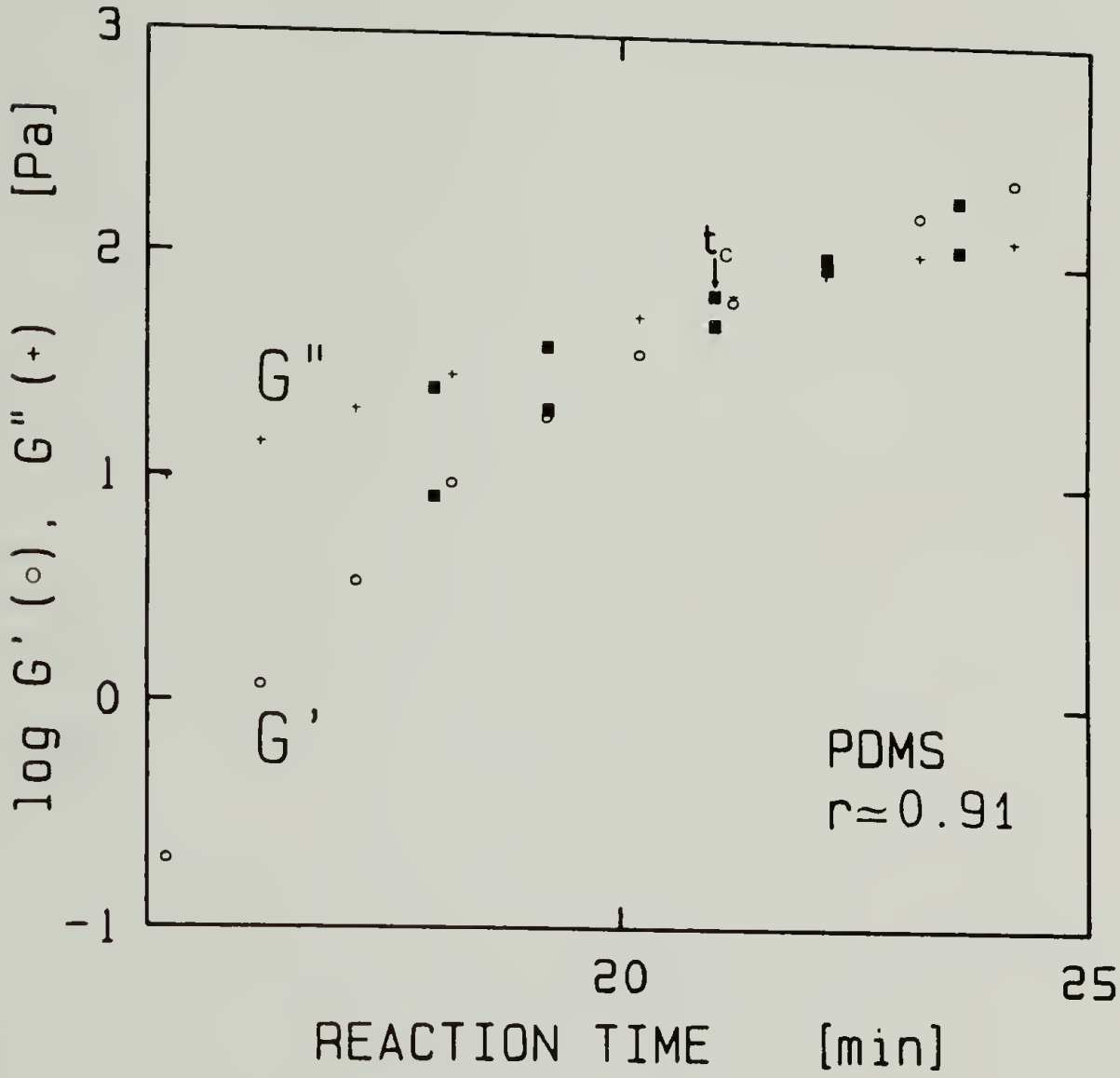

Figure 4.3. Curing curve of PDMS with imbalanced stoichiometry, at T=34°C and ω_0=0.5rad/s. The loss and storage moduli of the poisoned samples are represented by the dark squares.

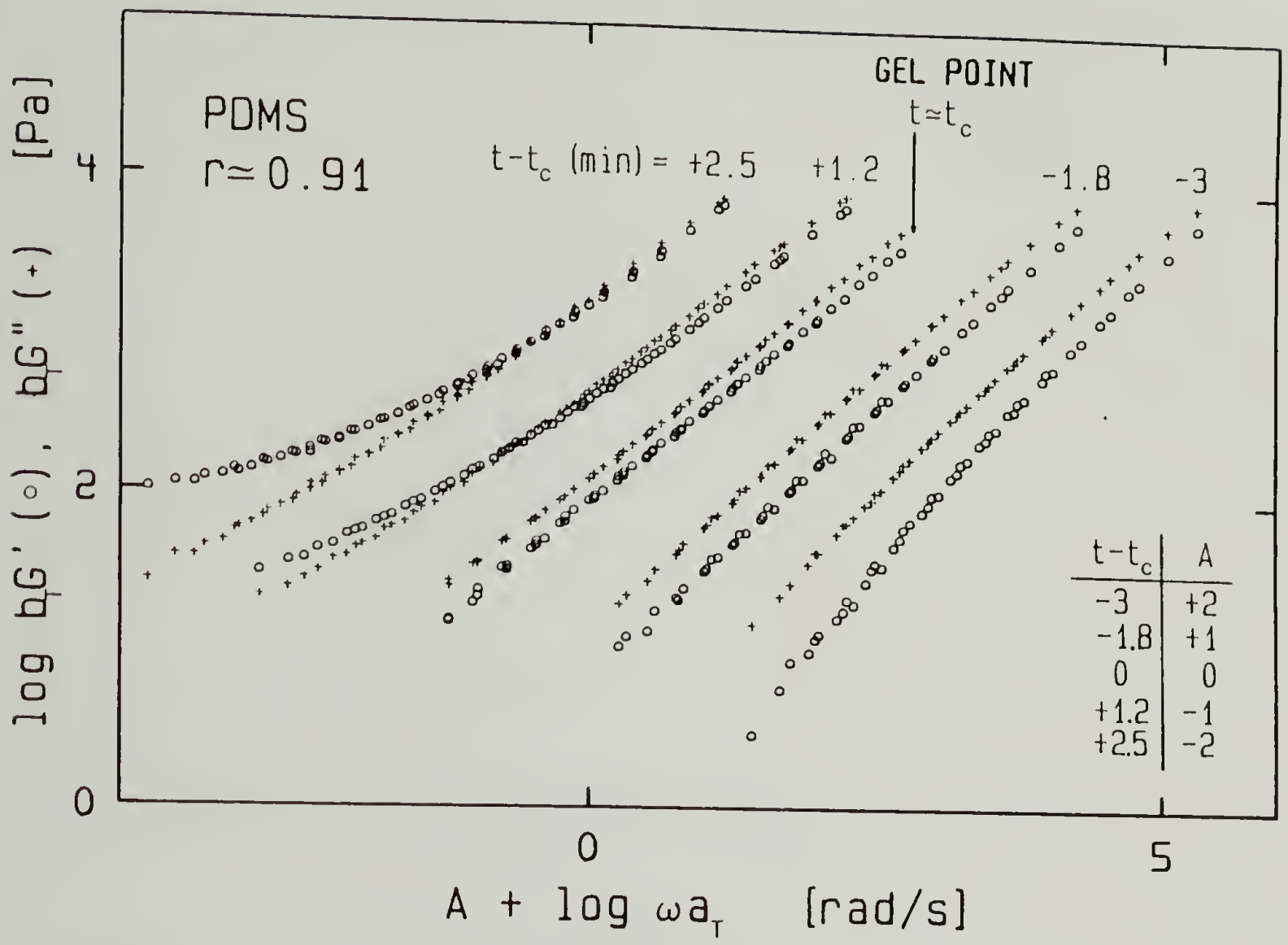

Figure 4.4. Reduced storage and loss moduli at intermediate states of conversion for PDMS with imbalanced stoichiometry. t_c is not the instant of intersection (see Figure 4.3) of G′ and G". The curves were shifted side-ways (factor A) to avoid overlap.

Figure 3.7) is observed. At t_c-3min and t_c-1.8min, both G′ and G″ are expected to decrease to zero at low frequency while at t_c+1.2min a plateau value of G′ has appeared which indicates that GP has been passed. Solubility tests discussed in section 6.4 confirmed this fact. A major difference is observed between the evolutions shown in Figures 4.4 and 3.7. For the network with imbalanced stoichiometry, the plateau in G′ appears before the occurence of the congruent behavior of G′ and G″. As a result, the crossover point of the loss and storage moduli on the curing curve no longer coincides with GP for networks of imbalanced stoichiometry.

A remarkable result comes from the repeated observation of a power law behavior for $G'(a_T\omega, t_i)$ and $G''(a_T\omega, t_i)$ over nearly five decades of frequency at $t \simeq t_c$. Analysis of similar results with an exponent n=1/2 showed that the power law behavior coincides with the instant of gelation for stoichiometrically balanced gels. The previous analysis is now generalized to demonstrate that the earlier conclusion is valid for a range of power law exponents.

4.2. Analysis of Linear Viscoelasticity at GP

A general power law behavior for the loss and storage moduli is hypothesized over the entire range of frequency. At $t=t_c$,

$$G'(\omega) \sim D(\omega^n) \qquad 0 < \omega < \infty \qquad (4.1)$$

$$G''(\omega) \sim E(\omega^n) \qquad (4.2)$$

where D and E are two material constants. The consistency of this hypothesis with the principles of the theory of linear viscoelasticity is tested by introducing Eqs. (4.1) and (4.2) into the Kramers-Kronig relation, Eq. (3.6), without specifying the value of n. The resulting equation, after arrangements,

$$1 = \frac{E}{D}\frac{2}{\pi}\int_0^\infty y^{n-1}(1 - y^2)^{-1}\, dy, \qquad (4.3)$$

has solutions

$$E = D \tan(n\pi/2) \quad \text{with} \quad n < 1 \qquad (4.4).$$

The only valid solutions, however, are for $0<n<1$ since $n<0$ would predict an increasing relaxation modulus and would therefore violate thermodynamics principles. As a result at $t=t_c$,

$$G' = \frac{G''}{\tan(n\pi/2)} = D\,\omega^n, \qquad 0< n < 1 \quad \text{and} \quad 0< \omega < \infty \qquad (4.5).$$

The verification of Kramers-Kronig relation indicates that a power law behavior with $0<n<1$ for dynamic moduli over the entire frequency range does not violate the rules of linear viscoelasticity. Equation (4.5) predicts that: G′ is greater than G″ for $n>1/2$, G′ is less than G″ for $n<1/2$, and G′is equal to G″ for $n=1/2$. These predictions are quantitatively verified with the cross-linking PDMS at $t\simeq t_c$, as shown in Figure 4.5.

The linear relaxation modulus can be obtained by solving Eqs. (3.11) and (3.12) together with Eq. (4.5). The unique solution for the relaxation modulus is

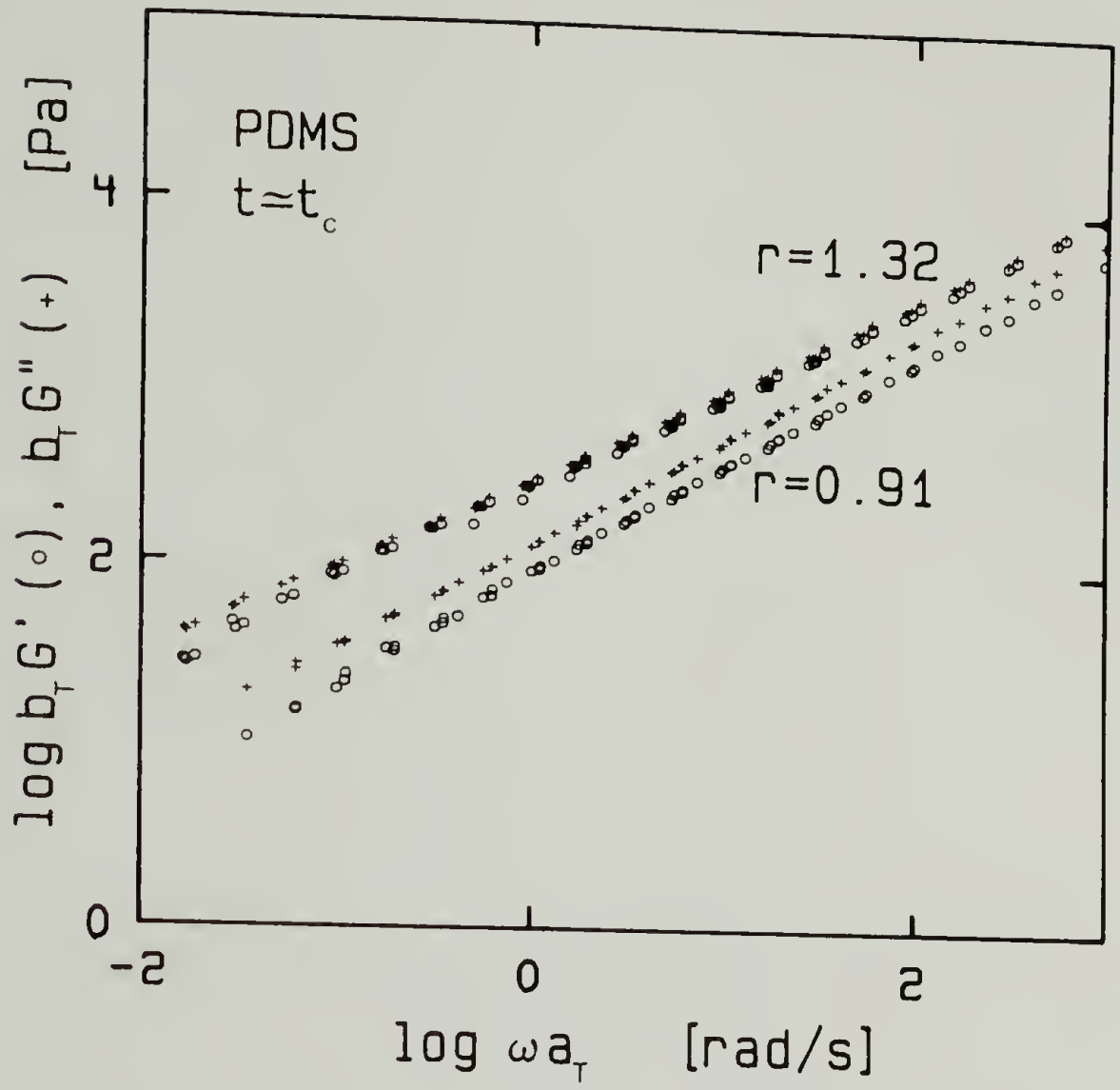

Figure 4.5. Reduced storage and loss moduli at $t \approx t_c$ for PDMS with balanced stoichiometry and with imbalanced stoichiometry.

$$G(t) = St^{-n}, \qquad 0< n < 1 \quad \text{and} \quad 0< t < \infty,$$
$$\text{with} \quad S = \frac{2\,\Gamma(n)}{\pi} \sin(n\pi/2)\, D \qquad (4.6).$$

Therefore at $t=t_c$ the relaxation modulus will exhibit a power law behavior with a slope -n. For n=1/2, Eq. (4.6) predicts the result observed for PDMS with balanced stoichiometry, Eq. (3.13). It remains to be shown that, for any value of the power law exponent $0<n<1$, the material defined at $t=t_c$ is at the gel transition.

The steady shear viscosity is defined by the theory of linear viscoelaticity as

$$\eta_0 = \int_0^\infty G(t)dt \qquad (4.7).$$

by introducing Eq. (4.6) into Eq. (4.7), the steady shear viscosity is seen to diverge to infinity for any value of n between 0 and 1.

Linear viscoelastic theory, as applied to Eq. (4.6), predicts an equilibrium modulus

$$G_\infty = \lim_{t\to\infty} G(t) = S \lim_{t\to\infty} (t^{-n}) = 0, \qquad 0< n < 1 \qquad (4.8).$$

Therefore the material at $t=t_c$ as defined above exhibits the classical attributes of the gel behavior in addition of the experimentally observed power law dynamic moduli. At GP the value of the exponent, n, is not limited to n=1/2 but rather to a range of values between 0 and 1. This new result is now included in the Gel Equation.

4.3. Generalization of the Gel Equation

Analysis of the experiments indicates that the relaxation modulus obeys a power law at GP, Eq. (4.6). It is observed however that the exponent, n, of the power law is a function of the stoichiometric ratio of the reactants, r,

$$n \begin{cases} = 1/2 & \text{for } r = 1.32 \\ > 1/2 & \text{for } r = 0.91 \end{cases} \qquad (4.8).$$

In order to model these differences in the rheological behavior at GP the Gel Equation developed in chapter two, Eq. (3.18), has to be modified. This is done by introducing the general expression for the relaxation modulus at GP, Eq. (4.6), into the general equation for viscoelastic materials defined in chapter three, Eq. (3.13). The generalized Gel Equation takes the simple form

$$\underline{\underline{\tau}}(t) = S \int_{-\infty}^{t} (t-t')^{-n} \, \underline{\underline{\dot{\gamma}}}(t') \, dt', \qquad 0< n < 1 \qquad (4.9).$$

Two material parameters are now needed, the gel 'strength', S, and the power law exponent, n. These two parameters depend on the molecular structure in a way which is not yet known. An attempt to relate the exponent n to molecular structure is presented in section 4.4.

Equation (4.9) predicts that the steady shear viscosity will never be reached at small strains (i.e. infinite steady shear viscosity), and that the equilibrium modulus relaxes to zero after a rapid strain . This can be easily seen by replacing the exponent n=1/2 in Eqs. (3.21)

and (3.24) by values of n with $0<n<1$. However these two properties involve limiting behaviors which do not distinguish among different gel behaviors.

Of higher interest is the prediction by Eq. (4.9) of a power law relaxation behavior at GP. The common behavior between two different gels is the power law type of relaxation (i.e. universal relaxation behavior) while the difference lies in the speed of the relaxation process (e.g. exponent of the power law). In the special case where $n=1/2$, Eq. (4.9) predicts congruency of the dynamic moduli. In this case only, the instant of gelation can be determined from the intersection of the loss and storage moduli on the curing curve, as shown in Figure 3.6. However, this method to measure the gel time is of limited interest since it will apply only in very specific cases.

By contrast, for any value of the exponent n, Eq. (4.9) predicts that the tangent of the loss angle at GP is,

$$\tan\delta(\omega) = \frac{G''(\omega)}{G'(\omega)} = \tan(n\pi/2) \qquad (4.10)$$

independent of the frequency, ω. This result is of direct practical interest since it indicates that any method able to detect the occurence of the power law behavior will be suitable to determine the instant of gelation. Such an experiment is suggested for future research in chapter 7.

4.4 Fractal Behavior at GP

A Rouse model with infinitely long relaxation time was suggested in section 3.4.2 to explain the power law behavior of stoichiometrically balanced PDMS gels. It was shown, however, that a Rouse type relaxation spectrum could not predict the rheological behavior in the vicinity of GP (see Figure 3.11). This raised some questions about the ability of the Rouse spectrum to model the rheological behavior in the vicinity of the gelation transition. Results obtained on the PDMS polymer with imbalanced stoichiometry, clearly show that the general rheological behavior at GP cannot be explained in terms of a Rouse relaxation spectrum since the power law exponent is not always 1/2. It is therefore concluded that the Rouse theory is not adequate to relate rheological behavior and molecular parameters at GP.

Principles of self-similarity define the fractal dimension of a molecular cluster as,

$$R \sim M^{1/d_f} \tag{4.11}$$

where R is the radius of gyration and M is the molecular weight. The fractal dimension at the gel point is predicted by different gelation theories and is found to be (Stauffer, Coniglio and Adam, 1982)

$$d_f \begin{cases} = 4 & \text{Zimm-Stockmayer} \\ = 2.5 & \text{percolation cluster at threshold.} \end{cases}$$

However, recent computer modeling (Hermann, Landau and Stauffer, 1982; Termonia and Meakin, 1985) of the kinetic gelation suggest that different values for d_f should be expected.

Recently, theories have been derived (Muthukumar, 1985; Cates, 1985) which predict the dependence of the complex viscosity in terms of the arbitrary fractal dimension of the molecular cluster. From Muthukumar (1985) theory, in the regime of large molecular weights but ignoring the entanglement effect, the frequency dependence of the viscosity is shown to be

$$\eta^*(\omega) \sim \omega^{-2/(d_f+2)}, \qquad 0< \omega \qquad (4.12)$$

$$\eta^*(\omega) \sim M^{2/d_f}, \qquad \omega \to 0 \qquad (4.13).$$

Since the molecular weight of the growing cluster diverges at GP, the experimental complex viscosity also diverges in accordance with Eq. (4.13).

From the Gel Equation, Eq. (4.9), power law loss and storage moduli are predicted at GP, Eq. (4.5). The complex viscosity is defined from the theory of linear viscoelasticity as

$$\eta^*(\omega) \sim [(G'/\omega^2) + (G''/\omega^2)] \qquad (4.14)$$

which becomes at GP,

$$\eta^*(\omega) \sim \omega^{n-1} \qquad 0< n < 1 \quad \text{and} \quad 0< \omega < \infty \qquad (4.15).$$

The combination of Eqs. (4.12) and (4.15) leads to the fractal dimension at GP as,

$$d_f = \frac{2n}{1-n} \qquad 0< n < 1 \qquad (4.16).$$

As discussed by Muthukumar and Winter (1986), the experiments suggest that the PDMS with balanced stoichiometry has a fractal dimension of 2, which is very close to the value of 1.94 predicted by the the kinetic percolation model of Termonia and Meakin (1985).

The fractal dimension is not expected to exceed the value of 3. This indicates an upper value for the power law exponent of $n_{max}=3/5$ as calculated from Eq. (4.16). This value is very close to the experimentally measured power law exponent for PDMS with imbalanced stoichiometry.

In conclusion, the predictions of the Gel Equation, Eq. (4.9), are consistent with recently developed fractal theories for polymeric materials. Both approaches predict a universal rheological behavior for cross-linking polymers at the gel point. That behavior is described by a power law relaxation spectrum. The exponent of the power law is directly related to the fractal dimension of the cluster at GP, a parameter which can be easily determined from rheological experiments. Additional tests on different systems and on a broader range of stoichiometric ratios are needed to confirm the universal validity of these findings. Such experiments are presented in chapter five.

C H A P T E R V

LINEAR VISCOELASTIC PROPERTIES OF CROSS-LINKING PU DURING GELATION

The universality of the Gel Equation is tested with different cross-linking polyurethanes (PU). As with the PDMS systems which were used in the previous experiments, these PU networks are formed by an end-linking reaction of well defined chemical species. However, the cross-linking process occurs by a different reaction and the PU cross-link functionality is 3 instead of 4 (for the PDMS). PU networks with balanced stoichiometry but with different strand lengths between cross-links are studied first. The influence of the stoichiometric ratio over the entire possile range for gelation is then investigated. At GP, all the PU networks studied exhibit the same rheological behavior as PDMS. This is shown in the following.

5.1 Rheology of PU Gels with Balanced Stoichiometry

PU samples with balanced stoichiometry, $r=1.0\pm0.02$, were prepared by following the procedure described in section 2.2. After mixing at 90°C, the samples were quickly transferred to the rheometer. Small strain oscillatory shear experiments were performed with a Rheometrics Dynamic Mechanical Spectrometer using 25mm diameter parallel disks and a nitrogen atmosphere. All the samples were reacted isothermally at 30°C.

The evolution of the storage (G′) and loss (G") moduli at constant frequency was recorded as a function of the reaction time (time sweep). At chosen stages of the cross-linking process, the time sweep experiments were interrupted to measure the frequency dependence of G′ and G" (frequency sweep). Both types of experiments could be performed on the same reacting sample since the duration of a frequency sweep (about 6 minutes) was always very short compared to the total curing time (at least 15 hours with PPO425). Thus the samples could be regarded as unchanged during the short frequency sweep, and the evolving viscoelastic response of the partially cured networks could be analyzed.

5.1.1 Time Sweep Measurements

Figure 5.1 shows the isothermal evolution of G′ and G" versus reaction time for the network synthesized with PPO1000. Only the most interesting part of the curing curve is presented since the complete leveling off of both moduli required more than 24 hours at 30°C in this case. In a typical curing curve, the viscous behavior dominates the initial part of the experiment (G">>G′) and the elastic behavior dominates the end of the experiment (G′>>G"). Both moduli increase as a result of the increasing cross-link density but the elastic component rises more sharply than the viscous component. Such an evolution of the dynamic storage and loss moduli is characteristic for networks formed by end-linking reaction whith balanced stoichiometry. The same general behavior is observed for the networks prepared with PPO425 and PPO2000, as shown in Figures 5.2 and 5.3 respectively. The main differences

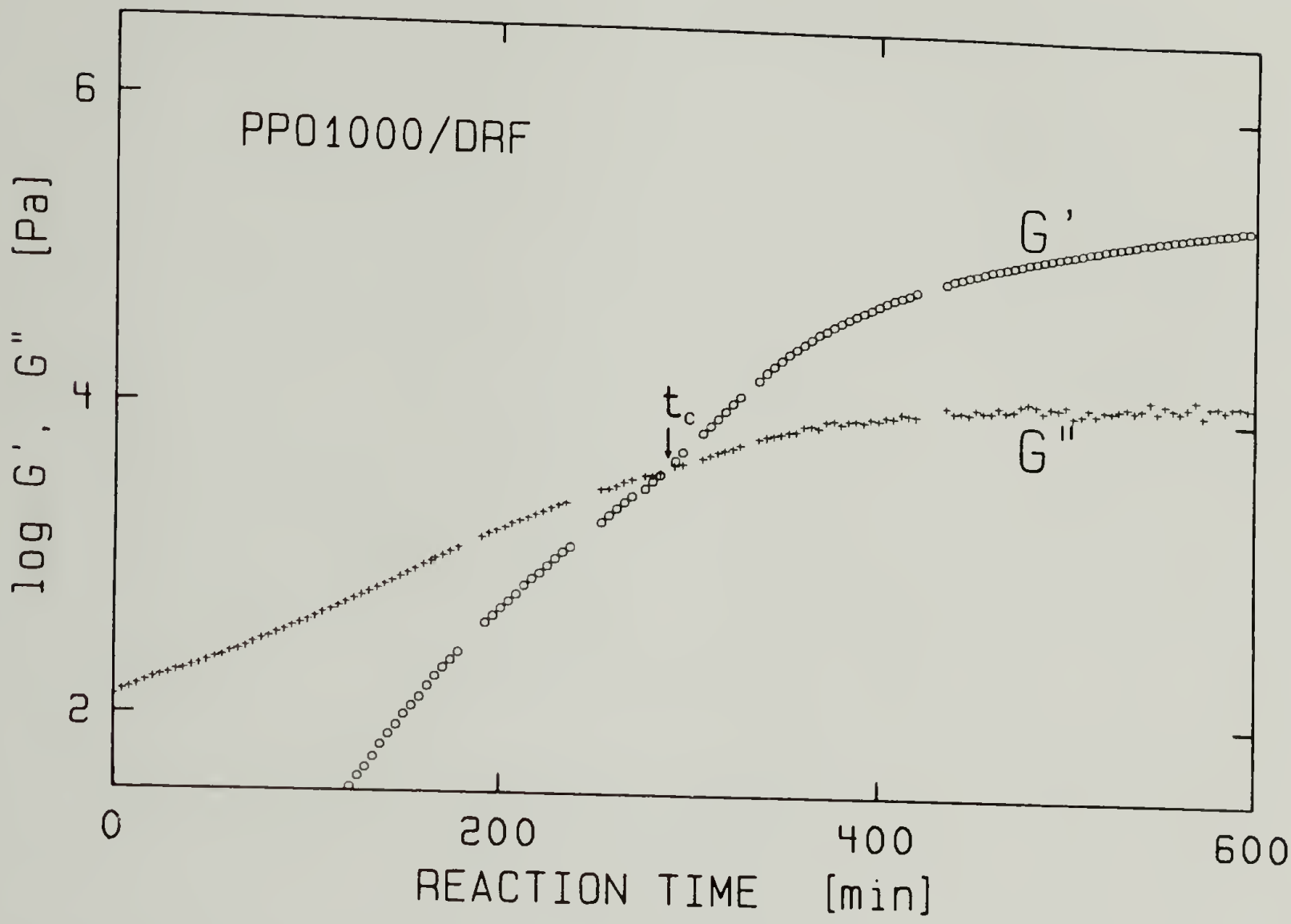

Figure 5.1. Curing curve of PPO1000/DRF with r=1.0 in an oscillatory shear experiment at constant temperature, T=30°C, and constant frequency, ω_0=0.5rad/s. t=0 marks the beginning of the rheological measurement but not the beginning of the crosslinking process.

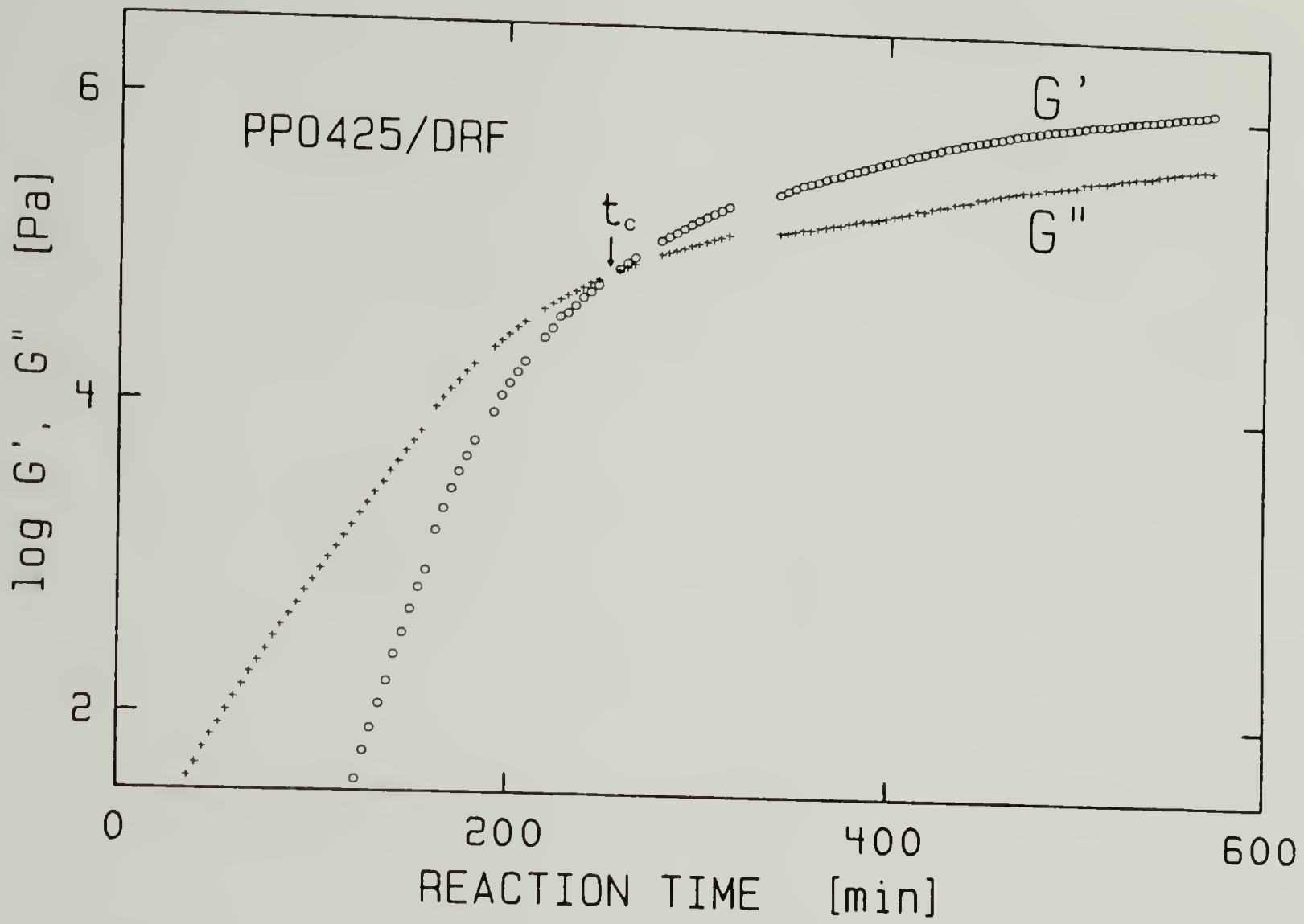

Figure 5.2. Curing curve of PP0425/DRF with r=1.0 at T=30°C, and ω_0=0.5 rad/s.

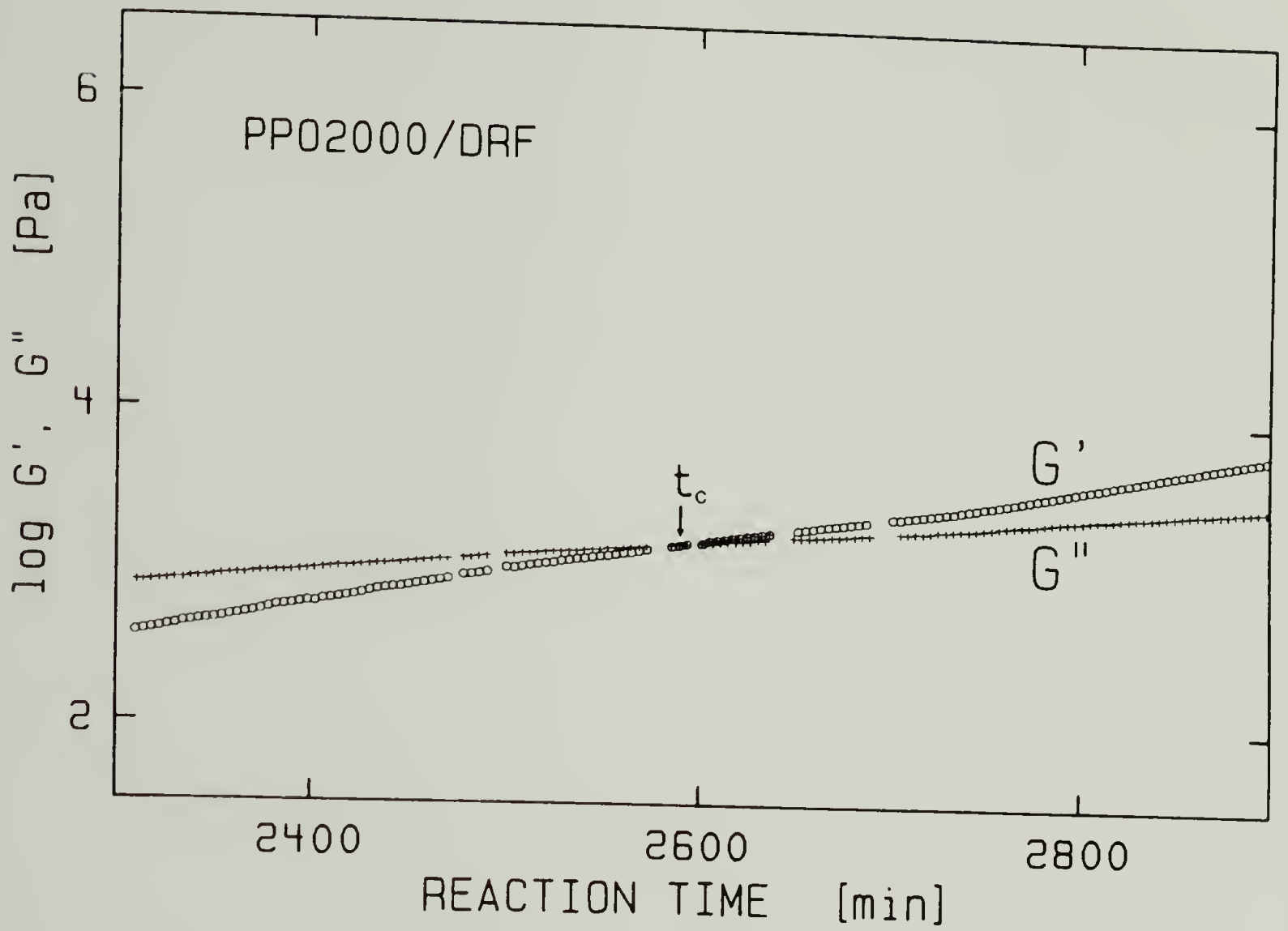

Figure 5.3. Curing curve of PPO2000/DRF with r=1.0 at T=30°C, and ω_0= 0.5rad/s.

between these curing curves are the magnitude of the moduli and the reaction rates. As the molecular weight increases the material becomes softer and the reaction rate slower.

The curing curves, Figures 5.1, 5.2 and 5.3, have been interrupted repeatedly. Sections of missing data points mark the intervals of time during which the viscoelastic properties of the partially cured networks have been studied by frequency sweep experiments.

5.1.2 Frequency Sweep Measurements

Frequency sweeps were performed in the vicinity of GP and are first presented for the network synthesized with PPO1000, as seen in Figure 5.4. The curves have been purposely shifted horizontally by a factor A (see table in Fig. 5.4) for easier comparison. Analysis of these data indicates that, as previously observed for the PDMS system, section 3.3.2,the crossover of G′ and G" on the curing curve occurs at the instant of gelation t_c, Figure 5.1. Shortly before t_c, the material is still a liquid and so both moduli decrease to zero at low frequency. Shortly after t_c, the storage modulus G′ tends towards a limiting value at low frequency demonstrating the existence of permanent elasticity characteristic of a solid material. Solubility tests described in section 6.4 supported this conclusion. The shapes of both $G'(\omega)$ and $G"(\omega)$ change smoothly as the reaction proceeds (i.e. G′ and G" approach each other, superimpose, and pass each other in a continuous fashion). These experiments confirm that the crossover in Figure 5.1 occurs at the instant of gelation and that rheological experiments can provide a very

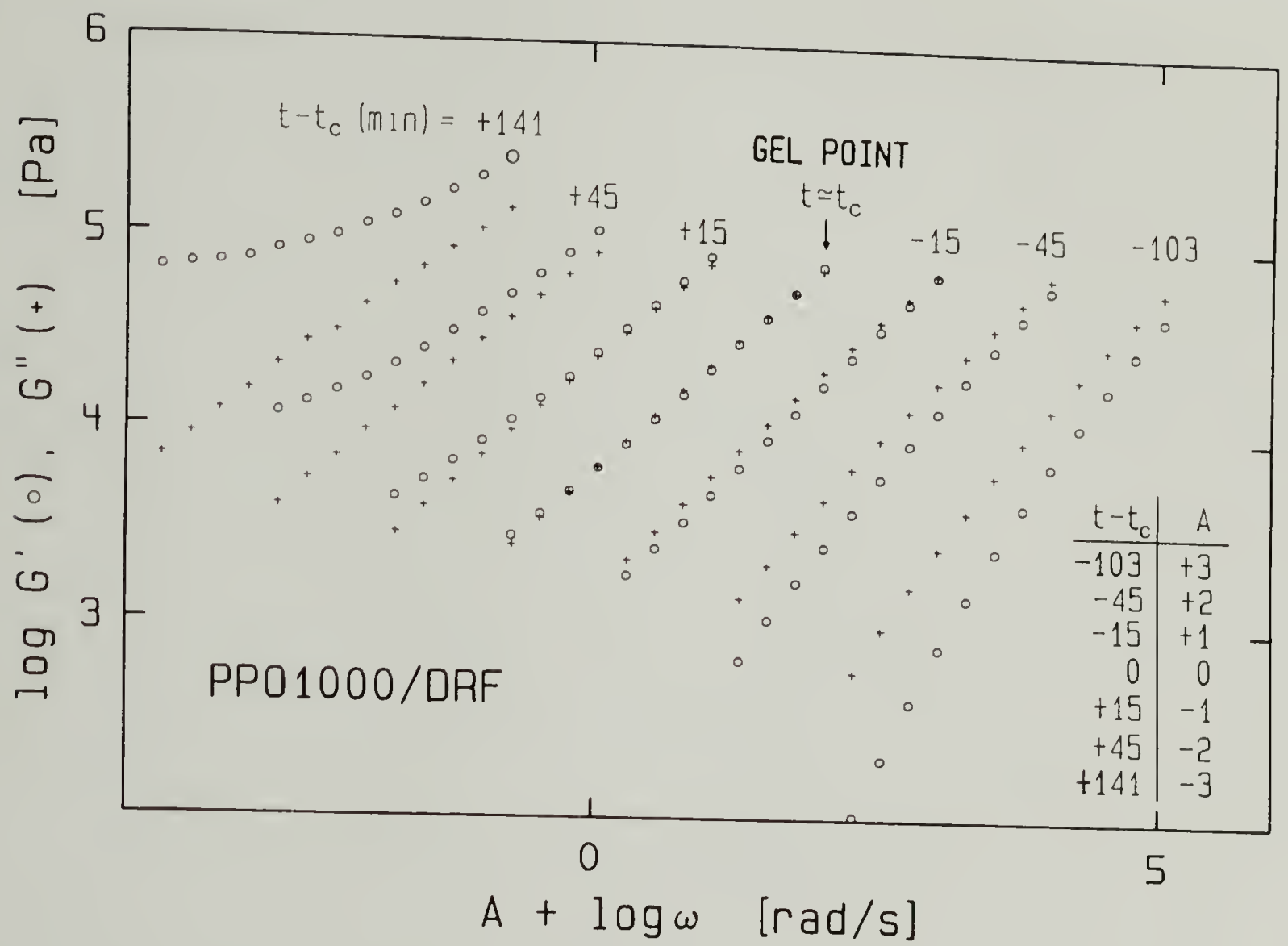

Figure 5.4. Storage and loss moduli at intermediate states of conversion for PPO1000/DRF with r=1.00. t_c is the instant of intersection (see Figure 5.1) of G' and G". The curves were shifted side-ways (factor A) to avoid overlap.

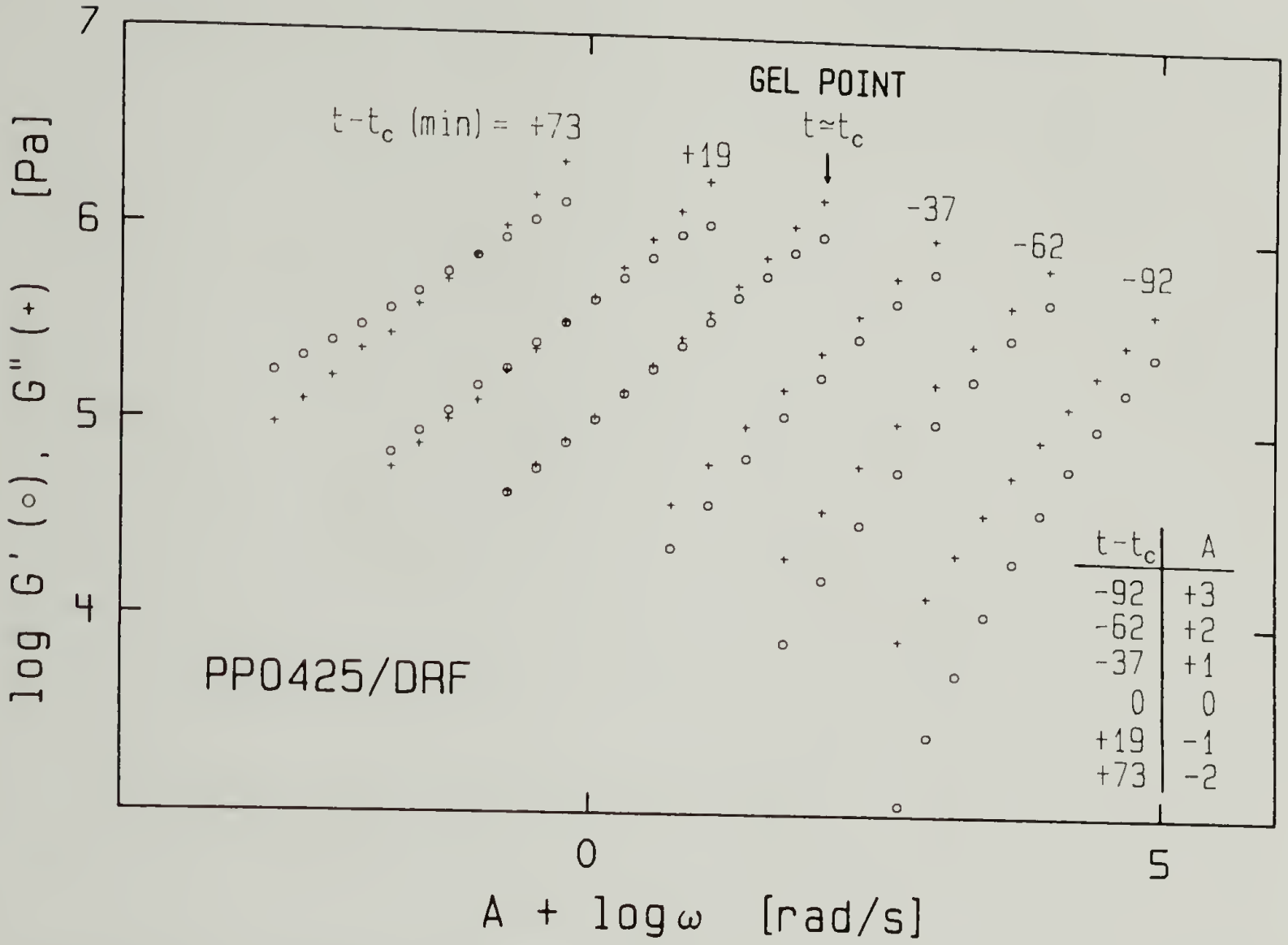

Figure 5.5. Storage and loss moduli at intermediate states of conversion for PP0425/DRF with r=1.00. t_c is the instant of intersection (see Figure 5.2) of G′ and G".

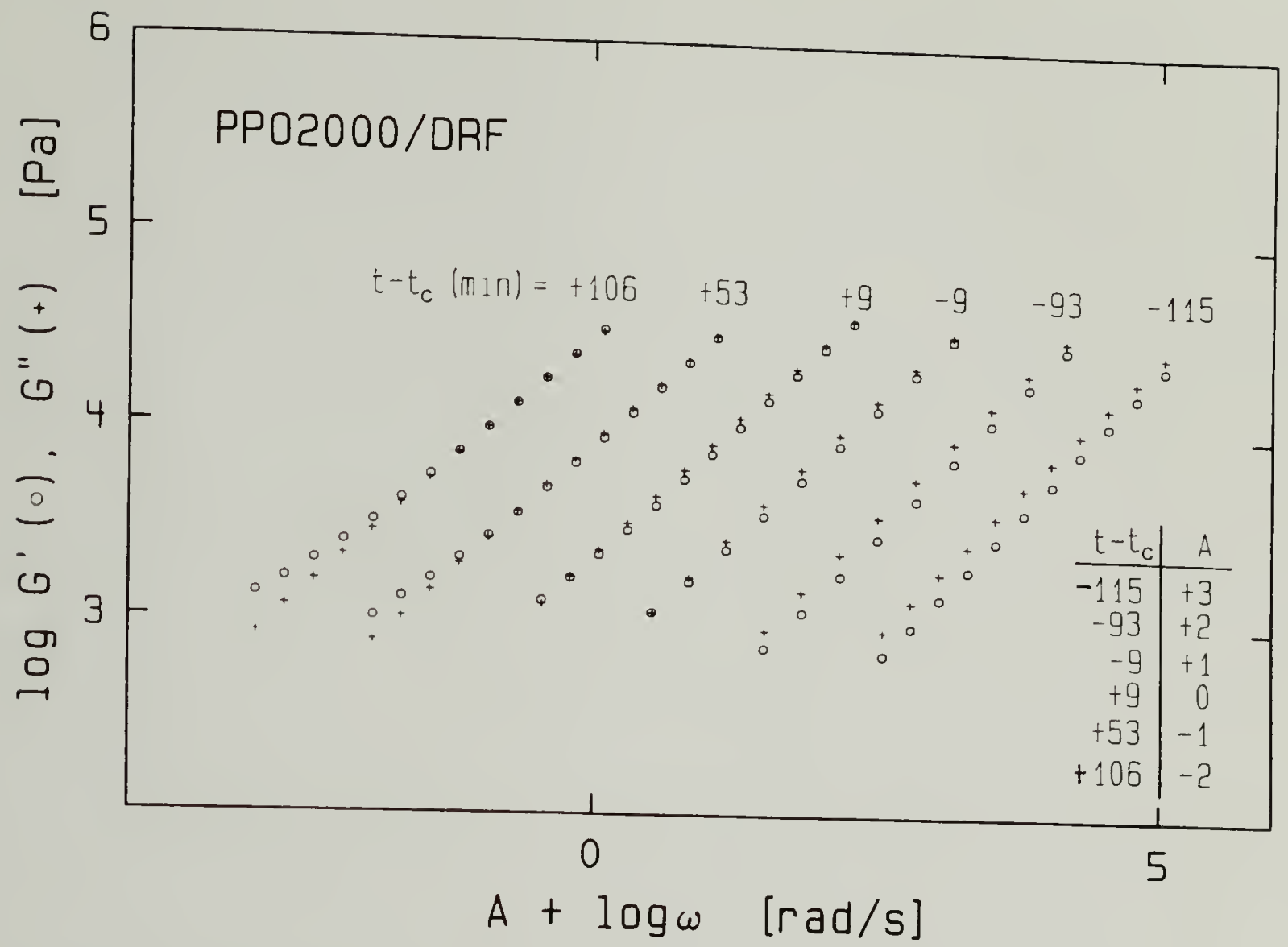

Figure 5.6. Storage and loss moduli at intermediate states of conversion for PPO2000/DRF with r=1.00. t_c is the instant of intersection (see Figure 5.3) of G′ and G".

sensitive tool to accurately localize GP.

The same general evolution of the rheological properties is observed for the samples prepared with PPO425 and PPO2000. However, with PPO425, presented in Figure 5.5, the determination of GP is not as straightforward. In this case, vitrification interferes with gelation and causes a deviation from the predicted behavior at high frequency. This effect is discussed in more detail in section 5.1.3. With PPO2000, shown in Figure 5.6, the reaction kinetics are very slow at 30°C and the exact instant of gelation is difficult to determine from the available range of measurements. In this case, t_c has been determined from the crossover of G′ and G" on the curing curve (time sweep experiment). However two states, t_c-9min and t_c+9min in Figure 5.6, are asymptotically close to GP and exhibit the moduli congruency predicted by the Gel Equation, Eq. (4.9).

The cross-linking reaction continues during the frequency sweeps which require about 6 minutes. The augmentation of G′ and G" during that time can be estimated using the slope of the curves in Figure 5.1, 5.2 or 5.3. At the gel point and for PPO1000, G′ increases by about 15% and G" by about 7% at 0.5 rad/s. Increases of less than 17% and 3% were found for G′ at the gel point of PPO425 and PPO2000 respectively. This systematic error is small and can be detected in Figure 5.7 as a very slight increase in slope beyond the expected value of 1/2.

For PPO1000 near the gel point, the 6 minutes time interval corresponds to an increase of the extent of reaction of about 0.2% as indicated by Feger et al. (1984) who studied the curing kinetics of a similar material. From their equation 7, and with a critical extent of

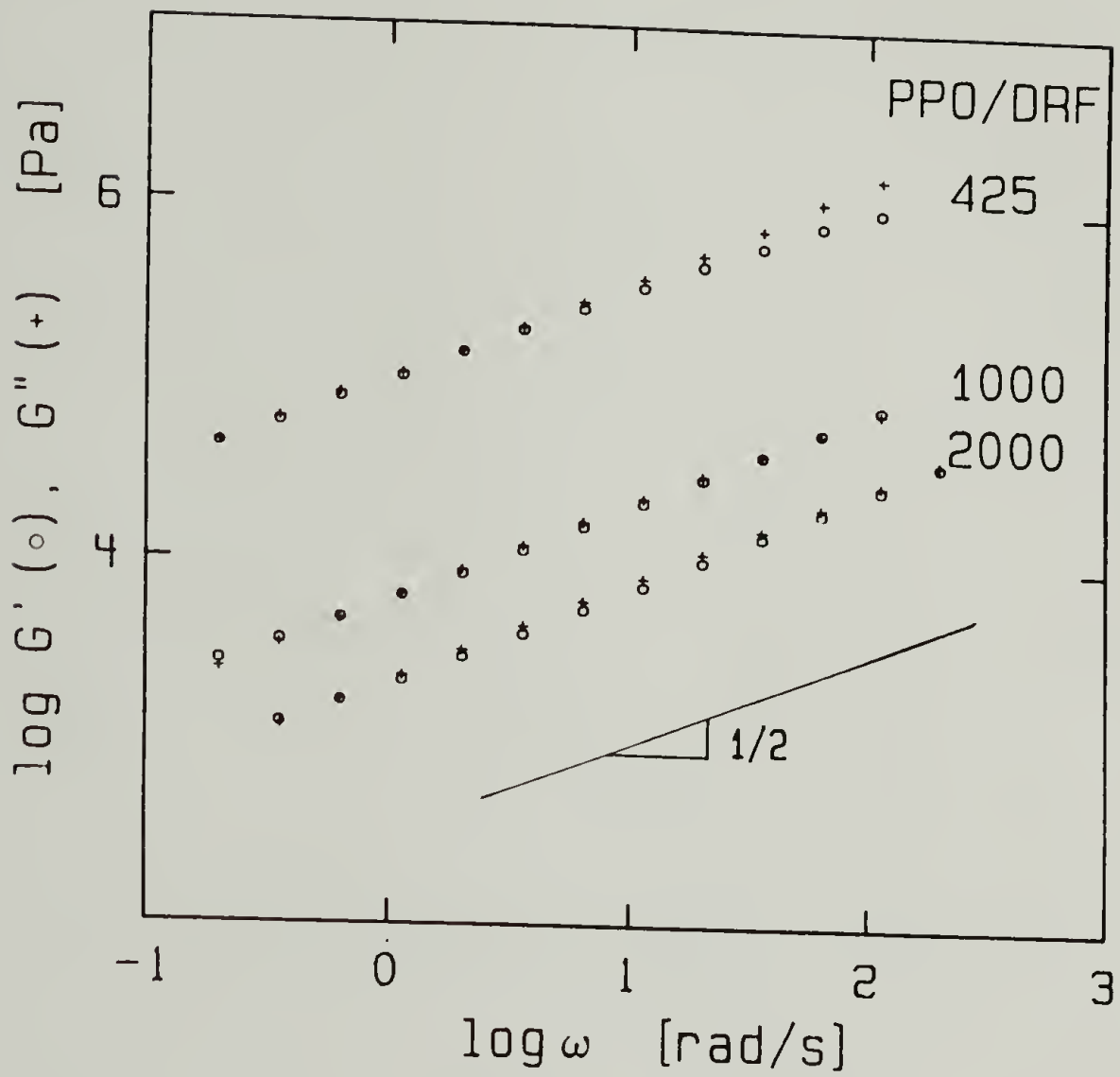

Figure 5.7. Storage and loss moduli at $t \simeq t_c$ for PPO1000/DRF, PPO425/DRf and PPO2000/DRF.

reaction as given by Flory's theory, the isothermal gel time t_c of PPO1000 at 30°C is calculated to be 530 minutes. The relative length of the frequency sweep is therefore $\Delta t/t_c=6/530=0.011$. Comparison with data of Adam et al. (1985) for the same value of $\Delta t/t_c$ indicates that our samples exhibited considerably smaller changes of the measured rheological parameters. This can be explained by the different range of shear rates used for the two experiments.

The range of measurements is limited to only 3 decades of frequency. Time-temperature superposition (Ferry, 1980) could not be applied at intermediate stages of the cross-linking process since the curing reaction of the PU had not been stopped. However, this limited range is sufficient to show that $G'(\omega)$ and $G''(\omega)$ grow together at $t=t_c$, and that they follow a power law with an exponent of 1/2 at that instant. The behavior which had been observed with a PDMS system over nearly 6 decades of frequency is now observed with the PU system, as shown in Figures 5.4, 5.5 and 5.6. This result is highly significant since the functionalities of the two systems are fundamentally different (i.e. PU with f=3 and PDMS with f=4).

5.1.3 Effect of Strand Length between Cross-Links on Rheological Properties at GP

The complex modulus of GP-networks with different strand lengths between cross-links is compared in Figure (5.7). Congruent moduli, $G'(\omega)=G''(\omega)$, and frequency dependence proportional to $\omega^{1/2}$ are observed for the networks prepared with PPO1000 and PPO2000. With PPO425 the

congruent behavior is only observed at low frequency. The deviation at high frequency is attributed to the interference of vitrification with gelation. DSC measurements performed on fully cured networks (Petrovic and MacKnight, personal communication), Table 5.1, suggest that the temperature of vitrification of the gel (T_{gg}) prepared with PPO425 must be relatively close to T=30°C . This results in a sharper rise of G"(ω) at frequencies above 10 rad/s while G'(ω) still exhibits a slope of 1/2. The same phenomenon may explain the results of Tung and Dynes (1982) who observed a frequency dependence for the reaction time needed to reach the crossover point of G' and G".

The material parameter S, called the gel 'strength' (see Eq. (4.9), appears to be extremely sensitive to changes of the strand length between cross-links, Figure 5.8. When the strand length is increased, the cross-link density is decreased thus resulting in a softer gel characterized by a lower value of S. The parameter S is related to T_{gg} through the cross-link density and so a gel with a lower value of S should exhibit a broader frequency range in which moduli are congruent.

In summary, it has been shown that cross-linking PU with balanced stoichiometry exhibit the same rheological behavior at the gel point as cross-linkinking PDMS with balanced stoichiometry; this behavior is described by a power law relaxation with a slope of 1/2. Consequently, the crossover time of G' and G", as measured during the cross-linking reaction, corresponds to the exact instant of gelation. However this result remains valid only if the frequency of the experiment is sufficiently low or if the experimental temperature is sufficiently far from the temperature of vitrification of the gel. Further comparisons with

Table 5.1. Glass temperature of the fully PU cured networks

Polymer	T_g midpoint (°C)
PPO425/DRF	+33
PPO1000/DRF	-20
PPO2000/DRF	-50

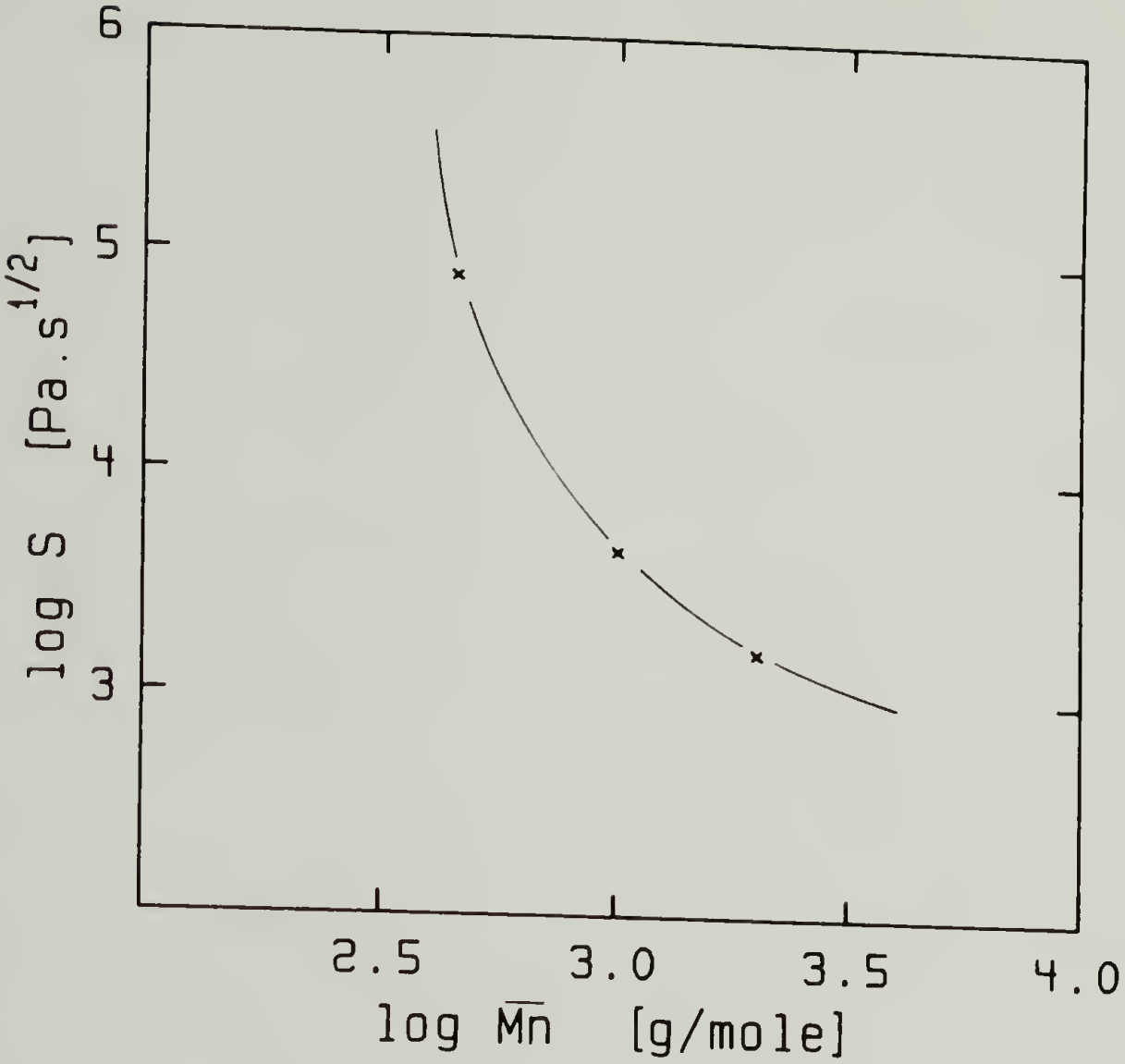

Figure 5.8. Measured gel strength as a function of PPO strand length.

the PDMS behavior now require the study of PU gels with imbalanced stoichiometry.

5.2 Rheology of PU Gels with Imbalanced Stoichiometry

The stoichiometric ratio, r, of the PU system is defined here as the ratio of isocyanate to hydroxyl groups. From Flory's (1953) theory of gelation, and assuming an ideal cross-linking process, the PU system is expected to reach the gel state for stoichiometric ratios ranging from $1/2<r<2$. PU samples with stoichiometric ratios r=0.596, 0.743, 1.48 and 1.72 were prepared by following the procedure described in section 2.2.2. The sample with balanced stoichiometry was already studied in section 5.1. In order to avoid the interference of vitrification with gelation, and to obtain some reasonably fast reaction rates, PPO1000 was selected for this investigation.

The experimental conditions used to measure the changes in dynamic storage and loss moduli during isothermal cure were similar to those described in section 5.1. The curing curves obtained with the two most extreme stoichiometric ratios are presented in Figures 5.9 and 5.10, and can be compared to the evolution with balanced stoichiometry shown in Figure 5.11. As expected, a strong dependence of the reaction rates upon the stoichiometric ratio is seen. With imbalanced stoichiometries, the rate of the cross-linking reaction decreases and the elasticity of the final material decreases. The influence of the stoichiometric ratio upon the properties of the final PU networks is discussed in section 5.3. For the moment, we limit ourselves to the study of the developing

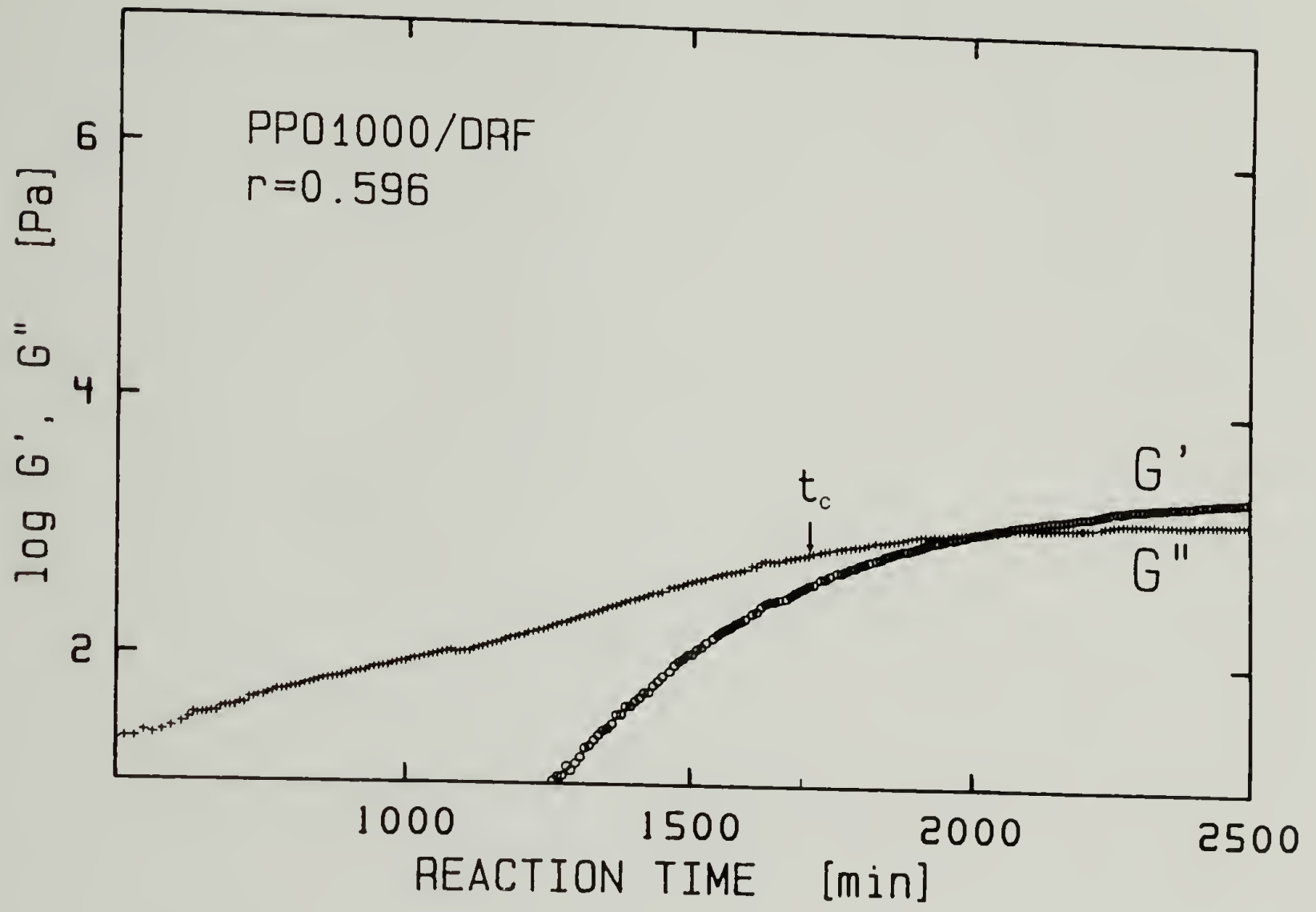

Figure 5.9. Curing curve of PPO1000/DRF with r=0.596 at T=30°C, and ω_0=0.5rad/s.

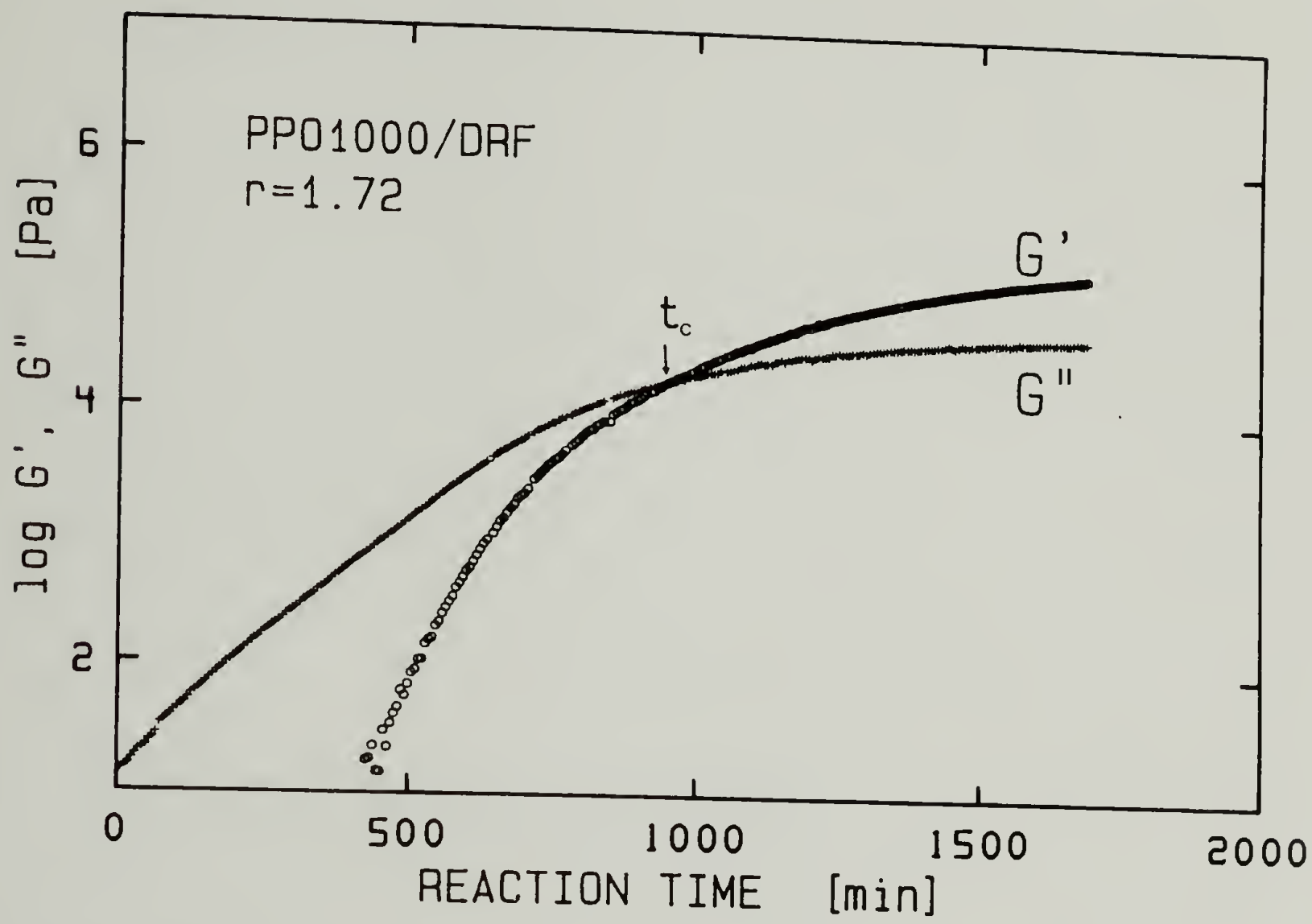

Figure 5.10. Curing curve of PPO1000/DRF with r=1.72 at T=30°C, and ω_0=0.5rad/s.

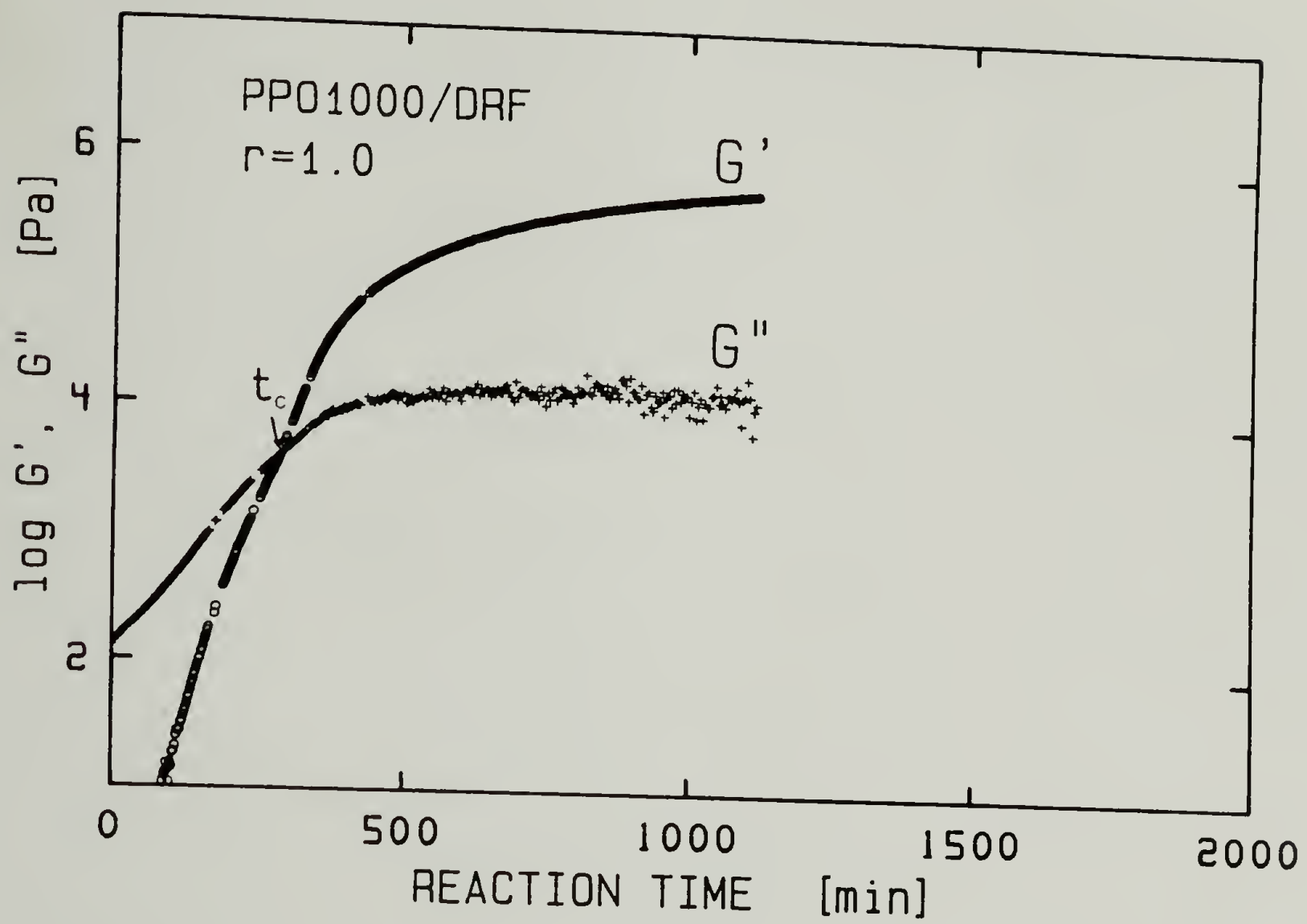

Figure 5.11. Curing curve of PPO1000/DRF with r=1.00 at T=30°C, and ω_0=0.5rad/s.

network.

Frequency sweeps were performed at intermediate states during the cross-linking process. The curves obtained are presented in Figures 5.12 to 5.15. A similar evolution from liquid to solid state is seen for all the stoichiometric ratios for which gelation is possible. The remarkable common behavior, however, is the occurence of a critical time, t_c, at which the dynamic moduli follow the power law evolution predicted by the Gel Equation. For gels with a deficiency of cross-linker, the same variation as previously observed with the PDMS is seen in Figure 5.16. With decreasing values of r below the balanced stoichiometry, the slope of the power law increases above n=1/2, and G" is greater than G' as predicted by Eq. (4.5). Surprisingly, such an evolution of the power law behavior is not observed for gels with an excess of crosslinker. In this case the power law exponent of n=1/2 is conserved and seems to be a limiting value. For systems with an excess of crosslinker, the instant of gelation can be easily determined from the crossover point of the loss and storage moduli on the curing curve, Figure 5.10. In contrast, this crossover point is far away from the gel transition for r=0.596, as seen in Figure 5.9.

The systematic error due to the fact that the material is changing during the frequency sweep experiment (i.e. reaction not stopped) was shown to be small in the case of the balanced stoichiometry. With imbalanced stoichiometric ratios, this error is even smaller since the reaction rates are slower. This can be detected in Figure 5.16 where the slope of 1/2 is more closely followed by the sample with r=1.48 than with r=1. However, a slight deviation from the power law behavior is

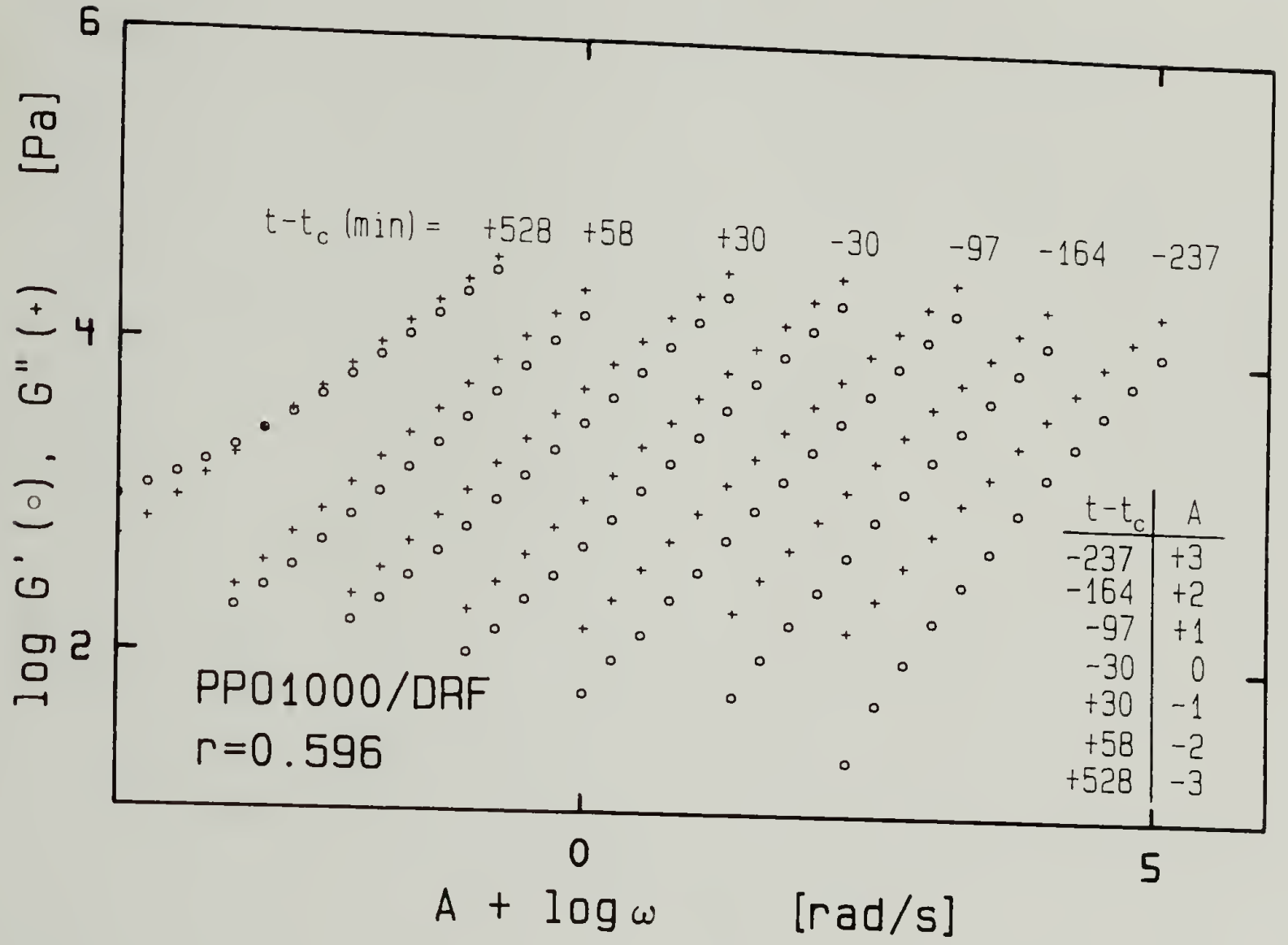

Figure 5.12. Storage and loss moduli at intermediate states of conversion for PPO1000/DRF with r=0.596. t_c is not the instant of intersection (see Figure 5.9) of G' and G".

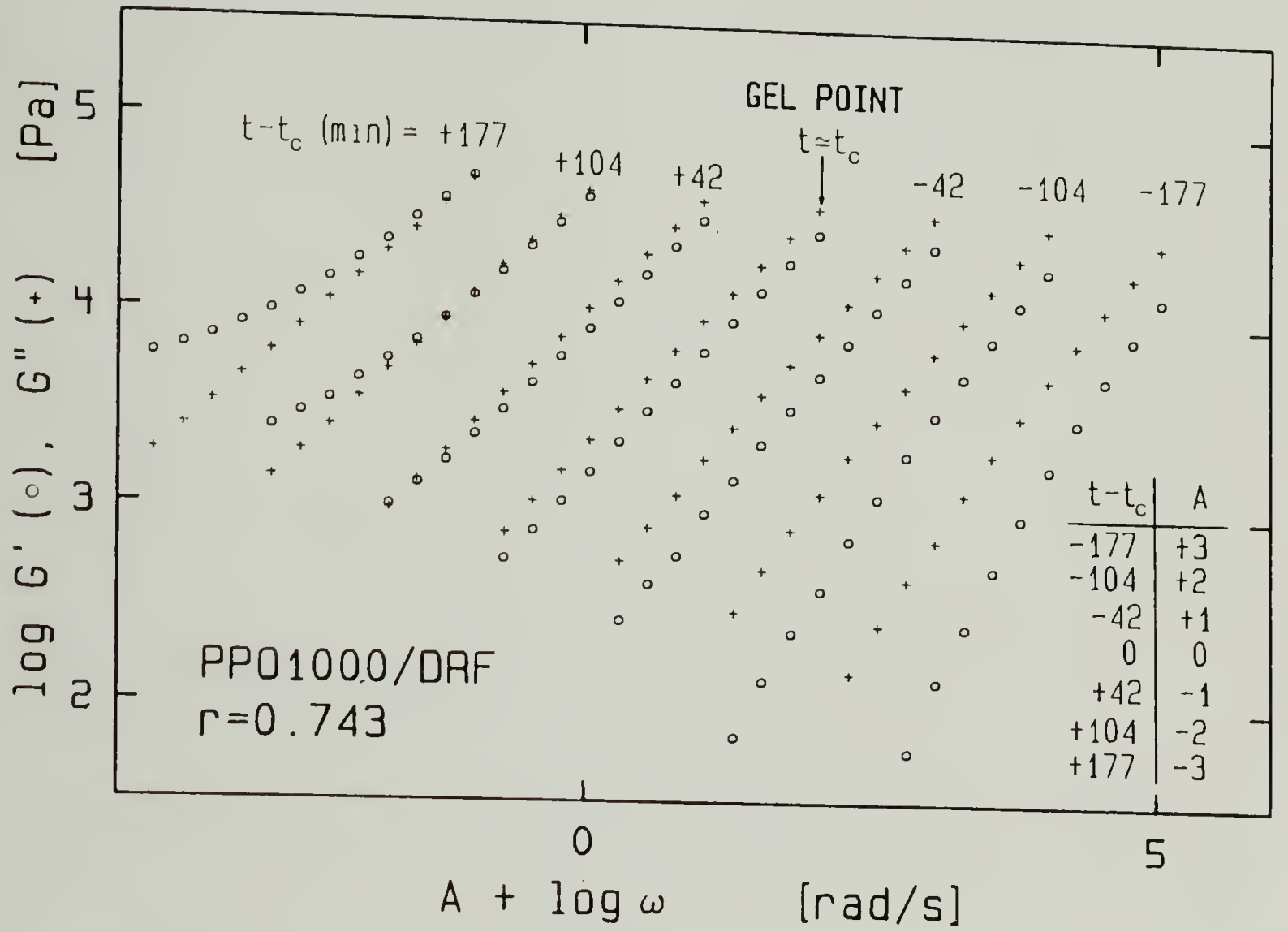

Figure 5.13. Storage and loss moduli at intermediate states of conversion for PPO1000/DRF with r=0.743.

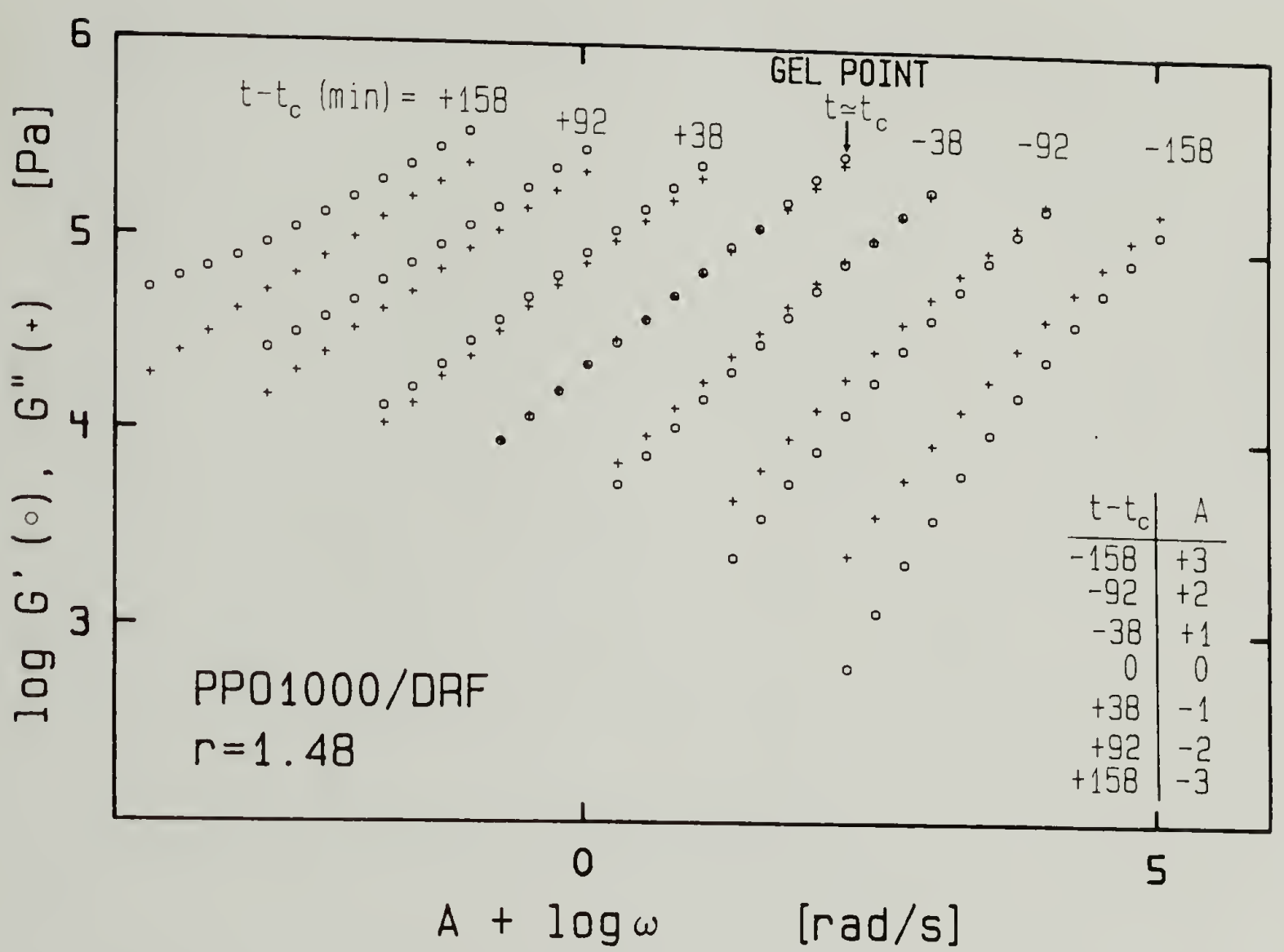

Figure 5.14. Storage and loss moduli at intermediate states of conversion for PPO1000/DRF with r=1.48.

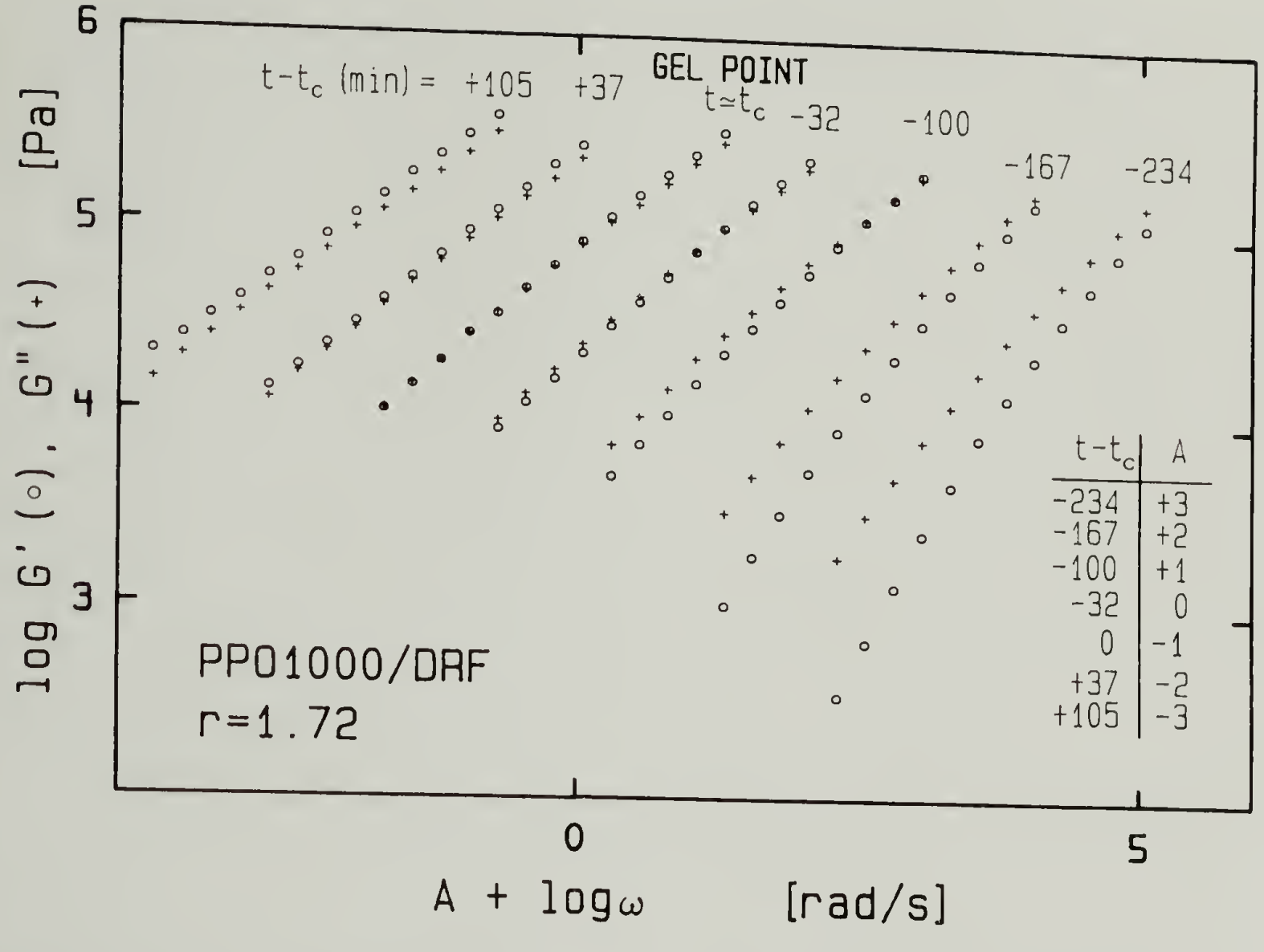

Figure 5.15. Storage and loss moduli at intermediate states of conversion for PPO1000/DRF with r=1.72. t_c is the instant of intersection (see Figure 5.10) of G' and G".

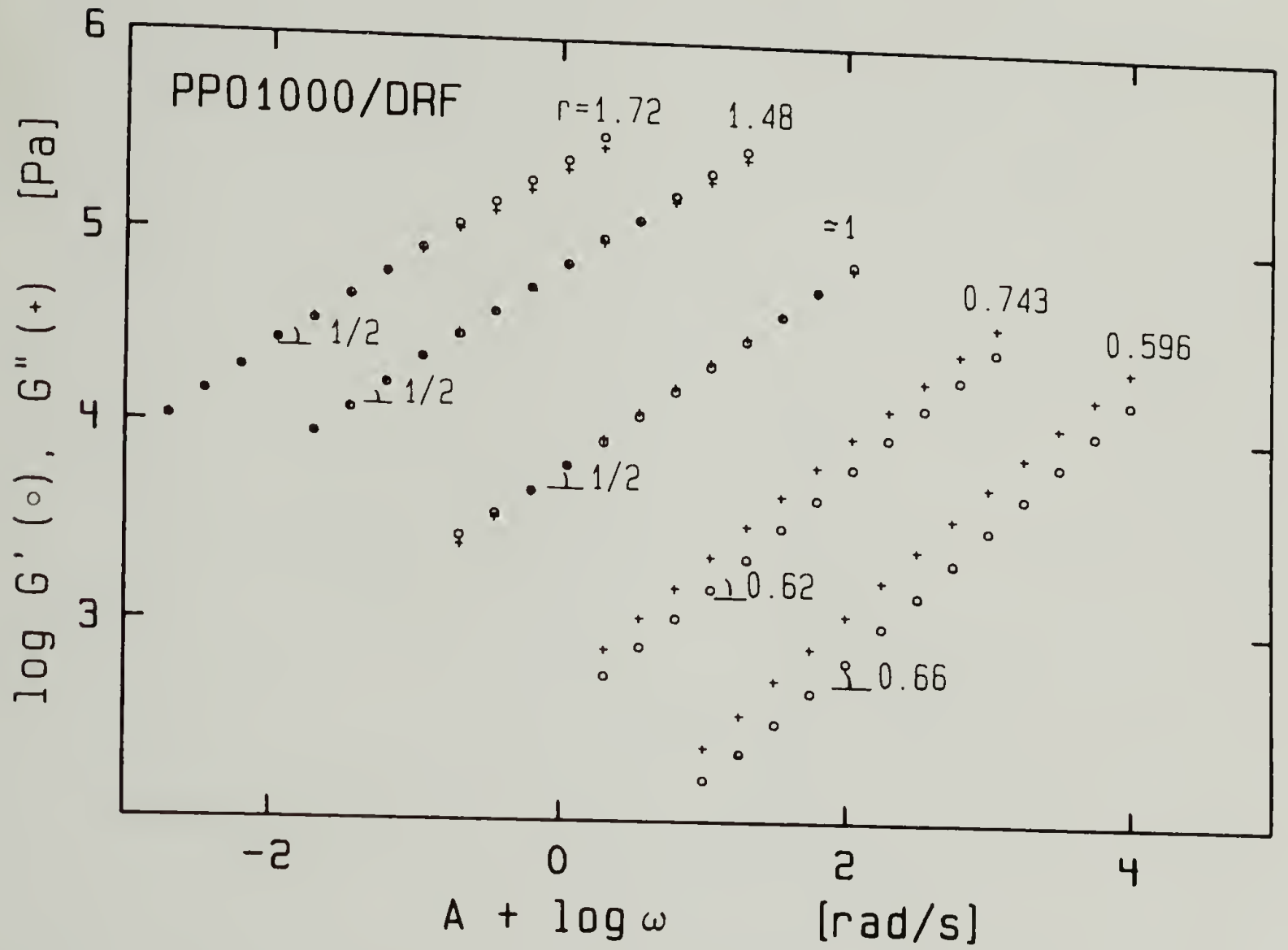

Figure 5.16. Storage and loss moduli at $t \approx t_c$ for PPO1000/DRF with r= 0.596, 0.743, 1.0, 1.48, 1.72.

seen at high frequency as the excess of cross-linker is increased. This has to be distinguished from the deviation which was observed with PPO425 (see Figure 5.7) and which was attributed to the interference of vitrification. In the present case where G" becomes lower than G' at high frequency, the behavior is most likely to be explained by an entanglement effect. A similar variation of the loss and storage moduli at high frequency is observed on the data of Roovers and Graessley (1981) who studied rather high molecular weight comb polymers. Data over a more extended frequency range would be needed to clarify this point. However, the power law behavior is quite well obeyed over the three decades of frequency studied, and moduli congruency is expected to continue at low frequency.

5.3 Discussion

The evolutions of the power law exponent and of the gel strength, as a function of the stoichiometric ratio are summarized in Figures 5.17 and 5.18. It is seen in Figure 5.17, that an upper value of the power law exponent exists for cross-linker deficient gels. This is in qualitative agreement with the fractal theory of Muthukumar (1985), Eq. (4.16). However the experimental value measured, n=0.66, is slightly higher than the theoretical prediction, n_{max}=0.6. A limiting power law regime is also evident in gels with an excess of cross-linker. This result suggests a lower limit of 2 for the fractal dimension. Equally interesting is the evolution of the gel strength, S, shown in Figure (5.18). For crosslinker deficient systems, a soft gel with low dynamic

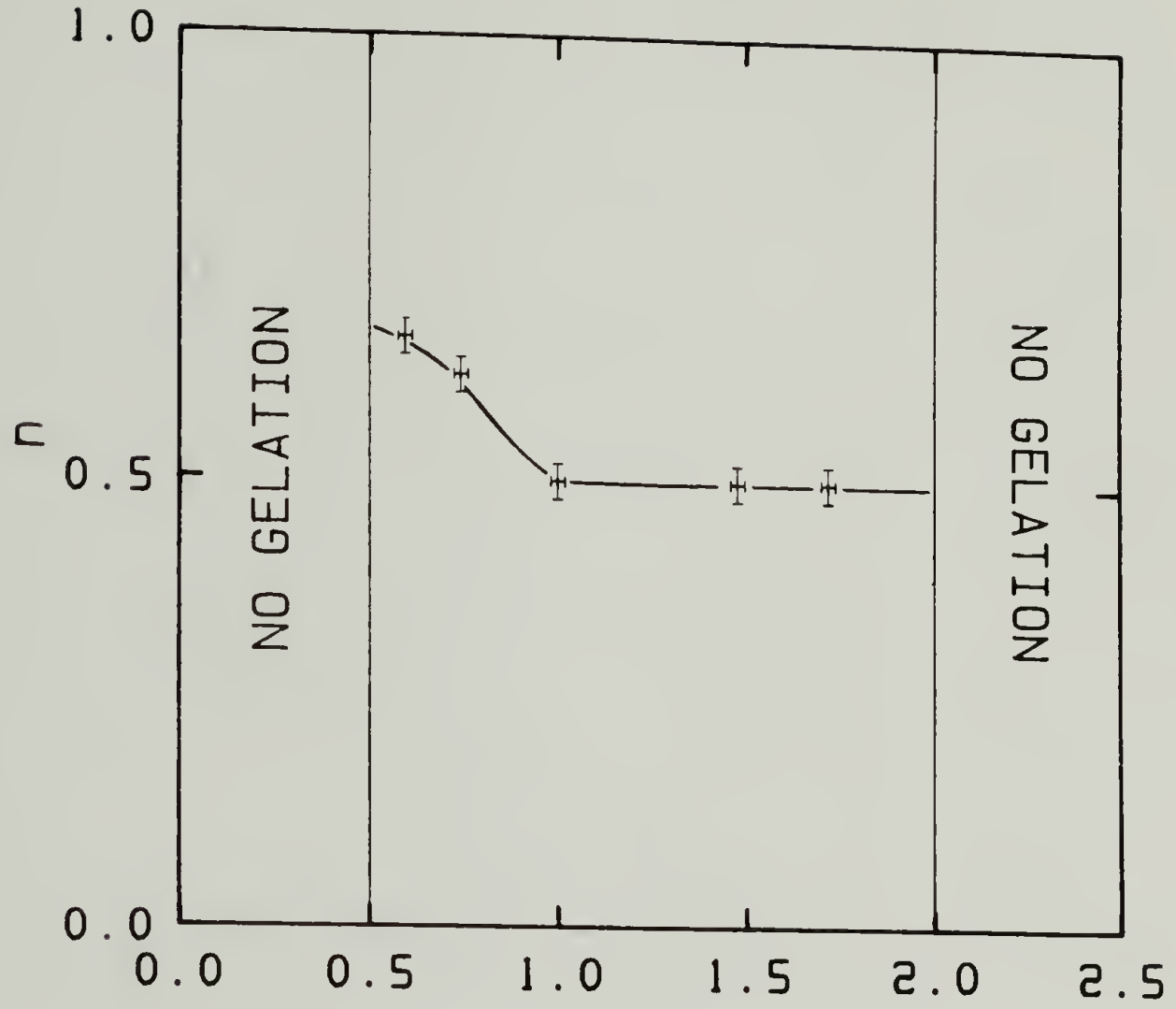

Figure 5.17. Measured power law exponent as a function of the stoichiometric ratio for PPO1000/DRF.

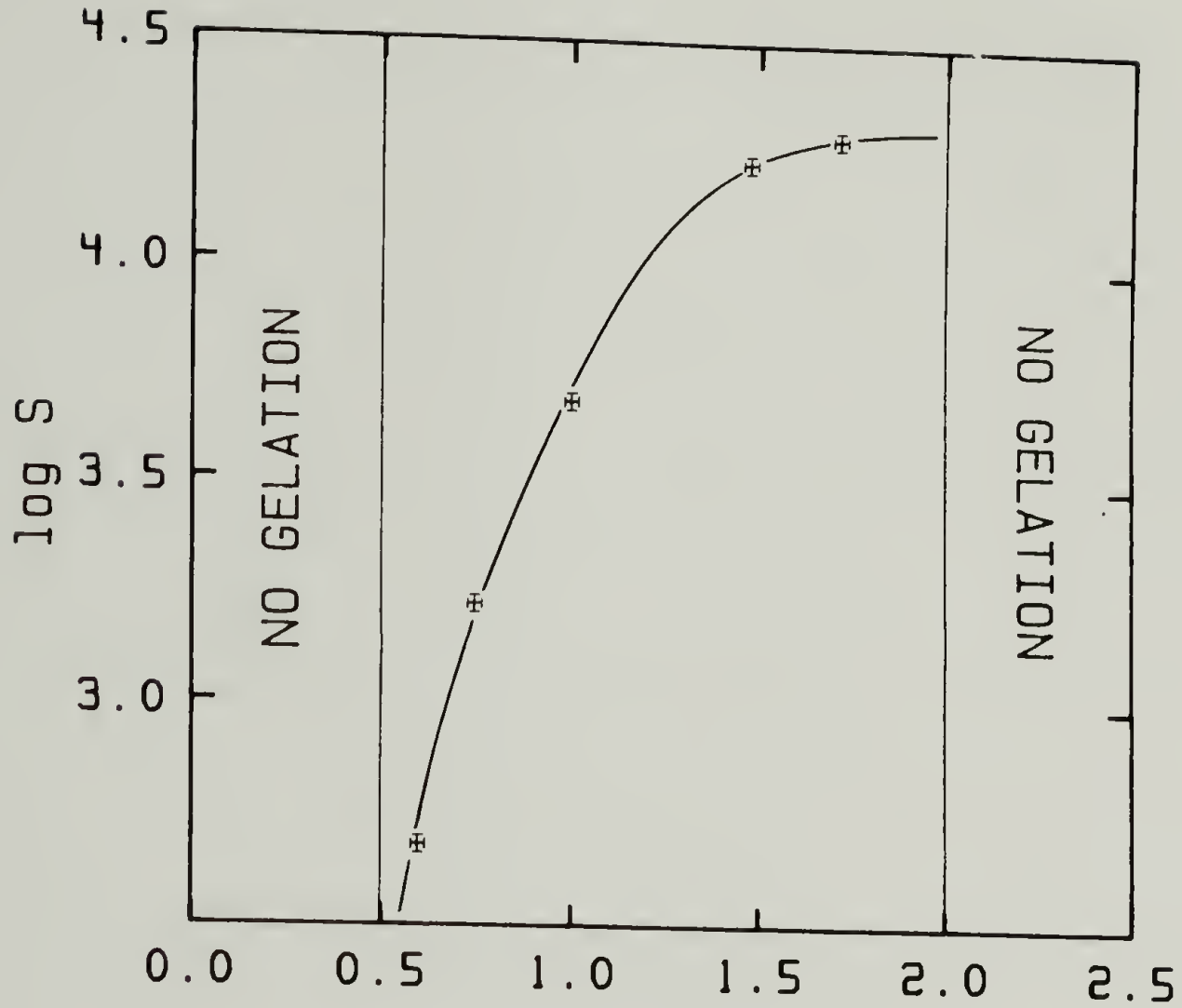

Figure 5.18. Measured gel strength as a function of the stoichiometric ratio for PPO1000/DRF.

moduli and therefore a low strength is produced. By contrast, the gel strength measured for networks with an excess of crosslinker reaches an upper value larger than the strength of the stoichiometrically balanced gel. This result, together with the evolution of the power law exponent, suggests that gels with a deficiency of crosslinker lead to more highly branched molecules and therefore to a higher fractal dimension than gels with an excess of cross-linker. By contrast, these latter produce longer but less branched molecules able to form entanglements which result in a higher strength.

The asymmetric variation of the power law exponent with stoichiometric ratio recalls the previously discussed asymmetric shape of the storage modulus as a function of the same parameter for fully cured PDMS (see Figure 3.1). A similar curve has been measured with the PU system and is presented in Figure 5.19. The maximum of the storage modulus seems to occur for values of r slightly higher than 1. Even though r=1 was considered to be the balanced stoichiometry of the PU system. More data points would be needed to confirm this result. As observed with the PDMS system, crosslinker deficiencies decrease the elasticity of the final network more efficiently than crosslinker excesses. It is also important to note that the minimum of $\tan\delta$ occurs at the same stoichiometric ratio as the maximum of the storage modulus. This result suggests that, as discussed in section 3.1, the network with the highest elasticity is also the most perfect.

In conclusion, the constitutive equation, Eq. (4.9), which was previously found to describe the viscoelastic properties of a PDMS network at GP is also valid for a PU system, independent of the cross-

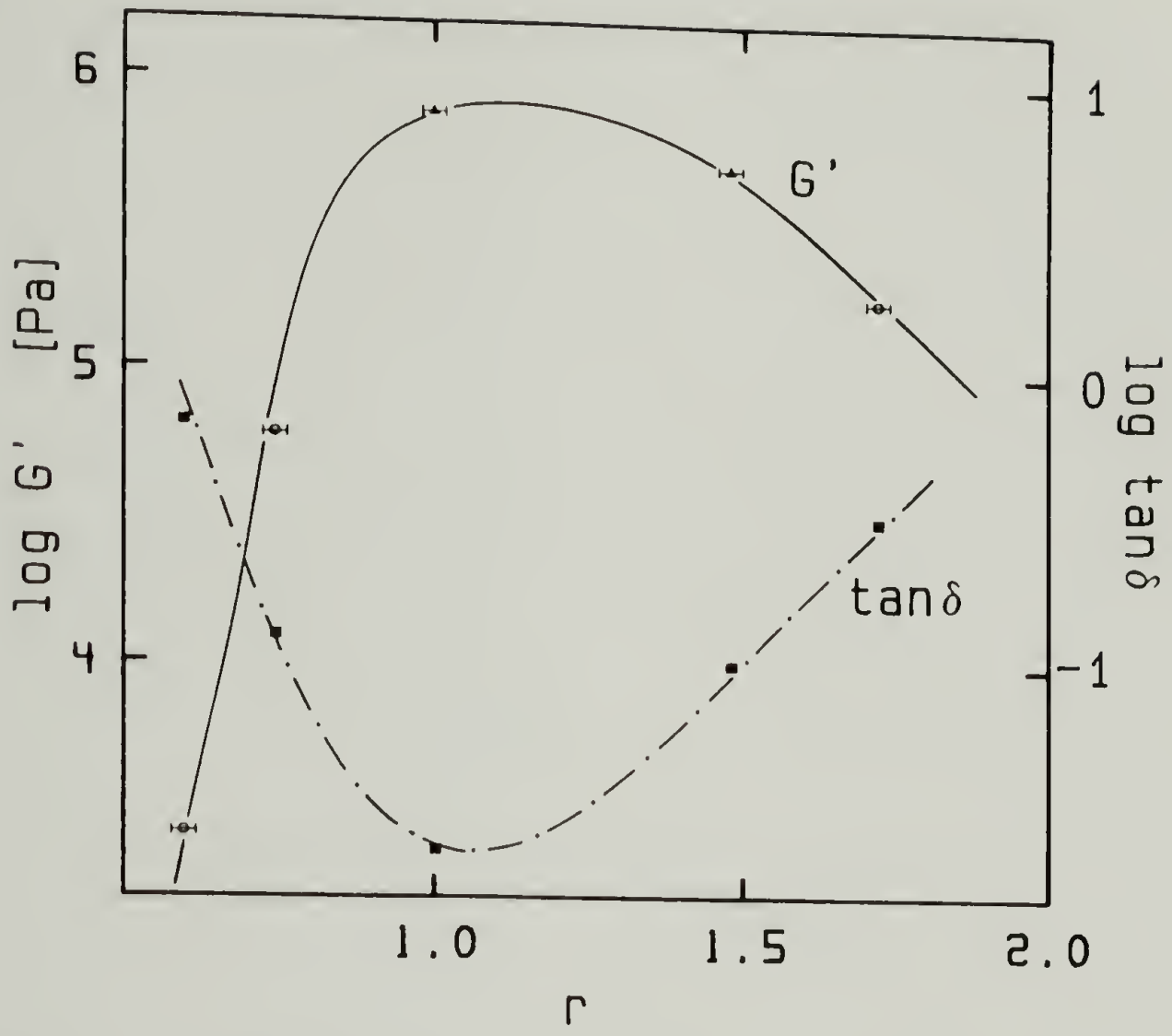

Figure 5.19. Storage modulus and tangent of the loss angle of cured PPO1000/DRF as a function of the stoichiometric ratio. (△) Fully cured at 90°C; (○) cured at 30°C, final moduli estimated from the curing curves (see Figures 5.9 and 5.11).

linker functionality. For balanced stoichiometry, $G'(\omega)$ and $G''(\omega)$ are found to be congruent and proportional to $\omega^{1/2}$, regardless of the strand length between cross-links. The gel strength, S, strongly increases as the strand length between cross-links is decreased. For imbalanced stoichiometric ratios, $G'(\omega)$ and $G''(\omega)$ are found to be proportional to ω^{n}, with $n=1/2$ for networks with balanced stoichiometry or cross-linker excesses and $0.66<n<1/2$ for networks with crosslinker deficiencies. The gel properties strongly depend on the stoichiometric ratio but molecular theories are needed to understand these variations.

C H A P T E R V I

PHYSICAL CHARACTERIZATION OF CROSS-LINKING PDMS

The purpose of this chapter is to present some physical experiments which complement the rheological study. These experiments are meant to be exploratory in nature and to suggest future research in the field of polymer gelation. Measurements of the degree of conversion for fully cured PDMS networks are discussed first. The curing kinetics of a PDMS network with balanced stoichiometry are measured by the infrared absorption intensity of the silane stretching band at 2134cm^{-1}. The extent of reaction at the gel point was determined and compared to the predictions of branching theory (Macosko and Miller, 1976). HNMR measurements during the curing reaction of a similar material are also presented. The molecular mobility at short scale length is demonstrated to decrease progressively through the gelation transition, and without any discontinuity at GP. Finally, solubility tests demonstrating the consistency of the rheological study are described.

6.1 Extent of Reaction of Fully Cured PDMS Networks

Effective cross-linking processes produce networks with a high degree of conversion. Networks with a low degree of conversion are usually the result of either an ineffective cross-linking reaction or an

improper sample preparation. Such imperfect networks can lead to erroneous conclusions and are not desirable for this study. In order to evaluate the 'quality' of the PDMS samples produced here, the degree of conversion of the fully cured networks utilized in section 3.1 was measured, and compared to previously reported data.

After curing in the rheometer (see section 3.1), the fully reacted PDMS networks were separated from the parallel disk assembly and transparent elastomers with a known thickness were obtained. These samples were subsequently placed on a KBr plate and were directly used for infrared measurements on an IBM IR/98 Fourier transform spectrometer.

Assuming that the change in SiH concentration between the initial mixture and the fully cured network is only due to the reaction between silane and vinyl, the degree of conversion can be evaluated by measuring the change of the infrared absorption of the SiH stretch at $2134cm^{-1}$ as seen in Figure 6.1. As already reported by Valles and Macosko (1979), the peak area at $1970cm^{-1}$ was found to be a function of the sample thickness only. It was therefore used as an internal standard to adjust for the slight thickness changes from one sample to another.

The linearity between absorbance and silane concentration was verified by mixing known amounts of prepolymer and crosslinker without adding any catalyst. A liquid cell with KBr plates and a 0.25mm spacer were used for these measurements. The peak area between 2107 and $2183cm^{-1}$ was determined as a function of the silane concentration. The resulting calibration curve is shown in Figure 6.2. Beer's law is seen to be valid for the range of silane concentrations of interest.

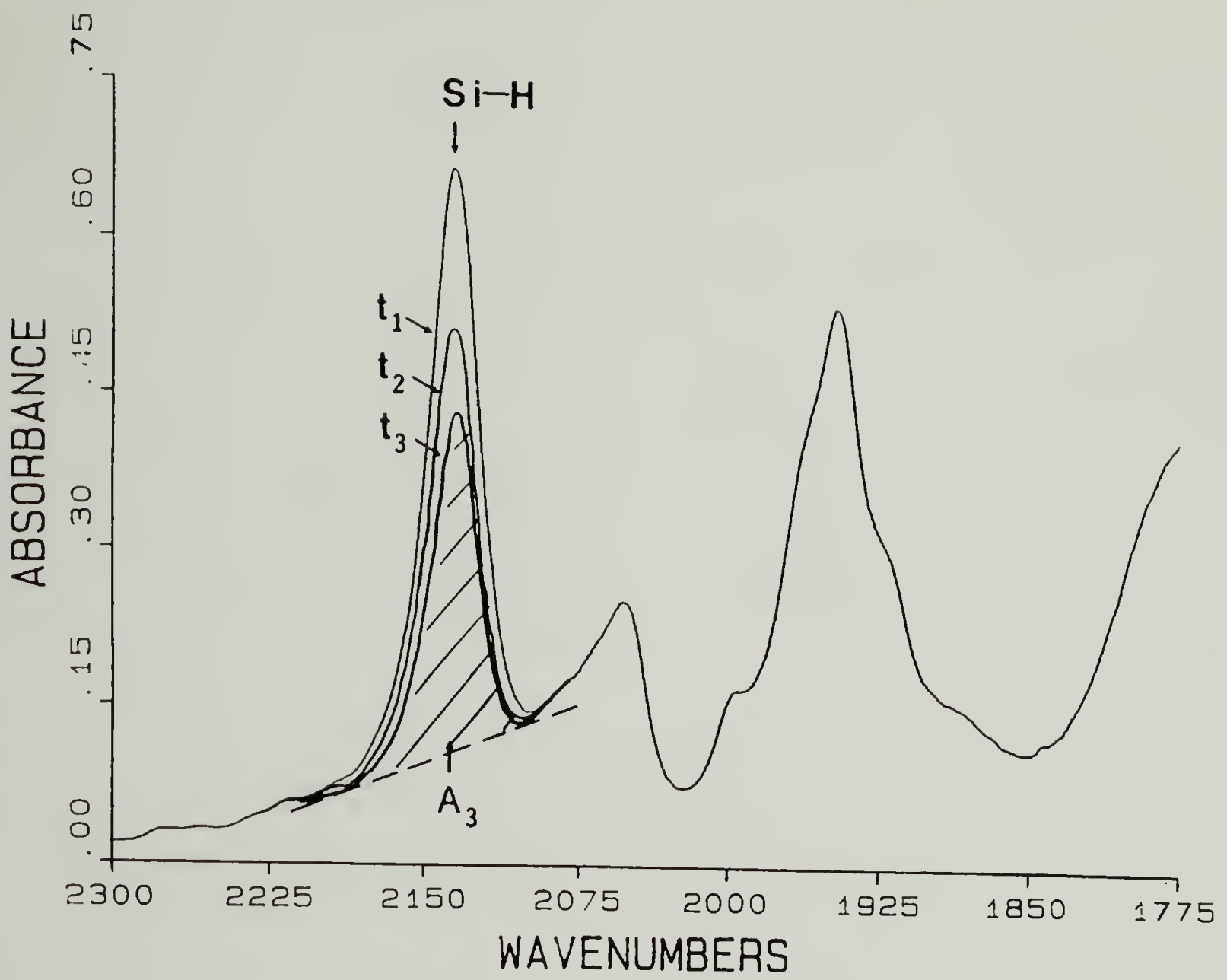

Figure 6.1 FTIR absorbance spectra of the curing PDMS at different times, t_i, and T=34°C.

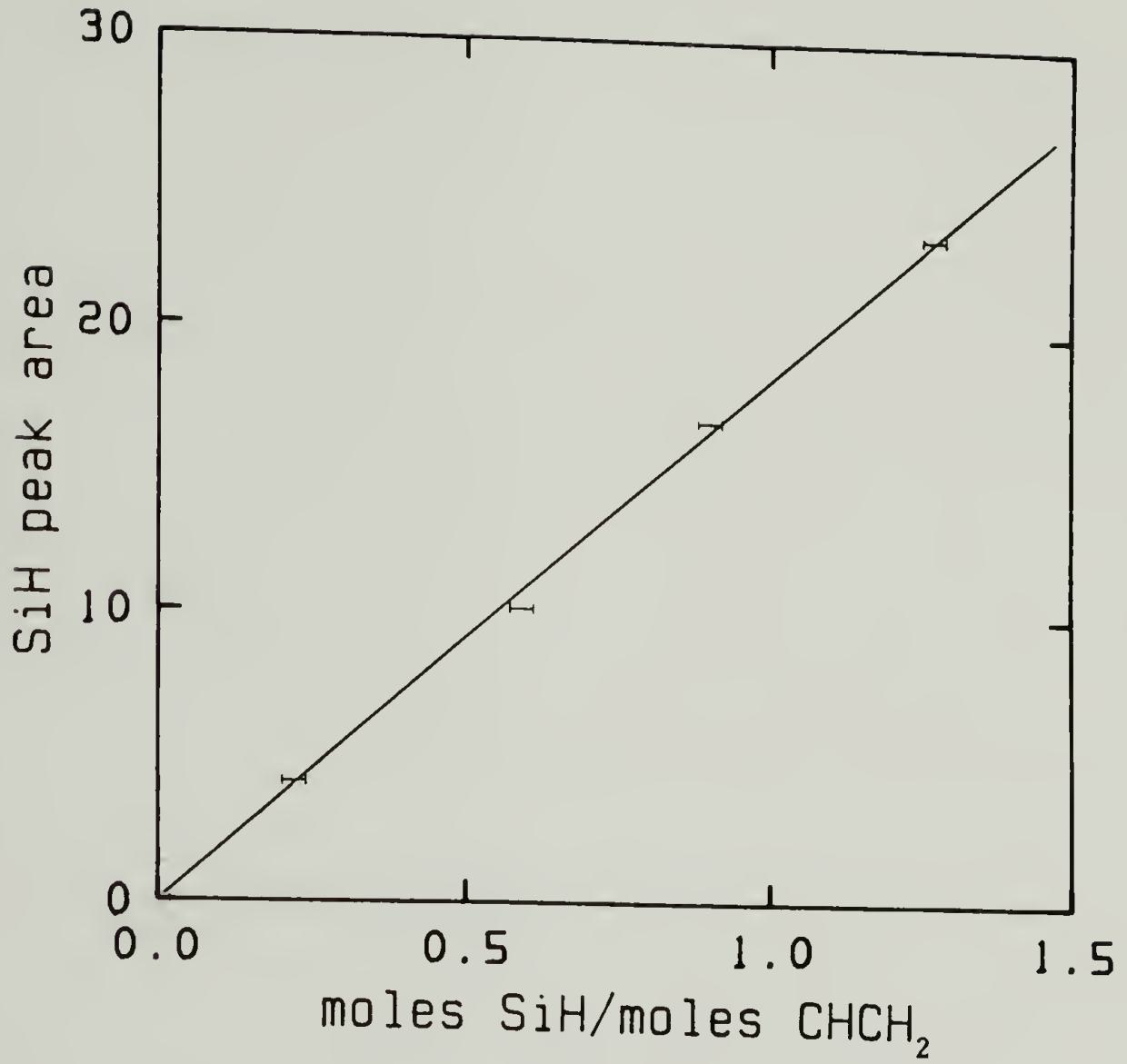

Figure 6.2. SiH absorption as a function of the ratio $SiH/CHCH_2$ at T=34°C.

The degree of conversion of the SiH groups, p_{SiH}, was determined as

$$p_{SiH} = \frac{A_0 - A_f}{A_0} \qquad (6.1)$$

where A_0 is the SiH peak area of the initial mixture (given by the calibration curve), and A_f is the SiH peak area of the fully cured sample reduced to a thickness of 0.25mm. The results of the measurements are presented in Figure 6.3. Their accuracy is within $\pm$ 2%.

For all the stoichiometric ratios, high degrees of SiH conversion are observed. The measured values are in good agreement with the previously reported p_{SiH} of more than 85% found by several groups on a similar system, and summarized in the revue article of Gottlieb et al. (1981). An upper limit of p_{SiH} is seen for networks with a defect of crosslinker. This suggests a plateau value for the degree of conversion of the vinyl groups of approximately 97%. Similar values were reported by Benjamin and Macosko (1981) and very recently by Fisher and Gottlieb (1986). For networks with an excess of crosslinker, $r>1.3$, p_{SiH} decreases as r increases. However the expected decay in 1/r for an ideal behavior is not obeyed. Instead, a slower decay is observed which suggests that a different process in addition of the hydrosylation consumes part of the SiH groups. This is discussed in more detail in the following section.

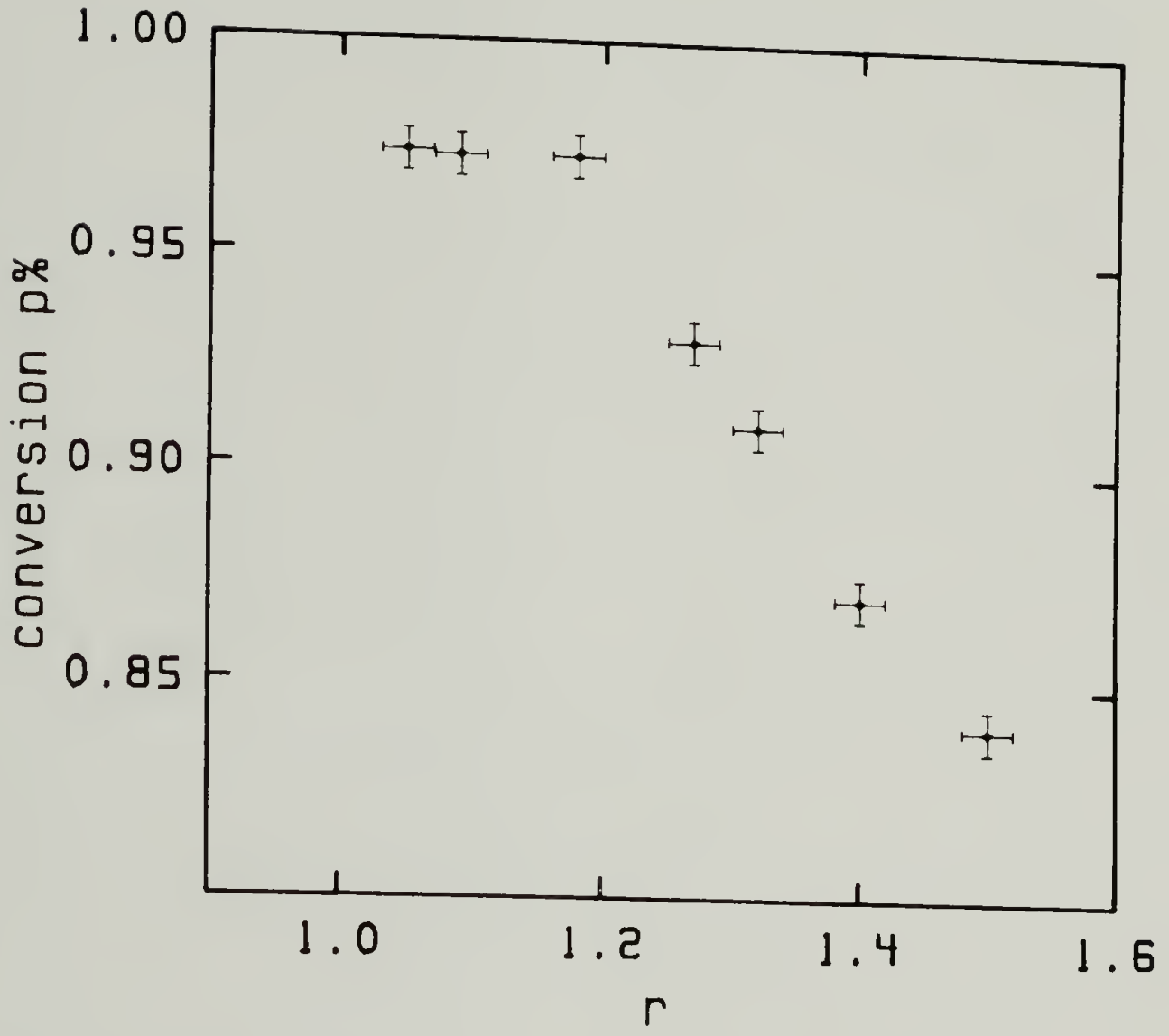

Figure 6.3. Degree of conversion, p, of fully cured PDMS as a function of the stoichiometric ratio.

6.2 Curing Kinetics of PDMS Networks with Balanced Stoichiometry

The curing kinetics of a PDMS network with balanced stoichiometry, r=1.32, were investigated by measuring p_{SiH} as a function of the reaction time. Spectra of the kinetics runs were taken automatically every 1.05 minutes. All the spectra were recorded at $2cm^{-1}$ resolution and were signal averaged for 48 scans.

To follow the kinetics, a frozen PDMS sample with balanced stoichiometry (see section 2.1) was thawed and transferred via syringe to thin KBr plates previously mounted in a preheated Harrick variable temperature liquid cell. A spacer thickness of 0.25mm was used. The temperature of the cell was maintained constant wihtin $\pm 0.5°C$. Prior to the experiment, the temperature indicators of the liquid cell and of the rheometer chamber were adjusted within $\pm 0.5°C$ agreement. A sample from the same batch was cured in the rheometer, and the results obtained with the two different instruments can be compared with a very high accuracy.

The extent of reaction, p_{SiH}, at a time t_i of the curing process is determined by Eq. (6.1). In this equation, A_f is replaced by A_{t_i}, where A_{t_i} is the SiH peak area at t_i ,as seen in Figure 6.1. The area of the peak at $1970cm^{-1}$ remained constant during the first 80 minutes of the curing process and its average value was used as an internal standard. The SiH peak areas recorded each minute were reduced to this standard value. The recorded kinetics of the PDMS are presented in Figure 6.4. The area A_{t_i} changes by approximately 0.5% from one measurement to another, which is close to the accuracy of the FTIR measure

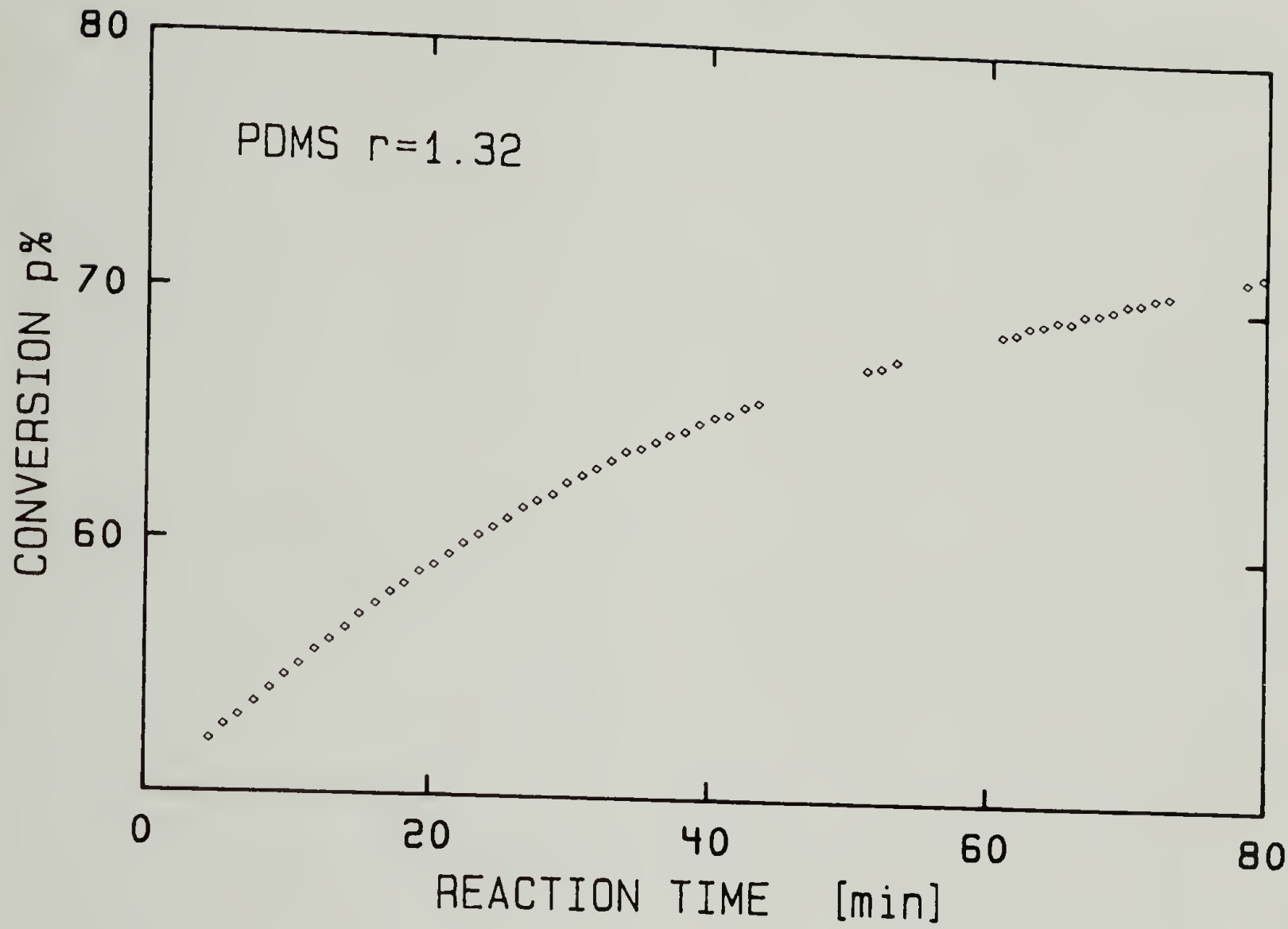

Figure 6.4. Degree of conversion, p, as a function of curing time for PDMS with balanced stoichiometry. p is measured by SiH absorption intensity.

ment for the range of p_{SiH} considered. As a result, the change of the SiH peak area during the recording of the 48 spectra is sufficiently small to be averaged precisely; hence the technique is suitable for this investigation.

Of great interest in this study is the combination of reaction kinetics data with rheological measurements taken on a similar sample and under the same conditions. This combination is done in Figure 6.5. Because of the reproducibility observed from one batch to another (see section 3.2), the curve in Figure 6.5 can also be compared with the results in Figure 3.7 where the rheological behavior at the intermediate states of the curing process is shown. It is known from the previous rheological study that the instant of gelation, t_c, of the PDMS network with balanced stoichiometry occurs at the crossover point of G' and G" in Figure 6.5. At this point, the degree of conversion is $p_{c_{SiH}}=0.5775\pm0.01$. This observed conversion can be compared with the critical extent of conversion predicted from branching theory (Macosko and Miller, 1976),

$$r(p_{c_{SiH}})^2 = \frac{1}{(f-1)(g-1)} \qquad (6.3)$$

where f and g are respectively the crosslinker and prepolymer functionalities (f=3.97, see section 2.1).

As seen in Table 6.1, the measured $p_{c_{SiH}}$ is far from the predicted value of 0.505 with r=1.32 and g=2. Several explanations can account for this discrepancy.

First, the prepolymer functionality, g, cannot be defined pre-

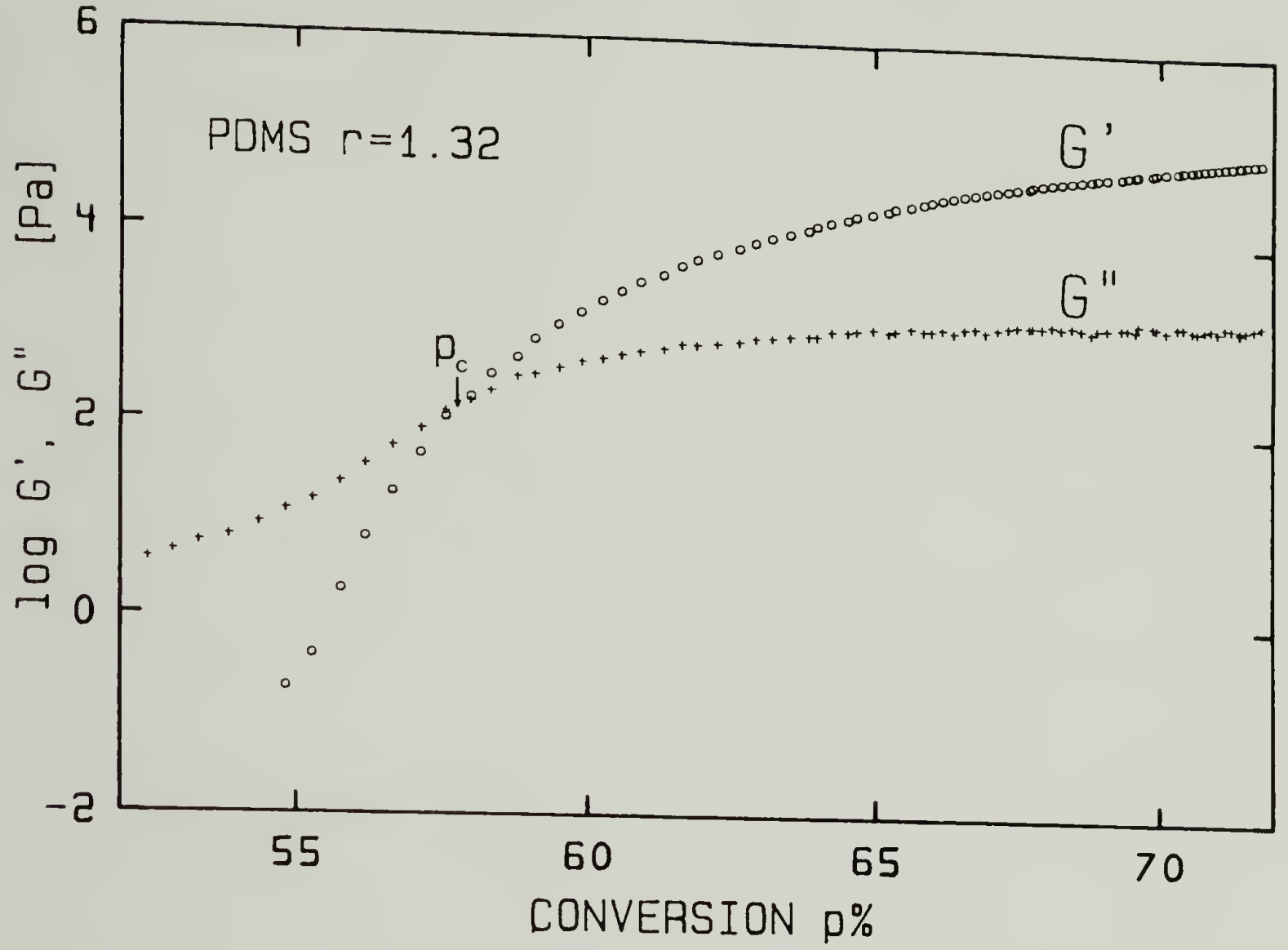

Figure 6.5. Curing curve of PDMS with balanced stoichiometry (see Figure 3.6) as a function of the degree of conversion. At the gel point p_c=57.75%.

Table 6.1. Critical degree of conversion, $p_{c_{SiH}}$, as predicted from branching theory.

r	g	$p_{c_{SiH}}$
1.32	2	0.505
	1.9	0.532
	1.8	0.603
1.0	2	0.580
	1.9	0.611
	1.8	0.648

cisely because of the inaccuracy involved in its molecular weight determination and because of its polydispersity ($\bar{M}_w/\bar{M}_n \simeq 2$) (see section 2.1). As mentioned in section 2.1.1, the most probable value of g is $1.9<g<2$. However, even in the case of $g=1.9$ an important deviation remains between the experimental and the predicted value of $p_{c_{SiH}}$.

A second contributing factor to this deviation is the fact that branching theory does not take into account intramolecular reactions. Computer simulation on a similar sample has shown (Shy, Lung and Eichinger, 1985) that about 2 to 3% of intramolecular reactions have occured at GP. However Shy et al. reported in the same study that, for end-linked polymers, cyclization nearly compensates for the inherent overestimation of the critical extent of reaction by branching theory. As a result, intramolecular reactions are not a satisfactory explanation for the important deviation observed.

Finally, a more consistent explanation seems to be the disappearance of SiH groups by a process which does not lead to elastically effective crosslinks. Such side reactions were previously estimated to consume 5 to 10% of the SiH groups, most of them in a reaction with water (Macosko and Benjamin, 1981). Very recent investigations on side reactions of the hydrosilation reaction (Macosko and Saam, 1985; Fisher and Gottlieb, 1986) reappraised this figure and reported that approximately 30% of the SiH groups are lost; 2 to 3% react with moisture and the remaining part, as much as 28%, is consumed in diverse redistributions reactions. These new findings explain the fact that the maximum of G' for fully cured samples is not found at $r \simeq 1.0$ but rather at $r \simeq 1.3$ (sec-

tion 3.1); however such a high percentage of side reactions is not expected to be reached at GP. Accurate determination of the amount of side reaction at GP would require a more thorough physical characterization of the curing samples and is outside the scope of this study. For the moment, the possibility of a substantial amount of side reaction is retained despite the purity of the chemicals and the careful drying conditions employed.

In summary, two main reasons can explain the discrepancy observed between the measured degree of conversion at the gel point and the prediction of branching theory. The first one, ill-defined prepolymer functionality, could be avoided by the use of monodisperse PDMS prepolymers synthesized by anionic polymerization. However such polymers are very difficult to prepare in large quantities (Holle and Lehnen, 1975). The second reason, side reactions of SiH groups, seems to be inherent to the hydrosilation process. This suggests that the disappearance of vinyl groups, which have been reported to be free of side reactions (Fisher and Gottlieb, 1986), should be followed rather than silane groups. Such measurements have been attempted by FTIR, but without success, since the concentration of vinyl groups in the sample studied was too low to be quantitatively measured.

Comparison of Figures 6.5 and 3.7 indicates that, between the times t_c-2min and t_c+2min, p_{SiH} has increased by less than 1.5%. This increase is only slightly greater than the accuracy of the technique employed. By contrast, a drastic change in the rheological properties was observed during this elapsed time. This leads to the conclusion that rheological measurements allow precise determination of the instant

of gelation, and that such precision is barely accessible to single evaluations of the extent of reaction.

6.3 NMR Peak Broadening of Curing PDMS Networks with Balanced Stoichiometry

The width of the NMR signal is strongly dependent on the molecular mobility of the media. In an attempt to determine the instant of gelation from NMR measurements, PDMS samples with balanced stoichiometry were prepared (section 2.1) and placed in NMR tubes before storage in liquid nitrogen. After thawing, the sample was transferred to the NMR chamber and allowed to cure at 34°C. A proton NMR spectrum was recorded every 0.9 minute, and the line width broadening at 275Hz was measured as a function of the curing time. The evolution obtained is presented in Figure 6.6.

A sharp broadening of the HNMR signal was expected as the material goes through gelation. Instead, a smooth and continuous change of the line width was recorded as the material solidifies, which does not allow a direct determination of GP. This result confirms that the liquid-solid phase transition occuring at GP does not involve important changes of the molecular mobility at short length scale. Instead, only the longest relaxation times due to the motion of large molecular segments are affected at GP, as was shown in the previous rheological study.

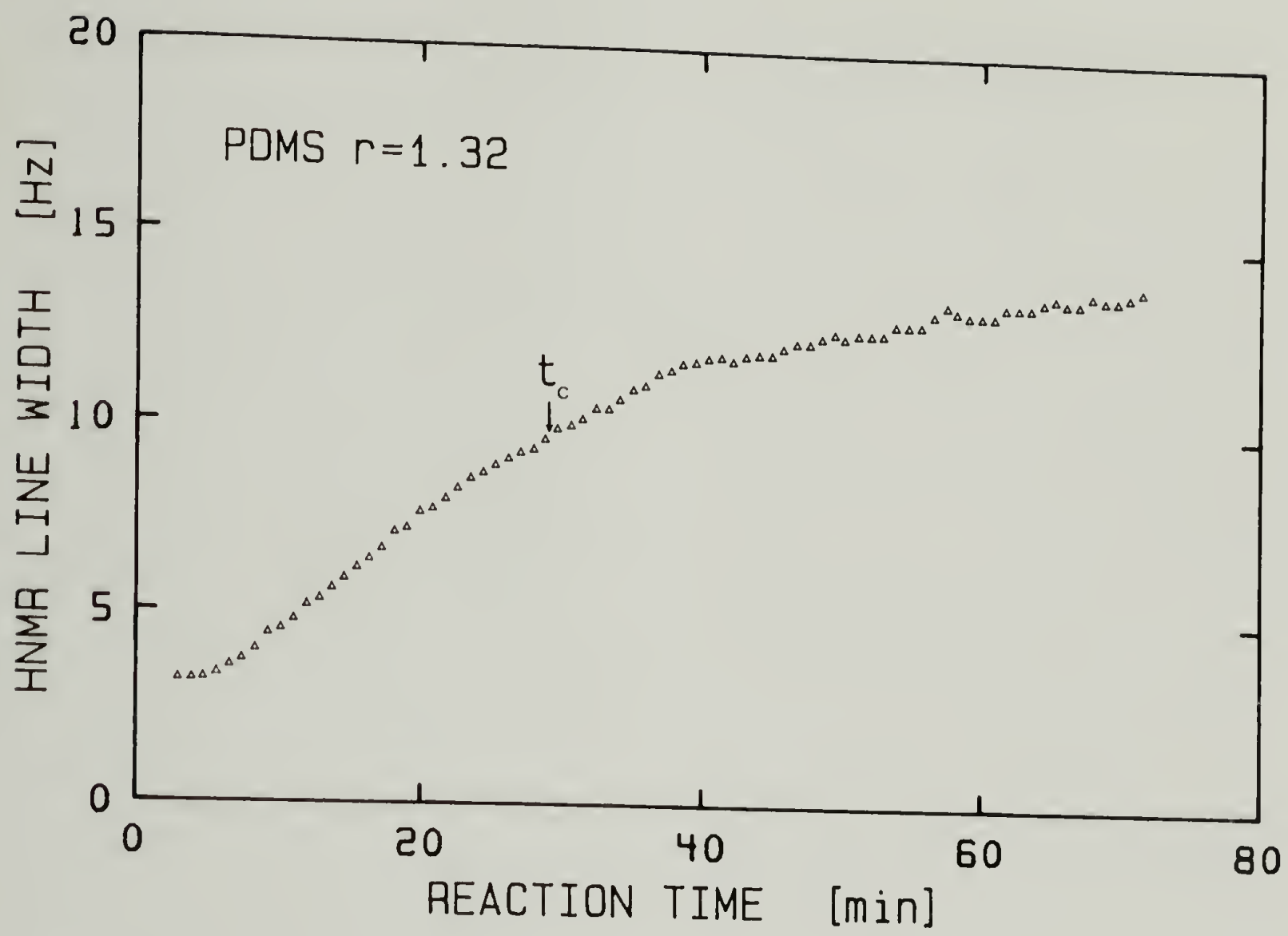

Figure 6.6. HNMR line width broadening at 275Hz as a function of the reaction time for PDMS with balanced stoichiometry. T=34°C.

6.4 Solubility Tests

The gel transition is defined by the appearance of an infinitely large macromolecule and therefore by an insoluble component in the material.

Subsequent to rheological characterization, three of the partially cured PDMS samples with imbalanced stoichiometry (see Figure 4.4) were immersed in toluene. The partially cured sample at t_c-1.8min dissolved after 24 hours in toluene. Filtration of the resulting solution through regular filter paper did not indicate the presence of any insoluble component. By contrast, the sample at t_c+1.2min did not dissolve in toluene. Instead, a fragile swollen PDMS film with a deformed disk-like shape was obtained. After 24 hours in toluene, the sample at $t \simeq t_c$ formed numerous swollen 'clusters', some reaching a size of several millimeters. It is important to note that an increase of the extent of reaction of less than 0.5% is expected between t_c and t_c+1.2min. This prediction is based on the kinetics study of PDMS network with balanced stoichiometry.

A similar solubility experiment was conducted with the PU system. A sample prepared with PPO1000 at balanced stoichiometry was cured in the rheometer up to a time slightly before t_c (see Figure 5.1). At that instant, the parallel plates assembly was quickly removed from the rheometer and immersed in liquid nitrogen. The frozen sample was then easily detached and plunged into a 50/50 (v/v) mixture of toluene and methanol (toluene is a good solvent for PU while methanol caps the crosslinker very effectively). Immediately after immersion in the

mixture, the PU sample dissociated into numerous clusters similarly to those described with the PDMS.

These experiments confirm the lack of connectivity throughout the samples at $t \simeq t_c$, and the inhomogeneous nature of the gelation process. Prior to t_c, the clusters formed may be insoluble, but they are not yet connected to each other. As a result, these samples do not possess any permanent elasticity; that is to say they are not gelled. By contrast, samples above t_c have clusters which are already connected and hence the material is no longer soluble; gelation has been passed. It is therefore concluded that these qualitative solubility tests fully support the rheological measurements already presented.

CHAPTER VII

CONCLUSIONS AND SUGGESTIONS FOR FUTURE RESEARCH

7.1 Conclusions

The transition from viscoelastic liquid to viscoelastic solid is a gradual one. There is no discontinuity in the rheological behavior at the gel point. The Gel Equation, Eq. (4.9), describes a limiting behavior as shown in Figure 7.1. The viscoelastic liquid is bounded by the purely viscous limit (Newtonian liquid) and by the gel transition limit (GP network); the viscoelastic solid is bounded by the gel transition limit and the purely elastic limit (Hookean solid). Each of the limiting behaviors is characterized by an extremely simple constitutive equation even though constitutive equations for intermediate materials (viscoelastic liquids and viscoelastic solids) are very complex. This is a highly significant result in several respects. First, viscoelastic liquids and solids can now be classified by their closeness to either one of the limiting rheological behaviors. Secondly, the existence of the limiting behavior at GP restricts the formulation of constitutive equations for viscoelastic liquids and solids. Finally, molecular theory for GP, if it were available, would help formulate molecular theories of the liquid and the solid state. The simplicity of the rheology at GP gives rise to the hope that a molecular theory, which

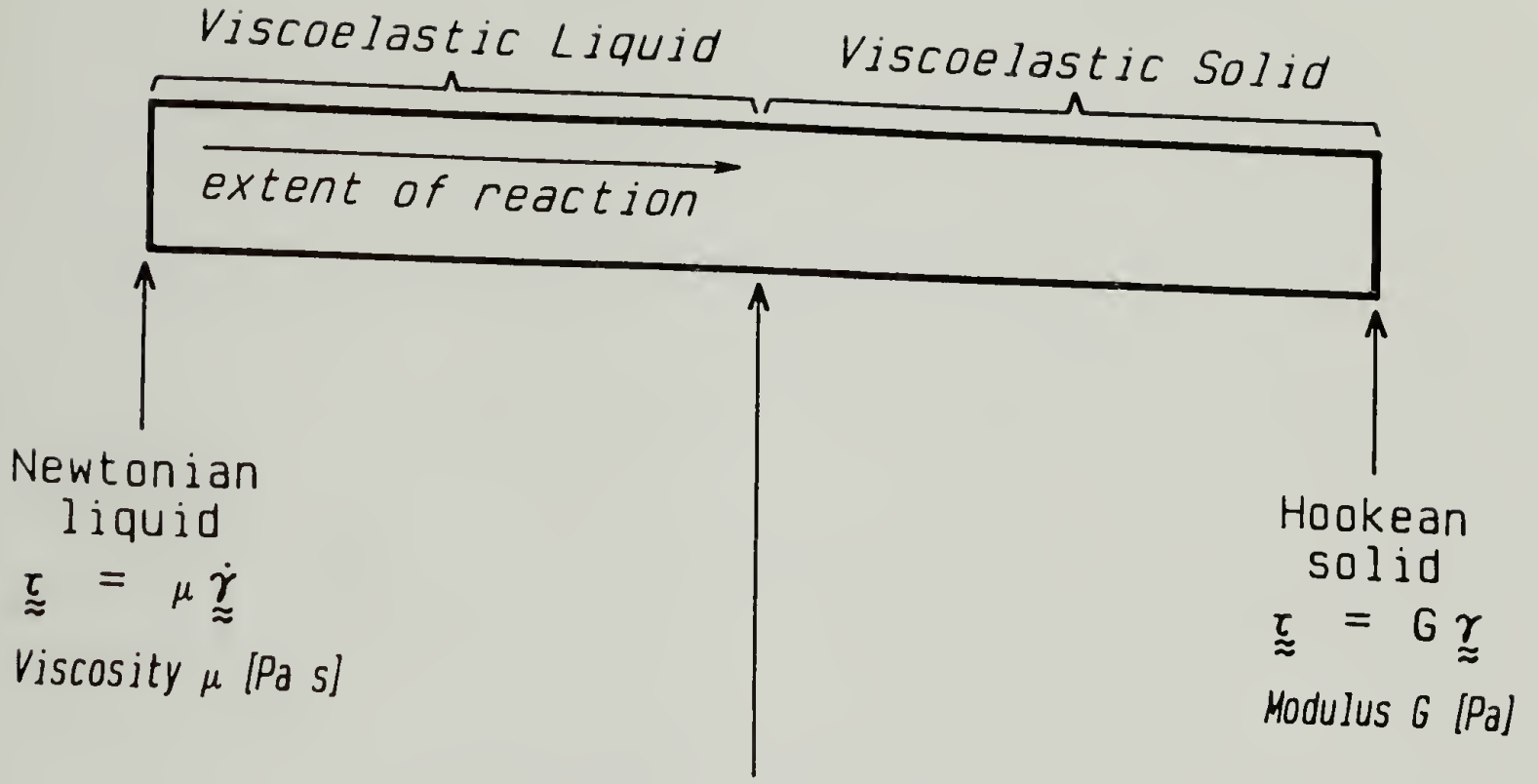

Figure 7.1. Evolution of the rheological behavior of a crosslinking polymer at constant density with three idealized states: the Newtonian liquid at the beginning of the reaction, the viscoelastic transition at a critical conversion, and the Hookean solid at completion of the reaction. Each of the three idealized states is described by a very simple constitutive equation. The equation of the Hookean solid and of the GP-network are written in a form which is limited to infinitesimal strain. At GP the power law exponent takes the values $n=1/2$ for $r>r_e$ and $1/2<n<1$ for $r<r_e$ (r_e=effective stoichiometry).

will predict an unusually extended power law relaxation zone, can be derived.

The Gel equation, Eq. (4.9), gives a new definition of the rheological behavior at GP. That is power law relaxation modulus and power law dynamic moduli. The commonly accepted definition (i.e. infinite steady viscosity, and zero equilibrium modulus) is too imprecise to accurately determine the instant of gelation, and inadequate to allow differences in gel behavior to be distinguished. The fact that the steady state shear viscosity cannot be reached at GP and the experimental difficulties encountered in measuring an actual zero equilibrium modulus imply that these two quantities may not be the pertinent rheological parameters to characterize GP. Instead, this study suggests that significant progress in understanding the gelation phenomenon will arise when gelation theories can predict other non-divergent rheological functions, such as dynamic moduli, at GP.

For chemically cross-linking polymers, there is an interesting difference between GP and other transitions such as the glass transition or the melting transition. A chemically cross-linked polymer at GP, such as the partially cured PDMS samples, cannot be moved in or out of this transition by changing the temperature or the frequency of the shearing experiment. In comparison, physically cross-linked networks undergo reversible GP at a critical temperature or pressure. Even so, a change in frequency should not shift GP. One might speculate that physical and chemical gels follow the same rheological law.

Finally, this study demonstrates that rheological measurements are sufficient to measure the instant of gelation and that they are more

precise than evaluations of the degree of conversion. However complementary physical characterization of the samples at GP would be of the greatest interest. Such experiments are proposed in the next section.

7.2 Suggestions for Future Research

A natural extension of this research is to precisely define the range of validity of the Gel Equation. An important aspect to be covered is the long time behavior near the gel point. Measurements at very low frequency were not accessible with the mechanical spectrometer in oscillatory shear. However creep experiments on stable PDMS samples near the gel point can give this information. Start-up of shear flow experiments on the gel are also of prime interest to test the predictions of the Gel Equation. At any shear rate within the range of linear viscoelasticity, the shear viscosity is expected to grow without ever reaching the steady state. It is of practical interest for reactive processing and for gel processing to investigate the large strain behavior of a gel and to define its range of linear viscoelastic response.

An interesting consequence of the power law behavior observed at GP is its application in measuring the instant of gelation. It has been shown in section 4.3 that at GP the tangent of the loss angle is independent of the frequency, Eq. (4.10). This property can be used to determine the instant of gelation in a single curing experiment. For instance, by subjecting the sample to a multi-frequency deformation, the tangent of the loss angle can be recorded as a function of the curing

time at different frequencies. From Eq. (4.10), the crossover point of these curves will occur at the gel point. It is interesting to note that this single experiment would give the value of the power law exponent, n, and therefore the fractal dimension of the gel. It is expected that rheologically-measured GP coincides with the transition of other properties such as cessation of large scale molecular motion (Schmidt and Burchard, 1981), divergence of the correlation length. Rheological measurements at GP support the arguments of self similarity. A great complement to this result would be a direct measurement of the fractal dimension at GP. Radiation scattering techniques are suggested to achieve this goal.

Finally, physical entanglements are avoided in this study, at least initially, by choosing prepolymer molecular weights below the entanglement limit. Surprisingly, rheological measurements at intermediate stages of the developing network do not show clearly any evidence for entanglements even in the vicinity of the gel region where large molecules are expected to be formed. It would be interesting to test the effect of entanglements on the validity of the Gel Equation. The addition of an inert filler in the cross-linking polymer would be equally interesting for composite processing. Preliminary experiments with a small quantity of filler suggest that filled gels still retain the power law relaxation property. However deviations from this behavior are expected at higher filler concentrations.

NOMENCLATURE

Roman Symbols

a_T	horizontal temperature shift factor
A_o	SiH peak area of the initial PDMS mixture, see Eq. (6.1)
A_f	SiH peak area of the fully cured PDMS mixture
A_{t_i}	SiH peak area at intermediate time of reaction t_i
b_T	vertical temperature shift factor
C	material constant, see Eq. (3.2)
$\underline{\underline{C}}^{-1}$	Finger strain tensor
d_f	fractal dimension
D	material parameter, see Eq. (4.1)
E	activation energy, see Eq. (3.1), or
E	material parameter, see Eq.(4.2)
f	cross-linker functionality
g	prepolymer functionality
G(t)	shear relaxation modulus
G_∞	equilibrium modulus
G'	shear storage modulus
G"	shear loss modulus
G'_c	shear storage modulus at the critical state
$G"_c$	shear loss modulus at the critical state
H	relaxation spectrum
M	molecular weight
$\bar{M}_n$	number average molecular weight
$\bar{M}_w$	weight average molecular weight
n	power law exponent, see Eq. (3.5)

n_{max}	maximum value of the power law exponent
P_{SiH}	degree of conversion of the SiH groups
$P_{c_{SiH}}$	critical degree of conversion of the SiH groups
r	stoichiometric ratio
r_e	effective stoichiometry
R	gas constant, see Eq. (3.1), or
R	radius of gyration, see Eq. (4.11)
t	time
t_c	critical time
T	absolute temperature
T_o	reference temperature
T_g	glass transition temperature
T_{gg}	glass transition temperature of the gel
v	velocity

Greek Symbols

$\underline{\underline{\gamma}}$	strain tensor
γ_{12}	shear strain
$\dot{\underline{\underline{\gamma}}}$	rate-of-strain tensor
$\dot{\gamma}_{12}$	shear rate
$\Gamma(n)$	gamma function with argument n
δ	phase angle between stress and strain
η	shear viscosity
η_0	steady-shear viscosity at vanishing rate
η^*	complex dynamic shear viscosity
η'	real part of complex viscosity
η''	imaginary part of complex viscosity

λ	relaxation time, argument of H
λ_{max}	longest relaxation time
ρ	density
$\underline{\underline{\tau}}$	stress tensor
τ_{12}	shear stress
ω	frequency in rad/s
ω_0	reference frequency, 0.5 rad/s.

REFERENCES

Adam, M., M. Delsanti, D. Durand, G. Hild and J.P. Munch, Pure & Appl. Chem., 53, 1489, (1981).

Adam, M., M. Delsanti and D. Durand, Macromolecules, 18, 2285, (1985).

Apicella, A., P. Masi and L. Nicolais, Rheol. Acta, 23, 291 (1984).

ASTM D 1638-74

Bibbo, M.A. and E.M. Valles, Macromolecules, 17, 360 (1984).

Bird, R.B., R. Amstrong and O. Hassager, 'Dynamics of Polymeric Liquids', J. Wiley, New York, 1977.

Bueche, F., J. Chem. Phys., 20, 1959 (1952).

Castro, J.M., C.W. Macosko and S.J. Perry, Polym. Com., 25, 82 (1984).

Cates, M.E., J. Physique, 46, 1059 (1985).

Choy, I. and D.J. Plazeck, to be published.

Cotton, F.A. and G. Wilkinson, 'Advanced Inorganic Chemistry', chap. 21, J. Wiley, New York, 1972.

Farris, R.J. and C. Lee, Polym. Eng. Sci., 23, 586 (1983).

Feger, C., S.E. Molis, S.L. Hsu, W.J. MacKnight, Macromolecules, 17, 1830 (1984).

Feger, C. and W.J. Macknight, Macromolecules, 18, 280 (1985).

Feger, C., personal communication.

Ferry, J.D., 'Viscoelastic Properties of Polymers', J. Wiley, New York, 1980.

Fisher A. and M. Gottlieb, Proc. of Networks 86, Elsinor Denmark, Aug. 1986

Flory, P.J., J. Am. Chem. Soc., 63, 3083, 3091, 3096 (1941).

Flory, P.J., 'Principles of Polymer Chemistry', Cornell Univ. Press, Ithaca, NY, 1953.

Gordon, M., Proc. R. Soc. London, Ser. A, 268, 240 (1962).

Gottlieb M., C.W. Macosko, G.S. benjamin, K.O. Meyers and E.W. Merrill, Macromolecules, 14, 1039 (1981)

Herrmann, H.J., D.P. Landau and D. Stauffer, Phys. Rev. Lett., 49, 412 (1982).

Holle, H.J. and B.R. Lehnen, Eur. Polym. J., 11, 663 (1975).

Kauffman, C.B. and D.O. Cowan, in 'Inorganic Synthesis' Vol. 6, E.G. Rochow, Ed., McGraw-Hill, New York, 214 (1960).

Kramers, H.A., Atti. Congr. Int. Ficici, Como, 2, 545 (1927).

Kronig, R de L., J. Opt. Soc. Amer., 12, 547 (1926).

Larson, R.G., Rheologica Acta, 24, 327 (1985).

Leung, Y.K. and B.E. Eichinger, J. Chem. Phys., 80, 3877, 3885 (1984).

Lipshitz, S. and C.W. Macosko, Polym. Eng. Sci., 16, 803 (1976).

Lodge, A.S., 'Elastic Liquids', Academic Press, new York, 1964.

Macosko, C.W. and F.G. Mussatti, ANTEC Tech. Papers, 18, 73 (1972).

Macosko, C.W. and G.S. Benjamin, Pure & Appl. Chem., 53, 1505 (1981).

Macosko, C.W. and J.C. Saam, "The hydrosilation Cure of Polyisobutene", to be published, (1985).

Malvern, L.E., 'Introduction to the Mechanics of a Continuous Media', Prentice-Hall, London, 1969.

Marin G. and Ph. Monge, Proc. Int. Congr. Rheology, Acapulco, 3, 455 (1984).

Mark, J.E. and J.L. Sullivan, J. Chem. Phys., 66, 1006 (1977).

Mark, J.E., Adv. Polym. Sci., 44, 1 (1982).

Meyers, K.O., M.L. Bye and E.W. Merrill, Macromolecules, 13, 1045 (1980).

Miller, D.R. and C.W. Macosko, Macromolecules, 9, 206 (1976); Polym. Eng. Sci., 19, 272 (1979).

Mooney, M., J. Polym. Sci., 34, 599 (1959).

Muthukumar, M., J. Chem. Phys., 83, 3161 (1985).

Muthukumar, M. and H.H. Winter, Macromolecules, 19, 1284 (1986).

Odian, G.,'Principles of Polymerization', p.108-109, J. Wiley, Ney York, 1981

Roovers, J. and W.W. Graessley, Macromolecules, 14, 766, (1981).

Rouse, P.E., J. Chem. Phys., 21, 1272 (1953).

Schmidt, M. and W. Burchard, Macromolecules, 14, 370, (1981).

Shy, L.Y. and B.E. Eichinger, Br. Polym. J., 17, 200 (1985).

Shy, L.Y., Y.K. Leung and B.E. Eichinger, Macromolecules, 18, 983, (1985).

Stauffer, D., Lec. Notes Phys., 9, 149 (1981).

Stauffer, D., Pure & Appl. Chem., 53, 1479 (1981).

Stauffer, D., A. Coniglio and M. Adam, Adv. Pol. Sci., 44, 74 (1982).

Sung, P.H. and J.E. Mark, J. Polym. Sci., Polym. Phys. Ed., 19, 507 (1981).

Stockmayer, W.H., J. Chem. Phys., 11, 45 (1943); 12, 125 (1944).

Termonia, Y. and P. Meakin, Phys. Rev. Lett., 54, 1083 (1985).

Tung C.Y.M. and P.J. Dynes, J. Appl. Pol. Sci., 27, 569 (1982).

Treolar, L.R.G., 'The Physics of Rubber Elasticity', 3rd ed., Clarendon Press, Oxford, 1975.

Valentine, R.H., J.D. Ferry, T. Homma, and K. Ninomiya, J. Polym. Sci., A-2, 6, 479 (1968).

Valles, E.M. and C.W. Macosko, Macromolecules, 12, 521 (1979).

Vinogradov, G.V., V.I. Gartsman, and B.M. Gorelik, Intern. J. Polymeric Mater., 3, 165 (1974).

Winter, H.H. and F. Chambon, J. Rheol., 30, 367 (1986).